APPLICATIONS OF FREQUENCY MODULATION

INTERFERENCE CANCELLERS TO MULTIACCESS

COMMUNICATIONS SYSTEMS

Thesis by

George A. Zimmerman

In Partial Fulfillment of the Requirements for the Degree of

Doctor of Philosophy

California Institute of Technology

Pasadena, California

1990

(Submitted May 17, 1990)

Acknowledgements

In many senses this thesis is the product of all the people I have been fortunate enough to share the last three years with. Almost everyone around me has had to put up with something above and beyond the boundaries of normal duty during the production of this thesis. What follows are only a few of those to whom I am especially indebted.

Professor Edward C. Posner, in title my Research Advisor, has been much more than that. Not only is he one of those responsible for getting me started on interference cancellation, but he has, even in my darkest hours, kept this research on track. At times when I refused to see that there was something worthwhile to be explored here, he subtly got me started again in the direction of discovery. In addition to helping me navigate the labyrinth of ideas to get me to this thesis, he has put in tireless hours editing this thesis for its final production. He calls this part of his job, but I think the effort he has put into it is far beyond the confines of his responsibilities.

Helmut Wilck and my co-workers in Section 331 at the Jet Propulsion Laboratory have put up with me during the difficult times when I had doubts, during the good times when I was exploding with enthusiasm, and during the stressful times when I was not the finest of individuals to be around. Their confidence in me has helped me through these past three years, and for this I am indebted to them . Their patience with some of my crazy ideas, and with my intense need to bounce them off the people around me, has been of incalculable value to both my mental well-being and the progress of my research.

I thank my wife, Christina. Christina has been there during all the hard times. She has certainly been more supportive and caring than I deserve. While I might not have produced this thesis without the contributions of the others, without her contributions I might not have survived the production.

I also thank my family, who have endured me during not only the past three years but also the many years before.

Abstract

Cancellation of interfering frequency-modulated (FM) signals is investigated with emphasis towards applications on the cellular telephone channel as an important example of a multiple access communications system. In order to fairly evaluate analog FM multiaccess systems with respect to more complex digital multiaccess systems, a serious attempt to mitigate interference in the FM systems must be made. Information-theoretic results in the field of interference channels are shown to motivate the estimation and subtraction of undesired interfering signals. This thesis briefly examines the relative optimality of the current FM techniques in known interference channels, before pursuing the estimation and subtracting of interfering FM signals.

The capture-effect phenomenon of FM reception is exploited to produce simple interference-cancelling receivers with a cross-coupled topology. The use of phase-locked loop receivers cross-coupled with amplitude-tracking loops to estimate the FM signals is explored. The theory and function of these cross-coupled phase-locked loop (CCPLL) interference cancellers are examined. New interference cancellers inspired by optimal estimation and the CCPLL topology are developed, resulting in simpler receivers than those in prior art. Signal acquisition and capture effects in these complex dynamical systems are explained using the relationship of the dynamical systems to adaptive noise cancellers.

FM interference-cancelling receivers are considered for increasing the frequency reuse in a cellular telephone system. Interference mitigation in the cellular environment is seen to require tracking of the desired signal during time intervals when it is not the strongest signal present. Use of interference cancelling in conjunction with dynamic frequency-allocation algorithms is viewed as a way of improving spectrum efficiency. Performance of interference cancellers indicates possibilities for greatly increased frequency reuse. The economics of receiver improvements in the cellular system is considered, including both the mobile subscriber equipment and the provider's tower (base station) equipment.

The thesis is divided into four major parts and a summary: the introduction, motivations for the use of interference cancellation, examination of the CCPLL interference canceller, and applications to the cellular channel. The parts are dependent on each other and are meant to be read as a whole.

Table of Contents

List of Figures

Chapter I

Introduction

One of the main advantages of wide-deviation, frequency-modulated (FM) signals is the FM threshold effect. Because of this, the detected signal-to-noise ratio (SNR) is markedly improved if the input is above a certain received SNR, with the amount and position of the improvement threshold being determined by the bandwidth expansion as given by the ratio of the modulating signal's bandwidth to the FM deviation [1]. In an environment where the main source of "noise" is interfering FM signals, usually co-channel, this effect, known as the FM capture effect, facilitates a simple method of providing multiaccess communications by dividing the service area into geographical regions. The allocation of frequencies for FM transmitters has been traditionally accomplished in this manner. The allowable geographical separation of co-channel and adjacent channel FM transmitters, be they high-power broadcast stations or low-power cellular telephones, has been regulated so that propagation laws will mitigate any interference problems.

As the frequency spectrum becomes more crowded, the search for more efficient uses of the available bandwidth intensifies. Complex digital combined modulation and coding schemes have been proposed to allow more robust communications in a denser interference environment. By allowing additional receiver complexity, many of these techniques provide greater spectral efficiency by actively mitigating the interference through advanced coding and modulation [2-7]. Among these are spread spectrum and other code division multiple access (CDMA) techniques. This raises the question of whether the spectral efficiency of more conventional modulation techniques, in particular analog FM modulation, can also be improved by additional receiver complexity.

1.1. An Approach to FM Interference Mitigation

The observed ability of an FM broadcast receiver to unambiguously receive one station or another at the same frequency in areas of interference leads one to speculate that there must exist situations where both mutually interfering signals could potentially be received with the right receiver. It is reasonable, for example, to consider that demodulated FM information, enhanced by the capture

effect, could be remodulated as an estimate of the interference. This estimate could then be subtracted from the input to a second receiver, leaving the originally weaker signal now the stronger and allowing its capture by the second receiver as in Figure 1. By using the remodulated phase estimates, the amplitude component of each interfering signal could be estimated, producing an estimate of the entire interfering signal. By tracking both the amplitude and phase of the interfering signals, the full separation of the interfering signals in signal space could be exploited. This can be contrasted with tracking only the phase, as is done in conventional broadcast FM receivers. Phase-only tracking can be seen as projecting the resultant of the interfering signals onto the surface of a sphere of constant amplitude. The loss of sometimes essential side information contained in the resultant's amplitude plagues these receivers. This loss will be examined in Chapter II. Such "power-division multiplexing" of FM signals has been proposed before [8], but the separation methods involved tuning a frequency domain "trap" filter, and are therefore fundamentally different from the coherent methods described here.

1.2. Brief History of Cross-Coupled Phase-Locked Loop Interference Cancellation

A version of this subtractive interference-cancelling technique known as the **cross-coupled phase-locked loop interference canceller** (CCPLL) was developed by the investigators cited in References 9-18. The research culminated in a hardware device combining amplitude- and phase-tracking loops detailed in the definitive Reference 18. The interference-cancelling assembly is renamed the **vector-locked loop interference canceller** in Reference 18, but for the sake of clarity with earlier work, the original name (CCPLL) is more commonly used, and will be used in this thesis. This promising interference-canceller assembly seems to have fallen to the wayside of communication theory with no significant further developments. The few potential applications of the interference canceller have focused primarily on military uses. Application to conventional multiaccess communication problems has not been previously made.

1.3. Use in Cellular Telephone Communications

A natural target for any technique to improve the spectral efficiency of FM is the cellular telephone channel. The number of users of cellular telephony has grown dramatically, beyond almost all

Figure 1

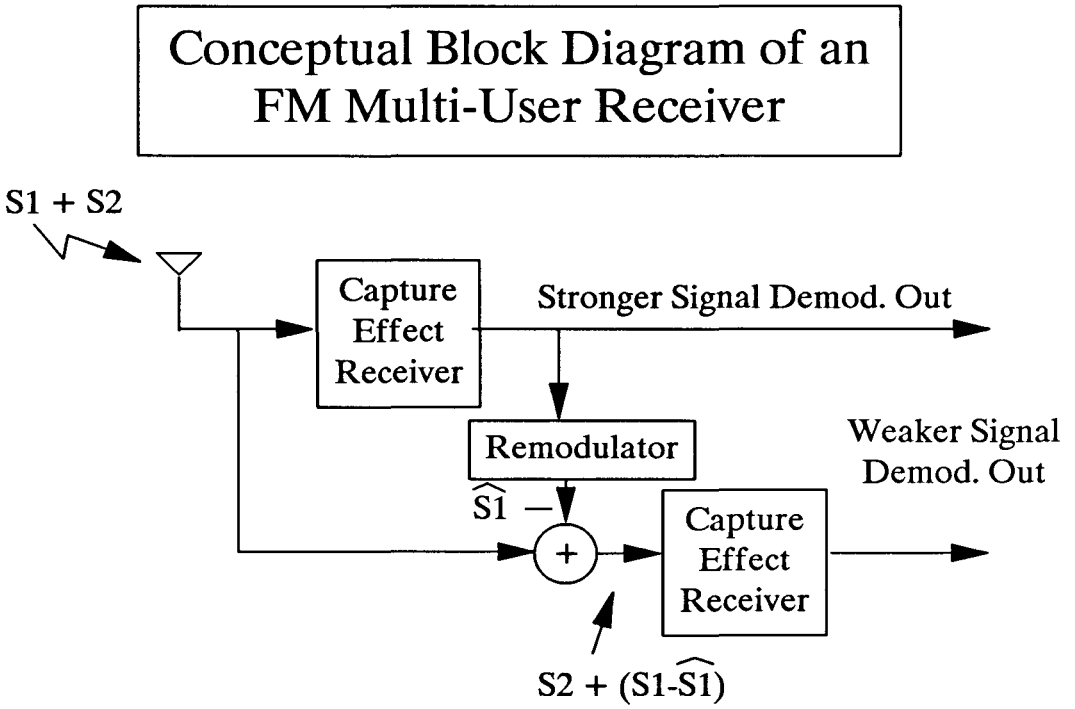
Conceptual Block Diagram of an FM Multi-User Receiver
S1 + S2
Capture Effect Receiver
Stronger Signal Demod. Out
Remodulator
Weaker Signal Demod. Out
Ŝ1
−
+
Capture Effect Receiver
S2 + (S1-Ŝ1)

expectations, putting an increasing burden on the spectrum allocated for this service [19]. The existing bandwidth allocation for cellular telephony effectively limits the number of subscribers who can be provisioned in any one service area at any one time. Competition with other uses for the frequency spectrum make additional allocations both expensive and difficult to obtain. Reuse of transmission frequencies across small areas, called "cells," is what improves the traffic handling capacity of a cell-based telephone system. However, the ability of the current United States cellular telephone system to handle traffic is constrained not only by the available spectrum, but also by frequency reuse rules designed to maintain call quality in the presence of interfering signals from the surrounding cells. It is reasonable that the application of interference-cancelling receivers to this channel will decrease the minimum frequency reuse distance, allowing the system to carry more traffic on the same allocated spectrum, i.e., more channels per cell. In addition, such a change in the cellular system could be implemented without the lengthy and expensive regulatory procedures required for changing the modulation schemes or obtaining additional bandwidth.

1.4. Outline of the Chapters

In Chapter II we examine the motivations for using interference cancellation in multiuser communications. We show that information theory naturally suggests that we utilize the discoverable structure of interference to mitigate its effects on desired transmissions. In Section 2.1 we review and further examine a special case where interference does not reduce capacity [20]. The preservation of capacity in this case requires decoding the interference information and hence implies active interference cancellation. We further show that the sufficient condition derived in [20], that the interference be decodable, is also necessary for unreduced capacity. We examine the applications of this result to the design of geographically distributed communications systems and show how reception regions might be mapped when using such interference cancellation. We discuss the relevance of such a system to analog FM transmission and briefly examine the capacity reduction that is due to the requirement for amplitude estimation. In Section 2.2 we examine traditional FM techniques and explore the losses incurred by the conventional practice of discarding amplitude information. The loss of the side information provided by the received signal amplitude is viewed both in terms of its potential use in

separating interfering signals and in terms of information-theoretic losses. The ability of amplitude side information to provide error-correction gains similar to erasure declaration in error-correcting codes is briefly discussed. In Section 2.3, the inherent ability of frequency division multiple access techniques to utilize the entire allocated channel capacity is demonstrated as a motivation for continued use of such systems in spite of newer but more complex multiple-access schemes.

In Chapter III we turn to the development of active interference cancellation for analog FM signals. The basics of the CCPLL interference-cancellation technique are reviewed in Sections 3.1 and 3.2. Section 3.3 examines the relation of the CCPLL to adaptive noise-canceller techniques (adaptive notch filter) and uses this relation to provide new understanding of the signal-acquisition process. The adaptive techniques also suggest a possible improvement to the CCPLL system, which is demonstrated to have a new and undesired stable steady-state solution. The proposed improvement is therefore discarded. The extension of the CCPLL to more than two interferers is also examined through its relation to adaptive systems. In Section 3.4 the capture effect in phase-locked loops is discussed since this effect is a major factor in CCPLL operation. Capture in PLL's is shown to be due primarily to the phase-detection operation itself, which in practical systems is accomplished by a bandpass limiter prior to the PLL. The ability of a PLL to track a signal based on a bandwidth proportional to the modulation bandwidth rather than to the FM signal bandwidth is discussed, showing how it improves capture over other FM receivers.

In Section 3.5, the effects of amplitude and phase-tracking errors on CCPLL performance are examined, and the relation between amplitude-tracking errors and weak-signal receiver input signal-to-noise ratio is presented. In Section 3.6, new interference-cancellation techniques related to the CCPLL are developed. The new systems are based on a closed-form solution to the two-weight, two-reference minimal mean-square error filtering problem for the special case found in the CCPLL where the reference inputs are orthogonal. This results in a feedforward rather than in a feedback amplitude estimator. Other hardware simplifications take advantage of the close phase tracking by the PLL to cut the amplitude-estimation hardware in half. The resulting system dynamics are examined for small perturbations from the desired steady state, showing its stability there. Similar examination of the

undesired equilibrium shows its instability near the undesired state. A variation of the feedforward amplitude estimator is also developed. This suppresses the undesired signal's corruption of the amplitude estimates by cross-coupling the amplitude-estimation process. The dynamics of this system are examined, and perturbation analysis shows it to have a stable, desired steady-state solution. The perturbation also confirms that corruption of the amplitude estimate is reduced in the desired steady state. Chapter III concludes with simulation of these new interference cancellers, confirming the analytically derived properties. The simulations serve to demonstrate the cancellers' effectiveness in separating co-channel FM interferers and also to elucidate the various advantages and disadvantages of the different canceller topologies.

In Chapter IV we examine the cellular telephone channel as an important multiuser channel and investigate the application of these interference cancellers to this channel. Section 4.1 provides background on the cellular telephone operating environment as it pertains to the need for greater spectrum efficiency. The aspects of the environment that might affect the operation of interference cancellers are examined. Section 4.2 examines the available channel capacity in proportion to the utilized capacity. The potential for improvement in this figure of merit through use of interference cancellation is estimated. Section 4.3 briefly discusses the FM receiver element of current cellular equipment and concludes that within the cost envelope of a cellular subscriber terminal, there is still much room for improvement. The relation of multipath fading to call degradation is discussed in reference to tolerable interference power in Sections 4.4 and 4.5. A simulator for multipath fading is detailed in Section 4.6. Sections 4.7 and 4.8 examine the potential mechanisms for spectrum-efficiency gains if the tolerable interference power level can be increased, while Section 4.9 details the simulation results from applying the interference cancellers of Chapter III to cellular telephony. The simulation results in Section 4.9 provide incentive for further development and field tests of interference-cancelling systems. Concluding Chapter IV, Section 4.10 discusses some of the economic constraints imposed on any modification to an existing cellular system, most notably the need for any subscriber equipment upgrade to be simple and inexpensive. Such an upgrade would be preferably a single integrated circuit, and the interference cancellers presented fit this criterion.

Chapter V summarizes the work of the preceding chapters and concludes with recommendations for future areas of research and development. Appendix A is a stand-alone attachment that focuses on specific recommendations to the cellular industry. Chapter V, however, deals with a more general scope. Implementation of interference-cancelling receivers in cellular telephony is considered, as well as the potential for application of these receivers in the areas of cordless telephones, wireless intercom systems and commercial broadcast FM radio. As long as the need for communication continues to grow, the available spectrum will be a resource to be managed wisely. Mitigation of interference either by careful coding techniques or by active cancellation or both will therefore be an important part of the future.

Chapter II

Motivations for Interference Cancellation in Multi-User Communications

Traditionally, analog communication is based on the assumption of a channel where one signal's power dominates all others. In multiaccess communications this is not going to be the case. Traditional multiaccess digital communications techniques do often assume that the interfering signal power will be comparable to the desired-signal power. Digital multiaccess communications actively mitigate this interference through the use orthogonal coding and modulation schemes. In this chapter we present information-theoretic motivations for the use of interference cancellation on analog channels. Clear reception of a powerful interfering signal provides information about the signal, and this information is used to improve the signal-to-noise ratio of other signals using the channel. For some special cases, the capacity region of an interference channel has been shown to be unrestricted by the interference. In addition, the use of side information is examined here in the mitigation of interference. The value of amplitude information is examined for a special case of interfering angle-modulated signals. Finally, the use of present frequency-allocation techniques (as frequency division multiple access) is compared to other multiple-access techniques in light of their ability to utilize the entire wideband frequency channel capacity.

2.1. Examination of a Case Where Interference Does Not Reduce Capacity

In order to better utilize available channels, communications systems that minimize the effects of interference must be examined. One proposed method for reducing the harmful effects of additive interference is to receive and decode the interfering signal, reconstruct it, and subtract the reconstructed signal from the input signal. If the reconstruction of the interfering signal is good enough, the original signal can then be successfully decoded. In [20], A.B. Carleial considers a discrete-time, multiple-terminal communication with linear interference and additive white Gaussian noise. By using the cancellation method described above, he proves that for sufficiently strong interference the multiaccess capacity region is not reduced by the presence of interference.

The topology used in [20] suggests an instance of a Cross-Coupled Phase-Locked Loop (CCPLL) receiver for demodulating the weaker of two FM signals. It also suggests the rather contrary notion that in order to gain in the overall capacity region, one should design the communication system so that the interfering signal, not the desired signal, is received with greater power at each receiver. This interpretation is not entirely correct since the communications receivers in [20] actually demodulate both the stronger signal and the weaker signal.

2.1.1. Channel Definition and Carleial's Result

The discrete-time, multiple-terminal communication channel with linear interference and additive white Gaussian noise used by Carleial is defined as follows:

1. There are two input terminals and two output terminals
2. The input and output alphabets are equal and real valued, $X_1 = Y_1 = X_2 = Y_2 = \mathbf{R}$.
3. The transmitted signals are independent and are constrained to have average energy of transmission P_1 and P_2.
4. The signals at the output terminals are given by:

$$y_1 = \sqrt{a_{11}}\, x_1 + \sqrt{a_{21}}\, x_2 + v_1$$
$$y_2 = \sqrt{a_{12}}\, x_1 + \sqrt{a_{22}}\, x_2 + v_2$$

where v_1 and v_2 are samples of zero-mean, white Gaussian random processes with variances N_1 and N_2, not necessarily independent. The constants a_{ij} represent the relative gain of signal i at receiver j, all positive, and without loss of generality take $a_{11} = a_{22} = 1$. The relative gains of the signals are assumed to be known.

The desired operating scenario is for receiver 1 to obtain signal 1 and for receiver 2 to obtain signal 2. Let R_1 and R_2 be the rates of transmission over links 1 and 2, respectively. Then, in the absence of interference, the capacity region has been shown to be the closure of the following:

$$R_1 < \frac{1}{2} \log\left(1 + \frac{P_1}{N_1}\right) \ nats/sec$$
$$R_2 < \frac{1}{2} \log\left(1 + \frac{P_2}{N_2}\right) \ nats/sec\ .$$

By showing through random coding arguments that a properly designed signal 2 can be successfully decoded with arbitrarily small probability of error at receiver 1, and likewise for signal 1 at receiver 2, Carleial proves that the capacity region is unmodified by the interference if:

$$a_{12} \geq (P_2 + N_2)/N_1 \quad \text{, and} \quad a_{21} \geq (P_1 + N_1)/N_2.$$

The condition above has only been shown to be sufficient for an unmodified capacity region [20], since the proof is based on construction of an interference-cancelling decoder topology which achieves the full capacity for each user. This does not prove that the condition is necessary.

An argument that the constraints on a_{12} and a_{21} are necessary as well as sufficient for the capacity region to be unmodified by the interference is obtained by noting the following. Since the transmitted signals were defined to be independent of one another, eliminating the effect of the interference is equivalent to decoding the undesired signal. The information rate required of the channel is then the sum of the individual signals' rates. By adding the received power from each signal, we then get the total received signal-to-noise ratio at each receiver. This can be used to express the information-bearing capacity of the channel. At the receiver for signal 1, the capacity is:

$$C_1 = \frac{1}{2}\log(1+\frac{P_1+a_{21}P_2}{N_1}) \ \ nats/sec$$

and at the receiver for signal 2:

$$C_2 = \frac{1}{2}\log(1+\frac{P_2+a_{12}P_1}{N_2}) \ \ nats/sec\ .$$

Under the condition that the information of the undesired signal must be decoded in order to completely eliminate the additional noise power that it presents to reception of the desired signal, the condition for an unmodified capacity region becomes:

$$R_1 + R_2 \leq \frac{1}{2}\log(1+\frac{P_1}{N_1}) + \frac{1}{2}\log(1+\frac{P_2}{N_2}) \leq \min(C_1\ ,\ C_2)$$

$$= \min(\frac{1}{2}\log(1+\frac{P_1+a_{21}P_2}{N_1})\ ,\ \frac{1}{2}\log(1+\frac{P_2+a_{12}P_1}{N_2}))\ .$$

A little algebra reduces this to:

$$\frac{P_1}{N_1} + \frac{P_2}{N_2} + \frac{P_1P_2}{N_1N_2} \leq \min(\frac{P_1}{N_1} + a_{21}\frac{P_2}{N_1}\ ,\ \frac{P_2}{N_2} + a_{12}\frac{P_1}{N_2})\ ,$$

which reduces to exactly the same constraints on a_{21} and a_{12} proven to be sufficient for the unmodified

capacity region by Carleial.

2.1.2. Further Examinations

Consider the case where both receivers are exposed to the same noise environment. In this case, $N_1 = N_2$, and the theorem states that the capacity region is unchanged if:

$$a_{12} \geq S_2 + 1 \quad \text{, and} \quad a_{21} \geq S_1 + 1 \,,$$

where S_1 and S_2 are the received desired-signal SNRs at their respective receivers. It is important to note that the interference at each receiver must be received with a gain greater than that for the desired signal. In addition, as the desired-signal SNR increases, thereby increasing the maximum information rate for the desired signal, the required gain for the interfering signal also increases. This is because the increased desired-signal power will produce more effective noise power in the first demodulation and decoding step where the interference is estimated. Hence, this analysis suggests that there are two locally optimum signal-power operating points for multiaccess communication systems: the usual one with low interference, and the one with high interference described here.

2.1.3. Reception Region Maps for the Additive White Gaussian Channel

Given a propagation law and the locations of the transmitters, the relations derived in [20] allow the user to draw maps of the reception regions capable of a given minimum information capacity for multiple signals. Given constant noise power throughout the region, let two signals of the same power be placed in the plane one unit apart. As an example, let the desired minimum information rate for each signal be that which can be achieved at a distance of two units from the transmitter with a signal-to-noise ratio at this position of 10 dB if there were no interference. Let the noise power be normalized to unity, and let the transmitter T1 be located at (0,0), with T2 at (1,0). The signal power at each transmitter, $P_{1,2}$, is then 10×2^k where k is the order of the propagation law, e.g., inverse square, fourth, etc. Then, at each point (x,y), the relative gains are:

$$a_1 = (x^2 + y^2)^{-k/2}$$

and

$$a_2 = ((x\text{-}1)^2 + y^2)^{-k/2}$$

for signals 1 and 2, respectively. The signal-to-noise-plus-interference ratio without cancellation is then:

$$SNR_1 = \frac{a_1}{a_2 + .1 \times 2^k}$$

$$SNR_2 = \frac{a_2}{a_1 + .1 \times 2^k} .$$

By the rate assumption above, if either SNR is greater than 10 dB, that signal can be received. Since that signal is then exactly removable, the only requirement for reception of both signals is that the weaker signal (i) satisfy $a_i > 2^k$, which is simply that the distance to its transmitter must be less than 2. Examples of reception regions for second- and fourth-order propagation laws are both shown in Figure 2.

2.1.4. Relevance to FM Interference Cancellation

The cancellation technique utilized by Carleial in his proof is strikingly similar to the application of Cross-Coupled Phase-Locked Loops in FM interference cancellation. Carleial's receivers, however, are only singly coupled rather than cross-coupled, and have *a priori* knowledge of the relative signal gains. Clearly, estimating the signal gains increases the rate at which information is extracted from the channel, although perhaps only slightly. This increase depends on the information rate or entropy of the gain factors. For Rayleigh fading multipath, this entropy of the relative channel gain is nonnegligible, but probably still recoverable. Recovery seems especially possible for the important FM voice case where the modulating information uses only a fraction of the theoretically available capacity.

2.1.5. Coherent Estimation of the Amplitude Components in FM Reception

In cellular mobile communications channels, the bandwidth of the amplitude modulation term depends among other things on the maximum doppler frequency generated by the motion of the mobile terminals. For cellular telephony (around 800-900 MHz) in automobiles traveling at up to 75 mph, this keeps the double-sided bandwidth of the range-variation-induced amplitude modulation (AM) components to less than 200 Hz, small with respect to the 24 kHz allocated for the information carrying FM voice signal. Recovery of the amplitude information from the input signal can be

Figure 2

Information Capacity Map of Multiaccess Communication System with Cancellation

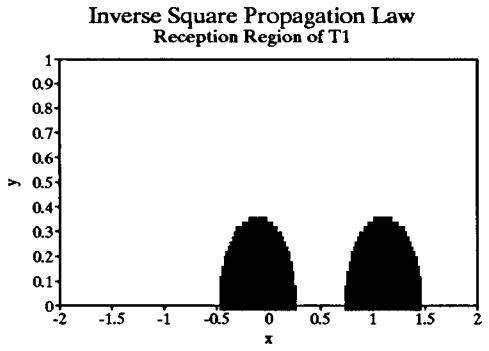

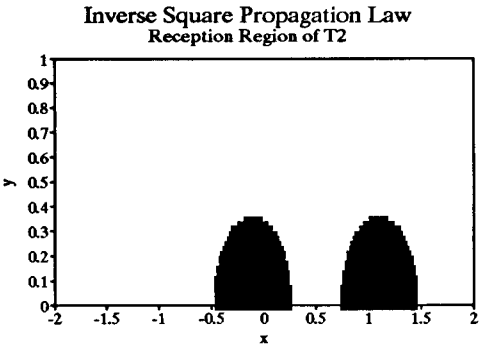

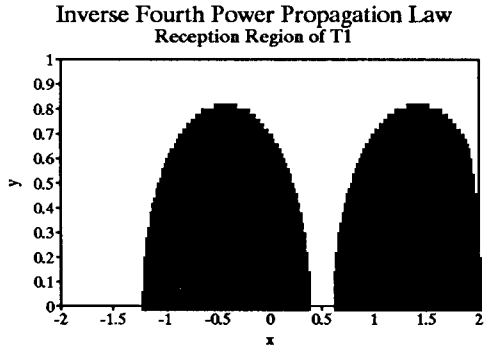

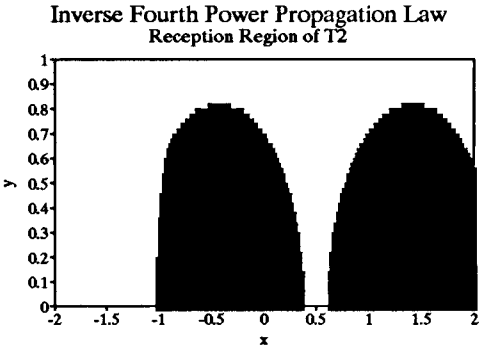

accomplished if a phase-coherent reference can be obtained. In this case, the proper amplitude estimator is a coherent AM receiver. For independent interfering signals with a perfect coherent reference, the requirement for interference-free, but not noise-free, recovery of the amplitude information is that the upper band edge of the amplitude information be lower than the lower band edge of the doppler-broadened frequency modulation information. This is due to the intermodulation terms that will be produced between the interfering signal and the coherent reference. The noise bandwidth of the process is simply the bandwidth of the amplitude-modulating information, giving the intuitive result that the more the constant-modulus property of FM signals is preserved by the channel, the easier they are to separate.

The rate at which information must be extracted from the channel in order to estimate the signal amplitude decreases the information rate that the communicator can use. Since infinitely precise measurement of a continuous process requires an infinite amount of information, the precision to which the amplitude function must be known for effective interference cancellation is an important part of the problem. For cellular communications, the amplitude of the received signal is a time-varying function, Rayleigh-distributed with a nonnegligible bandwidth on a short time scale, and with a lognormally distributed mean on a long time scale [21]. Errors will be made in the amplitude-estimation process. For the coherent amplitude estimation described above, the errors made can be modeled as adding white Gaussian noise to the actual amplitude. The mean-square error of this process (ε) , the variance of the white noise resulting from coherent AM detection, is a standard communications theory result [1]:

$$\varepsilon = N_0 W ,$$

where W is the bandwidth of the amplitude function, and N_0 is the input equivalent noise power spectral density. Errors in knowledge of the relative signal amplitude will add to the noise power. Therefore, for systems with amplitude-estimate errors, the capacity region achievable with an estimation and subtraction-based approach, such as Carleial uses, will be reduced in the presence of interference such that:

$$R_1 < \frac{1}{2}\log(1+\frac{P_1}{N_1 + \varepsilon_2 P_2}) \ \ nats/sec$$

$$R_2 < \frac{1}{2}\log(1+\frac{P_2}{N_2 + \varepsilon_1 P_1}) \ nats/sec \ .$$

The problems of amplitude estimation will return in Chapter III when specific interference-cancelling structures are discussed.

2.2. The Sin of Neglected Side Information

When the amplitude is not preserved by the channel, however, it has been traditional to ignore amplitude altogether. In fact, one of the main attractions of mobile FM radio systems has been their robustness under (amplitude) fading. Receivers have been analyzed and designed as if the input signals are of constant amplitude, so most receivers have been equipped with amplitude limiters to make this so. However, is it really so prudent to throw away possibly useful information ? The amplitude of a received FM signal contains, at the least, information as to the reliability of the phase estimate at that moment. The (wideband) time track of the amplitude can potentially tell even more, giving information about the interference environment through the dynamics of its behavior. Such information can be the key to separating otherwise inseparable signals.

For example, consider the case of two interfering frequency-modulated signals in negligible noise. The receiver knows nothing about the two signals except that there are either one or two of them, they are frequency-modulated, and they have constant amplitude. The resultant sum of the two signals is passed through two channels. One channel performs a complex limiting operation and removes all amplitude information from its output, exactly as a conventional FM receiver would do. Without additional *a priori* knowledge of the individual interfering signals, it would be impossible to tell even that two signals were present after transmission through this channel. So, at least one additional bit of information is required. However, the process for extracting the FM information is not particularly helped by this bit of information. Knowledge of the bandlimits of the frequency-modulating process, though, would aid the process by enabling the use of filters. These could be used to remove intermodulation products from the modulation estimate of the combined signal. In this way, if the modulation index and the power difference were both sufficiently large, the FM capture effect might allow for the recovery of the stronger signal's information. Even with this knowledge, we are still a long way

from being able to determine the modulating information on the second signal. The capture-enhanced estimate of the stronger signal might, for example, be used to drive a model of the interference environment and produce an estimate of the second signal, but in general this is algorithmically complex.

Now consider the same problem without the complex limiting channel. By observing the oscillating amplitude of the resultant signal, the presence of more than one signal would be readily apparent. The maximum and minimum of the amplitude track would give the sum and the difference of the individual signal amplitudes. The signal phases could now be resolved down to a single ambiguity by solving for the angles of the triangle formed by the phasors of the two signals plus the resultant signal (see Figure 3). This is now trivial since all three sides of the triangle are known. The problem is therefore reduced to resolving the ambiguity between the two possible triangles formed by the signal phasors, one on each side of the resultant phasor. Only one additional bit of information is therefore required to separate the two signals unambiguously. This is the same amount of information we needed just to get started in the case without amplitude information. Because of the side information provided by the amplitude of the resultant signal, the signals could be separated with far less knowledge required at the receiver. This example suggests that the demodulation of angle-modulated signals might best be carried out by estimating both the amplitude and the phase process of the received signal. This suggestion is further supported by detected SNR gains found in [22] for joint amplitude and phase estimation FM receivers, and by the interference-cancellation work presented in Chapters III and IV of this thesis.

The foregoing arguments raise the question of what the information-theoretic losses are in discarding the amplitude information. The information lost by discarding the amplitude is dependent on the amplitude process itself. Clearly, if the channel is known to have only one signal present and little narrowband noise, the amplitude information is of much less value than if two or more signals are present and/or the channel is noisy. The reason is that in the former case, the amplitude is relatively constant, and hence its average entropy rate over a long period of time is small, indicating that it can provide little additional information. However in the latter cases the amplitude significantly varies (randomly) with time and is capable of carrying much information. Its dynamics either represent the

Figure 3

Separation of Interfering Signals by Solving Side-Side-Side Triangle

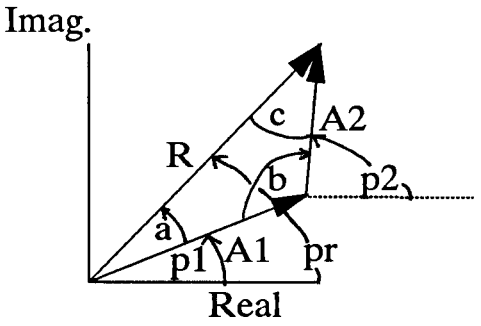

OR:

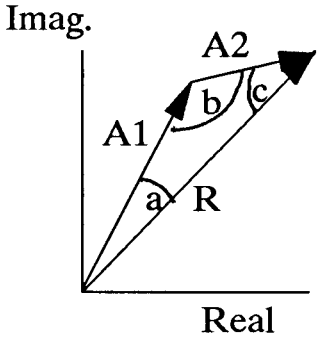

R, pr are measurable

A1 > A2

A1 = E [R]

A2 = .5* (max R - min R)

p1 = pr-a OR pr + a

p2 = pr+c OR c - pr - 2π

Let s = .5*(A1+A2+R)

$$\text{Let } x = \sqrt{\frac{(s-A1)(s-A2)(s-R)}{s}}$$

a = 2atan(x/(s-A2))

b = 2atan(x/(s-R))

c = 2atan(x/(s-A1))

relative phases and frequencies of the interfering signals, or they represent the instantaneous amplitude of the noise, both of which are indicative of the amount of corruption in the received version of the desired signal. If the entropy of the received amplitude process of a signal is a fixed constant; i.e., either the amplitude is constant over time, or it can at least be specified for all time by fixed parameters with finite entropy; the information rate required to remove any amplitude-induced uncertainty goes to zero as the total transmission time increases without bound. This reinforces the known result that for additive white Gaussian channels of infinite bandwidth without interference, constraining the amplitude to a constant should not reduce the capacity [23].

As an example, consider channel-induced amplitude variation as amplitude modulation on the input signal to an additive white Gaussian channel. Let the amplitude be zero-mean Gaussian with bandwidth W plus a known constant offset. Recovery of the amplitude information from AWGN at a signal-to-noise ratio S_A (noise is estimation error) would then require a rate of:

$$R_A = W \log_2(1+S_A)$$

bits per second extracted from the channel. Note that this information must be recovered from the same signal component as the frequency-modulating information. Assuming that the amplitude information is independent of the FM information, the useful rate at which FM information can be extracted from the channel is reduced by the rate necessary to extract the amplitude information. By the data processing theorem of information theory [24], it is not possible to circumvent this loss of FM information simply by ignoring the amplitude information. This relative information loss to the FM information is, however, clearly small when the amplitude is narrowband, or when the variance of the amplitude is small compared with the square of its offset.

It is, however, sometimes possible to use amplitude information to improve the detected SNR of an angle-modulated signal. Note that as the received SNR decreases and the FM threshold is reached, the detected SNR of the baseband FM information becomes more sensitive to the received SNR, a fact that can be found in any text covering FM communications [21,25,1]. This effect is caused by the increasing probability of origin encirclements (breaking) by the received signal's phase trajectory, demonstrating that for constant noise power, the FM information and the amplitude information are

not always independent. When the amplitude is small, the phase trajectory is more likely to "break" than at times when the amplitude is momentarily large. Hence by demodulating the amplitude information, the received signal can be post-detection filtered to remove some of the breaking during periods of low amplitude. Although the actual processing may be complicated, amplitude information could thus be used in a way similar to soft-decision decoding of error correction codes to improve the output signal-to-noise ratio.

Amplitude tracks can be used to provide erasure or soft-decision information for digital phase-modulated systems as well.[1] The declaration of erasures based on amplitude tracking in Rayleigh fading mobile channels can be quite useful. On such a channel where most of the error bursts could be detected in this way, the declaration of erasures would double the effective error-correcting capability of block (RS) codes. The maximum likelihood (Viterbi) decoder for convolutional codes on the Rayleigh fading channel likewise incorporates an amplitude-related "confidence measure" [26] to improve its error-correction capability.

2.3. Frequency Division Multiple Access Systems and Channel Capacity

The use of spread spectrum (code division) multiple access (CDMA) techniques has been proposed for use in multiaccess communications services to replace the existing cellular frequency division multiple access (FDMA) technique of assigning frequency slots to the given users [4, 7]. The simple analysis presented below shows that the total capacity of the spread spectrum multiple access channel must be less than or equal to the total capacity of the same bandwidth used with more traditional FDMA techniques, given the simple channel model. The model ignores multipath and fading, which might or might not treat CDMA even worse.

2.3.1. Channel Parameters

Assume that K users are operating on the channel asynchronously. The wideband channel to be used is a B Hz wide, additive white noise channel with power spectral density N_0. The capacity of this

[1] I thank fellow Caltech student Ivan Onyszchuk for pointing this out.

channel in bits per second for a single user at power S, by Shannon-Hartley Law, is:

$$C_c = B \log_2 (1 + \frac{S}{N_0 B}).$$

2.3.2. Frequency Division Multiplexing

Let the i *th* user, transmitting at signal power S_i, be allocated a fraction a_i of the bandwidth for his own private use. The total capacity achieved by this FDMA channel is:

$$C_{c\text{-}FDMA} = B \sum_{i=1}^{i=K} a_i \log_2 (1 + \frac{S_i}{a_i N_0 B}).$$

If we assume that all the users are on an equal footing, i.e., that all S_i are equal and $a_i = \frac{1}{K}$ for all i = 1,2,...K, the total capacity becomes:

$$C_{c\text{-}FDMA} = B \log_2 (1 + \frac{K S}{N_0 B}).$$

2.3.3. Comparison With Other Techniques

It is now clear that the total capacity given for the above FDMA channel is the total (single-user) capacity of the B Hz when KS Watts are transmitted. Therefore, no multiplexing technique could possibly exist that allows for a higher capacity, given the same total transmitted power from the K users. If such a technique did exist, a single user could act as K separate users and thus beat the (single-user) channel capacity for the B Hz channel. Hence, no such multiplexing technique exists.

It is important to mention here that while the potential to use the fully allocated channel capacity is a powerful tool of the FDMA access scheme, the information-bearing capacity of the available frequency spectrum for geographically distributed multiaccess systems can sometimes cloud more relevant measures of performance for these systems such as traffic carried over a fixed bandwidth in a given area. However, if the service area is divided into regions, as is done in cellular radio communications, and the interference from surrounding regions can be mitigated, as Carleial's result suggests may be possible, then the traffic-handling capacity is limited only by the efficiency with which the allocated bandwidth's capacity is used by the individual regions.

In order to achieve this ultimate limitation, however, the interference must first be mitigated. Techniques for actively mitigating interference in FM communications will now be explored.

Chapter III

Cross-Coupled Phase-Locked Loop Interference Cancellers

The CCPLL interference canceller (Figure 4) is an example of subtracting an estimate of interfering signals from the incoming corrupted signal to produce a clean output. The estimator-subtractor method (Figure 5) is quite general and can be applied to many different interference situations including FM multipath, co-channel FM interference, and AM-FM interference. Getting the best possible estimate of the interference environment is the most important and one of the most challenging aspects in developing one of these interference cancellers. Estimation approaches vary from those that utilize extensive *a priori* knowledge of the input to those that make as few restrictions as possible on the input signals.

3.1. Relation of CCPLL to MAP Receiver

The CCPLL interference canceller is based on the topology of a noncausal optimum (*Maximum a posteriori* (MAP)) FM receiver for suppression of interchannel interference with constant modulus (no AM component) [9]. Given an input signal mix:

$$v(t) = s_1(t) + s_2(t) + n(t),$$

where:

$$s_1(t) = A_1 \cos\left(\omega_1 t + x_1(t)\right)$$

$$s_2(t) = A_2 \cos\left(\omega_2 t + x_2(t)\right)$$

$n(t)$ is white Gaussian noise with zero mean and normalized two-sided power spectral density of 1 W/Hz.

$x_1(t)$ is the desired-signal angle modulation (here assumed a Gaussian process), for FM , $x_1(t) = \int^t m_1(u)du$, where $m_1(t)$ is the desired-signal frequency modulation information.

$x_2(t)$ is the interfering signal angle modulation (also assumed Gaussian).

A_1 and A_2 are the moduli of the two signals and are assumed constant.

Figure 4

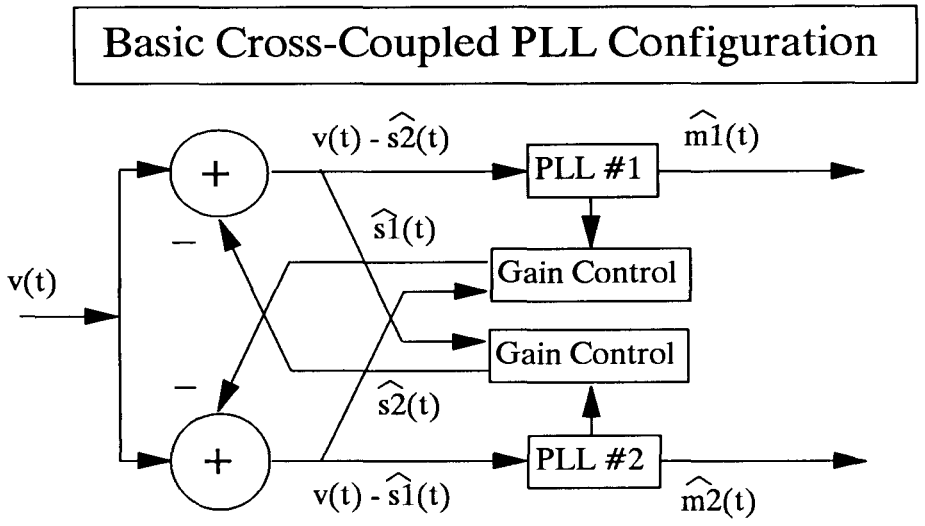

Figure 5

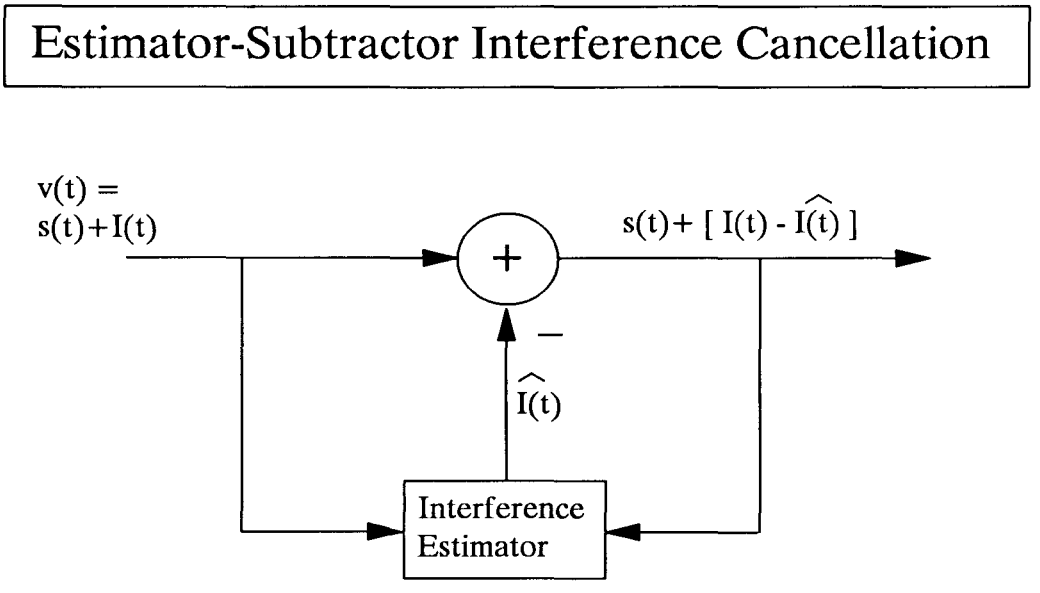

In [9] the MAP estimates of $x_1(t)$ and $x_2(t)$ are found to be:

$$\hat{x}_1 = k_1 \int_0^T R_{x_1} \frac{\partial \hat{s}_1}{\partial x_1} (v - \overline{s}_2)\, du$$

$$\hat{x}_2 = k_2 \int_0^T R_{x_2} \frac{\partial \hat{s}_2}{\partial x_2} (v - \overline{s}_1)\, du \ ,$$

where $k_{1,2}$ are constants, $R_{x_{1,2}}(t,u)$ are the impulse responses of lowpass filters, and $\overline{s}_{1,2}$ represent the minimum mean-square error (MMSE) estimates of $s_1(t)$ and $s_2(t)$. A correlator implementation of the optimum receiver for x_1 is depicted in Figure 6. Since for FM, $m_{1,2}(t) = \dot{x}_{1,2}(t)$, where $m_{1,2}(t)$ represents the desired information, the phase-controlled oscillator in Figure 6 can be replaced with a voltage-controlled oscillator (VCO). The result is a representation of the optimum receiver for $m_{1,2}(t)$ similar to a phase-locked loop (PLL). This optimum receiver topology inspires the use of the phase-locked loop structure as a causal approximation. However, note that even with noncausal correlation loops, the receiver is optimum only when the generated estimates are the MMSE estimates; i.e., $\hat{s}_{1,2}(t) = \overline{s}_{1,2}(t)$.

3.2. Basics of CCPLL Operation

The CCPLL system utilizes two important characteristics of the phase-locked loop (PLL) to produce its estimate:

1. A PLL is an unbiased estimator of phase.
2. PLL's, like other FM demodulators, exhibit FM capture effect and nonlinearly enhance the strongest signal when more than one signal is present.

The characteristics (loop bandwidths, gain control, etc.) of the CCPLL interference canceller can be fine-tuned to best accommodate different types of interferers; however, this requires *a priori* knowledge of both the input desired signal and the interfering signals. Modifications of the system to include amplitude-tracking loops inspired by Least Mean Squares (LMS) adaptive filters have been used [14, 16, 18] to produce a slightly more complex system that is fairly robust in the presence of co-channel AM-FM and pulsed RF (FM) interferers. The performance of CCPLL interference cancellers has been demonstrated against these types of interferers both in simulation [10-15,17,18] and by

Figure 6

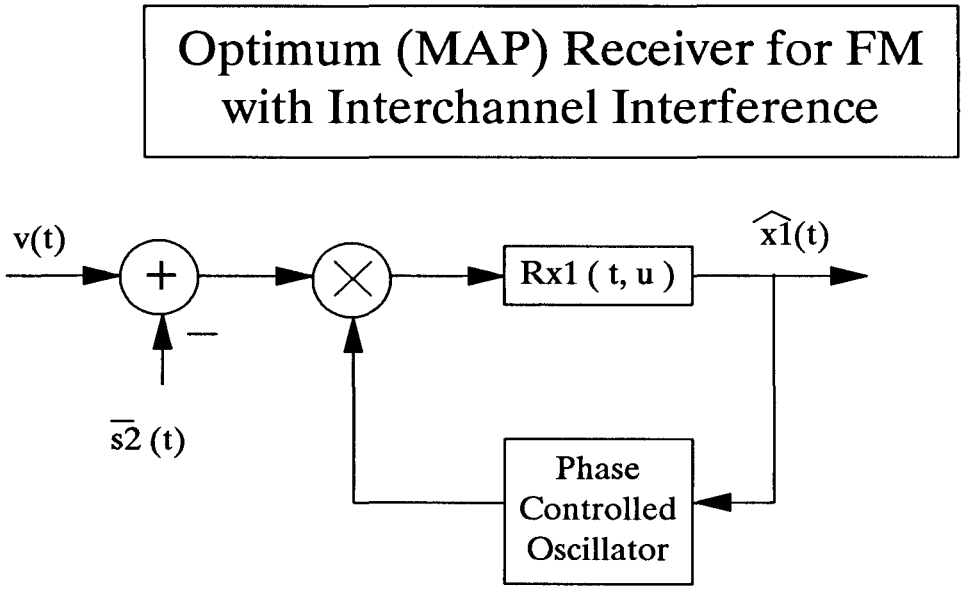
Optimum (MAP) Receiver for FM with Interchannel Interference
v(t)
+
−
$\overline{s2}$ (t)
Rx1 (t, u)
$\hat{x1}$(t)
Phase Controlled Oscillator

experiment [9-12,16,18], providing as much as 20 dB of interference suppression.

3.3. Relation of CCPLL to Adaptive Notch Filter

The addition of LMS-type amplitude-tracking loops to the CCPLL interference canceller [13,14,16,18] transforms the device from one based primarily on the FM capture effect into a more standard, adaptive noise-cancelling device similar to those used by Widrow [27]. In the adaptive noise cancelling topology, often called the "adaptive notch filter," a periodic reference is used in both inphase and quadrature (90 degree phase-shifted) forms to cancel correllated components in the input. The LMS algorithm is used to produce the inphase and quadrature multiplicative weights necessary to cancel the reference's component from the input. A block diagram of the adaptive notch filter is shown as Figure 7. This structure has been shown [28] to converge to a notch filter at the frequency of the reference for sinusoidal reference signals. The convergence analysis is dependent on considering the LMS algorithm and the reference input as a linear, time-invariant filter whose input is the residual signal (output of the "notch filter") and whose output is the amount to be subtracted from the signal input. The strict periodic nature of the sinusoidal reference input makes this analysis possible, and it is easy to see that the algorithm will perform adequately even if the input is not a pure sinusoid, so long as the phase and amplitude offsets between the reference and the input are slowly varying.

The realization of amplitude-control loops for the CCPLL interference canceller closely parallels the adaptive notch-filter approach. This is motivated by the convergence of the LMS solution to a minimum mean-square error estimate , and the MAP receiver topology's requirement that the subtracted interference estimate be an MMSE one. The implementation of the CCPLL interference canceller with amplitude control (the so-called Vector-locked Loops of [18]) are shown as Figure 8. From the figure, it is clear to see that each amplitude-control loop is separately a direct adaptation of the adaptive notch filter. The resulting implementation is a self-bootstrapping, continuous analog version of the discrete digital adaptive filter, with the reference inputs being provided by the VCO's in the capture effect PLL's. The system is called self-bootstrapping because it can acquire the interfering signals by itself because of the FM capture effect. Experimental trials with the CCPLL system [18] have

Figure 7

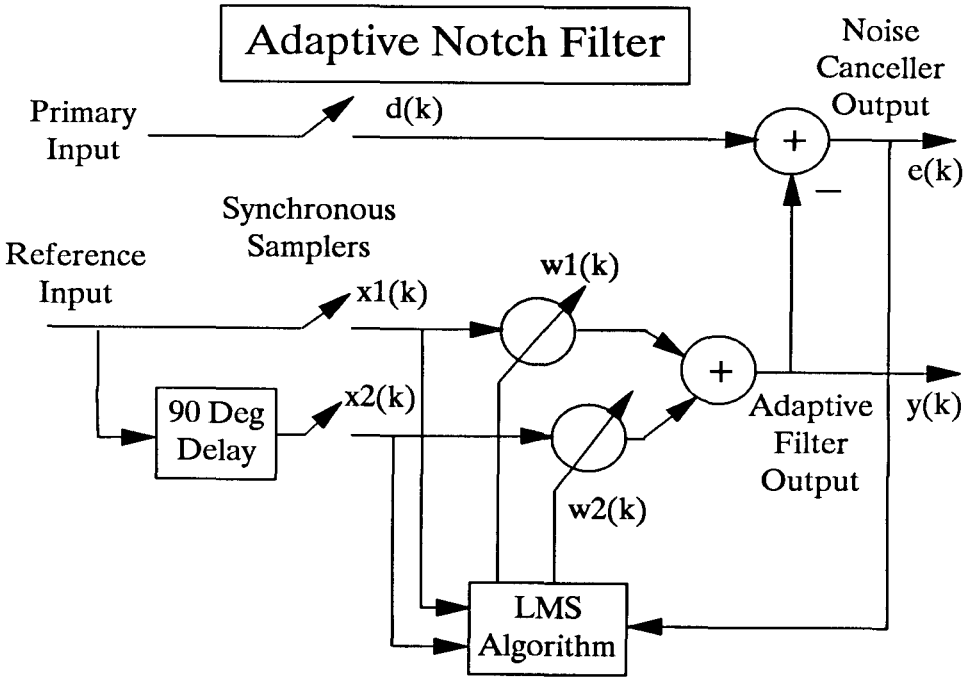

Figure 8

Cross-Coupled Phase-Locked Loop with Amplitude Control (from [18])

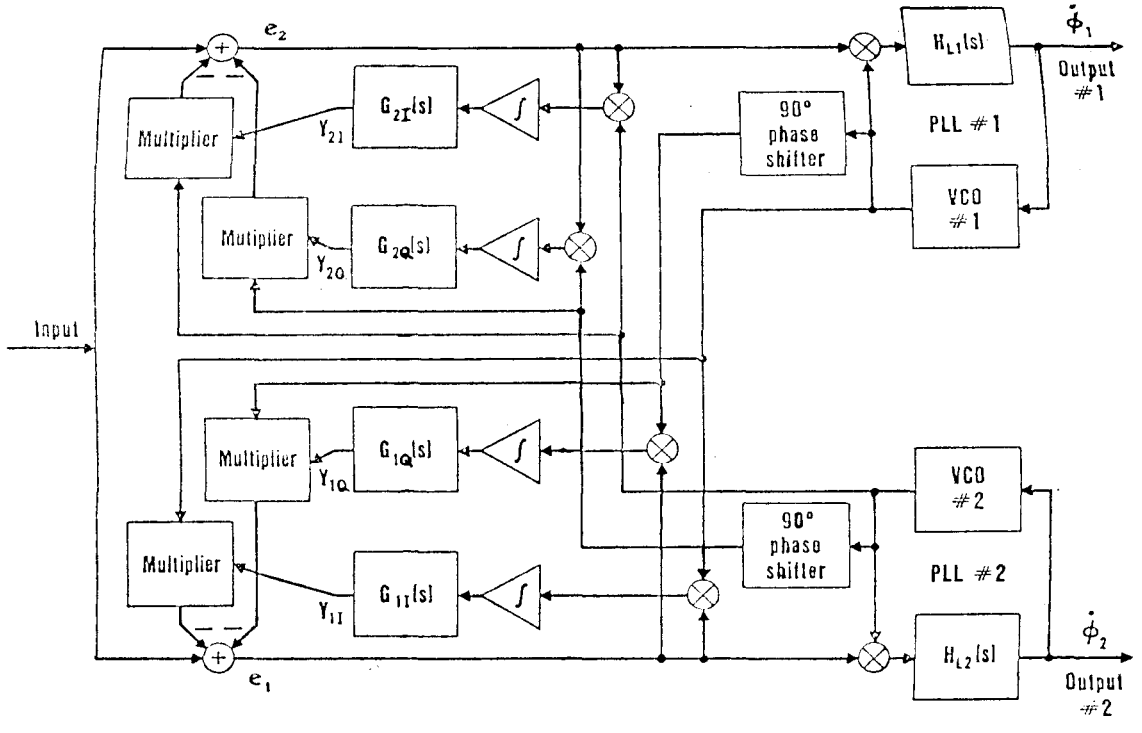

demonstrated that acquisition is a two-stage process, as might be expected. Software simulations [14, 18] have confirmed this finding. The first stage consists of a PLL capturing and locking to the strongest signal present. The second phase is marked by the convergence of the amplitude control weights. The two phases are then repeated by the second PLL, resulting in FM demodulation of both the weaker and the stronger signal.

3.3.1. Cross Leakage in the CCPLL

Because of error and delay in the frequency tracking of the PLL's, as well as imperfect capture, the inputs to the amplitude estimators often contain some leakage from the undesired signal. This cross leakage affects the convergence of the amplitude-control loops and results in further imperfections in cancellation. Because the CCPLL structure contains a reference for each signal present, it is tempting to think of recursively applying the adaptive noise canceller in an attempt to limit cross leakage. A successful second application of the adaptive noise canceller, cross-coupling the VCO references themselves, would serve to decrease components of the undesired signal in each reference, and therefore be potentially more robust. Such a scheme would have an additional feedback path within each PLL structure as shown in Figure 9. However, before considering this "leakage-control" topology further, we will investigate the effects of the leakage on the normal CCPLL canceller.

Following the analysis in [27], the effect of a residual, strong signal component in the VCO output of the weak signal tracking PLL (hence called PLL#2) on its amplitude-control loop (called loop #2) can be considered as leakage of signal into the reference input of an adaptive notch filter. This will cause some cancellation of the strong signal prior to the input of the strong signal tracking PLL (PLL #1). Let the strong signal be denoted s_1 and the weak signal s_2, and let the transfer function for the weak signal to the VCO of PLL #2 be $H_{2,2}(f)$. Consider the two signals to be uncorrelated and stationary. Similarly, let the transfer function for the s_1 into the VCO of PLL #2 be $H_{1,2}(f)$, and let the transfer functions for s_1 and s_2 into the VCO output of PLL #1 be $H_{1,1}(f)$ and $H_{2,1}(f)$, respectively. Neglecting intermodulation terms the power spectral density of the input to the amplitude-control loop #2, the VCO output of PLL #2, denoted x_2, is approximately:

Figure 9

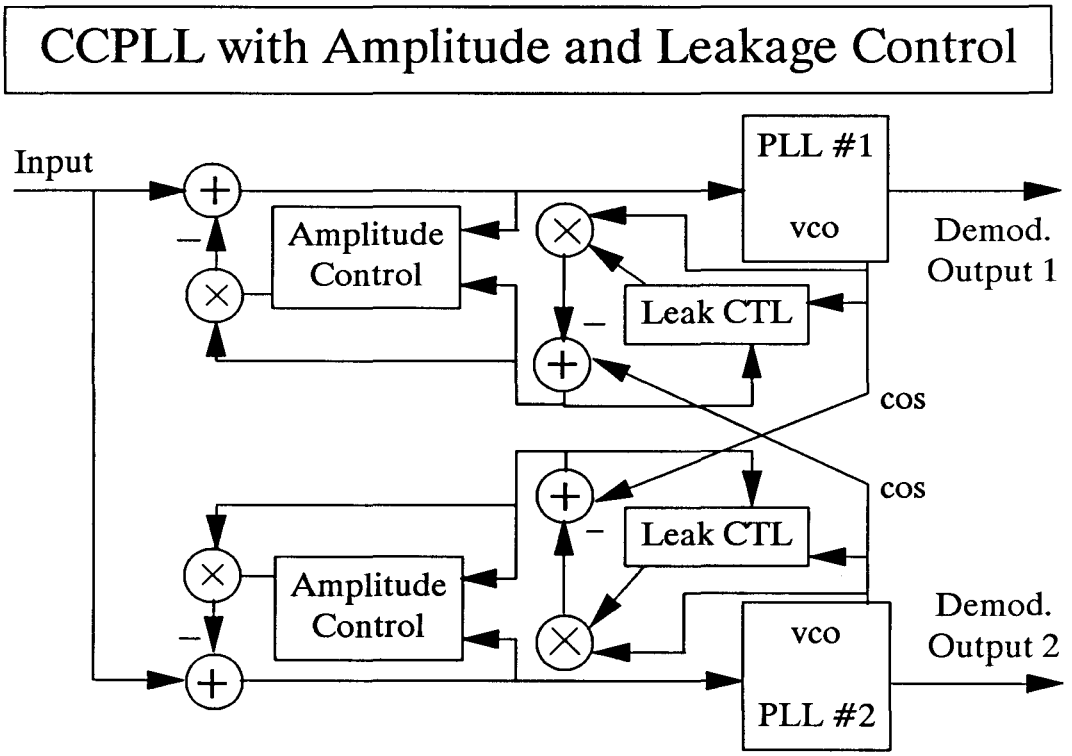
CCPLL with Amplitude and Leakage Control
Input
PLL #1
vco
Demod.
Output 1
Amplitude
Control
Leak CTL
cos
cos
Leak CTL
Amplitude
Control
Demod.
Output 2
vco
PLL #2

$$S_{x_2x_2}(f) = S_{s_2s_2}(f)\,|\,H_{2,2}(f)\,|^2 + S_{s_1s_1}(f)\,|\,H_{1,2}(f)\,|^2.$$

The cross spectrum between the input to the system, (s_1+s_2), and the VCO output of PLL #2, x_2, is:

$$S_{x_2(s_1+s_2)}(f) = S_{s_2s_2}(f)H^*_{2,2}(f) + S_{s_1s_1}(f)H^*_{1,2}(f)$$

where * denotes complex conjugation. Because of the feedback in the CCPLL structure, a causal solution must be achieved as opposed to the noncausal analysis given in [27].

However, examination of the noncausal case will demonstrate the same behavior seen for the real causal system. It is interesting to note that the noncausal analysis leads to an exact expression for the ratio of strong signal power to weak signal power at the inputs of the PLL's (under stationary signal conditions) in an uncoupled system. The signal power ratio follows a power inversion law as described by Widrow in [27]. For the uncoupled system, the unconstrained Wiener solution for the power ratio at the input of PLL #1 is

$$SIR_{in_1}\left(\frac{s_1}{s_2}\right) = \frac{1}{SIR_{out_2}\left(\frac{s_1}{s_2}\right)}$$

and, at the input to PLL #2,

$$SIR_{in_2}\left(\frac{s_2}{s_1}\right) = \frac{1}{SIR_{out_1}\left(\frac{s_2}{s_1}\right)}.$$

Heuristically, these expressions indicate that a canceller with desired signal leaking into its reference of the interference can do no better than to give an output signal-to-interference ratio equal to the reciprocal of the signal-to-interference ratio in the reference. Hence, strong desired-signal leakage into the interference reference will significantly limit the achievable cancellation.

By examining these two equations, we can perhaps gain some insight into how two identically designed PLL's would behave during acquisition. If both PLL's were to initially capture the same signal, say s_1 , each would decrease the other's $SIR_{in}(\frac{s_1}{s_2})$ according to the power-inversion relations above. Both amplitude loops would be headed for convergence at a point, making s_2 the stronger signal. FM capture effect provides gain preferentially to the stronger signal at the input of the PLL. One PLL input, say PLL #2, must cross the capture threshold for s_2 first, making its $SIR_{out}(\frac{s_1}{s_2})$ less than

one. This would reverse the direction of convergence for the amplitude-control loop #2, which uses that PLL's output as a reference. Thus $SIR_{in}(\frac{s_1}{s_2})$ for the PLL #1 increases, reinforcing its capture of s_1. The FM capture effect further reinforces $SIR_{out}(\frac{s_1}{s_2})$, and provides the feedback necessary to complete the self-bootstrapping process.

The actual causal system acquires the signal in much the same way, according to approximate solutions to the defining, coupled differential equations and signal-acquisition experiments given in [13], [14] and [18].

3.3.2. Summary of Experiments with the Leakage-Control Topology

The proposed topology adds "leakage-control loops" to the VCO outputs of the two PLL's. These adaptive noise-cancelling loops attempt to better orthogonalize the two VCO references, increasing capture in the interference-cancelling reference. The use of a second pair of adaptive noise-cancelling loops would cause the SIR at the input of the PLL's to converge to the inverse square of the SIR produced by the PLL's, rather than just to the inverse of the SIR at the PLL output. The resulting system should have decreased acquisition time, and I have performed simulations demonstrating this result (Figure 10). The simulated loops, however, did not hold lock onto the signals, indicating that the resulting system dynamics are sufficiently complicated that for signals in which the amplitude varies, the tracking does not always hold true. The simulated system showed much less stable outputs in the presence of such signals than the original CCPLL implementation, in that the track of the weak-signal PLL would occasionally switch and capture the strong signal.

Re-examination of the leakage-control topology (Figure 9) quite readily explains this phenomenon. The addition of the leakage-control loops creates a stable, steady-state solution where both PLL's are tracking the stronger signal. This new stable state is equivalent to an uncoupled system. While forcing the VCO outputs to be uncorrelated with respect to each other, the leakage-control loops produce the degenerate solution where both VCO outputs are uncorrelated to either signal. This in turn causes little or no cancellation of the strong signal at the input to either VCO, and strong-signal

Figure 10

Performance of CCPLL with Leakage-Control Loops (see Figures 21 and 23 for comparison)

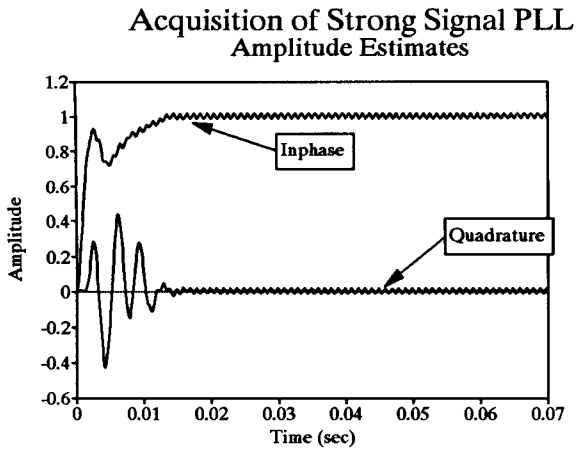

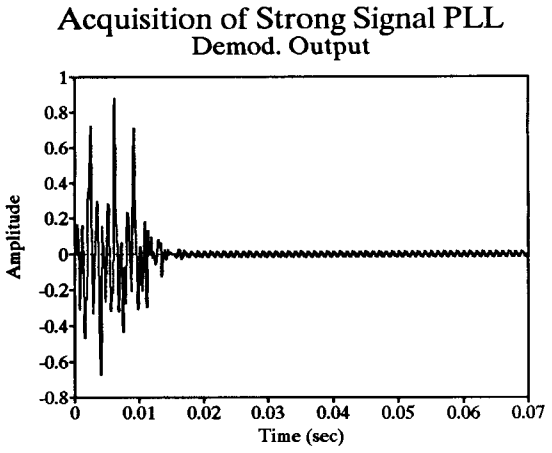

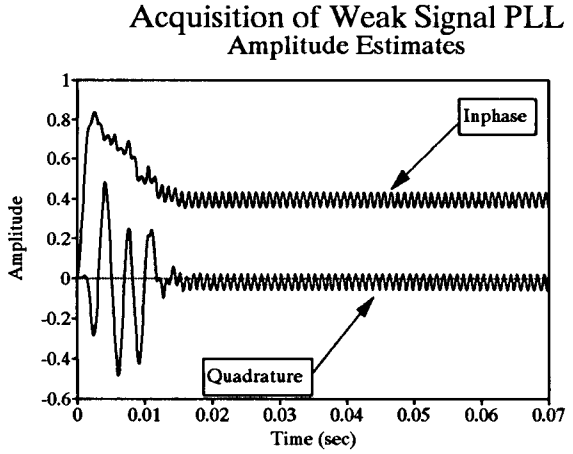

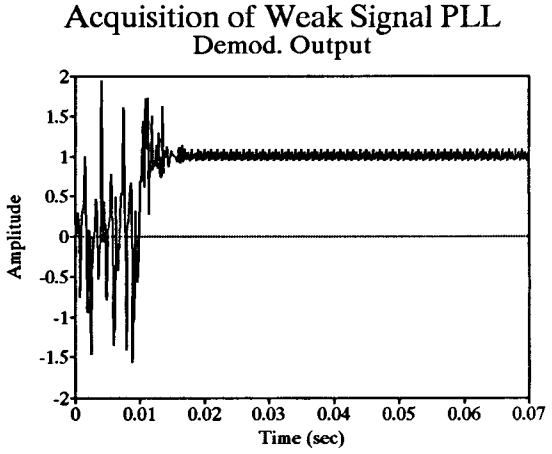

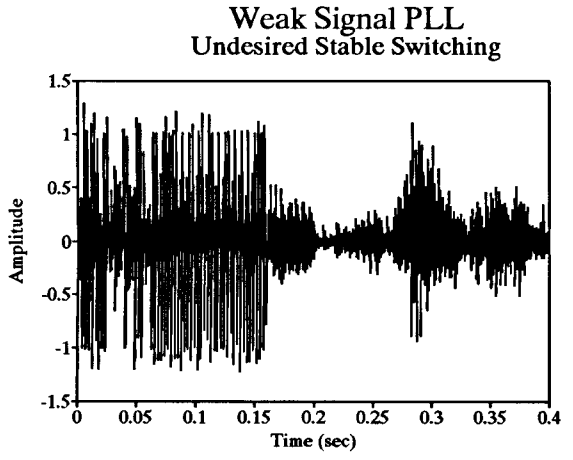

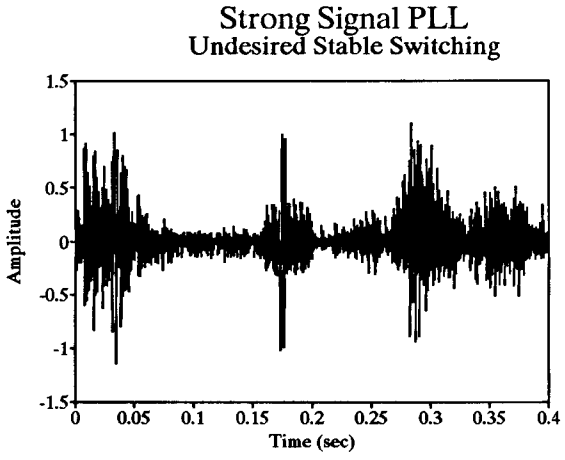

capture occurs in both PLL's, reinforcing the stable state. This example of an interference-cancelling topology is important in that it demonstrates how by strengthening a desired stable state of the system, i.e., the capture of both input signals, an additional, undesired stable state may be created, much as in neural networks [29]. As a result, the addition of leakage-control loops to the canceller was discarded, and the focus of improvements was shifted to systems with less complicated dynamics than the original CCPLL. Dynamically simpler systems are discussed later in this chapter, but first the investigation of the basic interference-cancelling receiver will be concluded with discussions of more than two signals and the capture effect in PLL's.

3.3.3. Extension of the CCPLL to More than Two Signals

If a CCPLL-based interference-cancelling receiver is to be extended to more than two signals, simply tracking the amplitude of each received signal is not sufficient. This is because a minimum mean-square error estimate for the sum total interference is desired, and the MMSE estimate of a sum is not necessarily the sum of the individual MMSE estimates. As a result, interference amplitude-tracking loops are associated with each desired signal rather than with each interfering signal. A block diagram of one desired-signal receiver component is shown in Figure 11a. The amplitudes of the interfering signal components to be subtracted from the input are estimated jointly for each desired signal in a method paralleling the multireference adaptive interference-cancellation techniques described in [27]. An example of the interference amplitude-tracking loops for the three-signal case is shown in Figure 11b. If the VCO-produced references of the summed interferers are uncorrelated with each other, the estimation of the amplitudes of the summed interference will be the same as separately estimating the amplitudes of the component signals.

3.4. Capture Effect in Phase-Locked Loops

In considering the capture effect in practical phase-locked loop receivers, it is important to first consider the effect of bandpass limiting of the input signal that ordinarily precedes the PLL. The primary purpose of the bandpass-limiting operation is to normalize the input signal amplitude so that the loop performance is independent of this parameter. The bandpass-limiting operation removes

Figure 11

Interference-Cancelling Topology for > 2 Signals

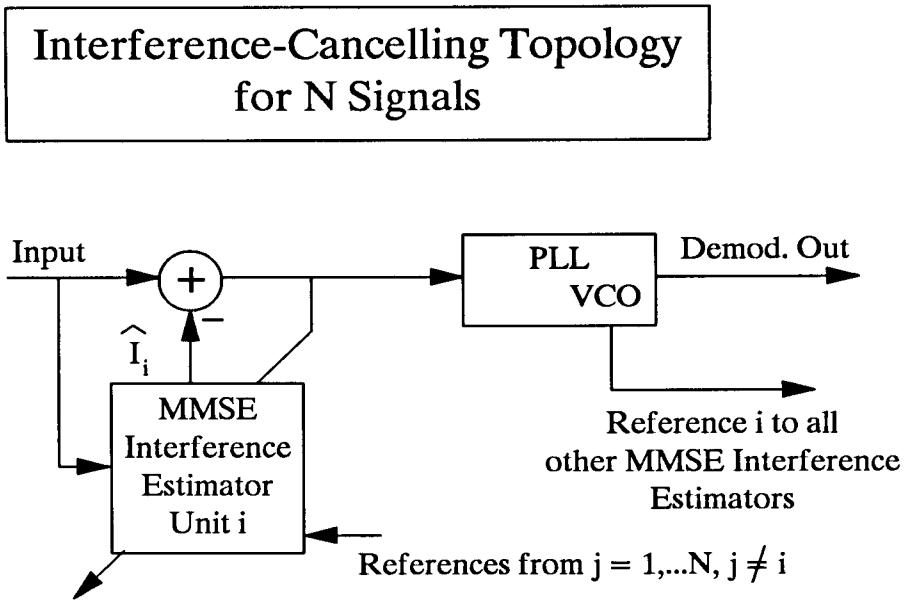

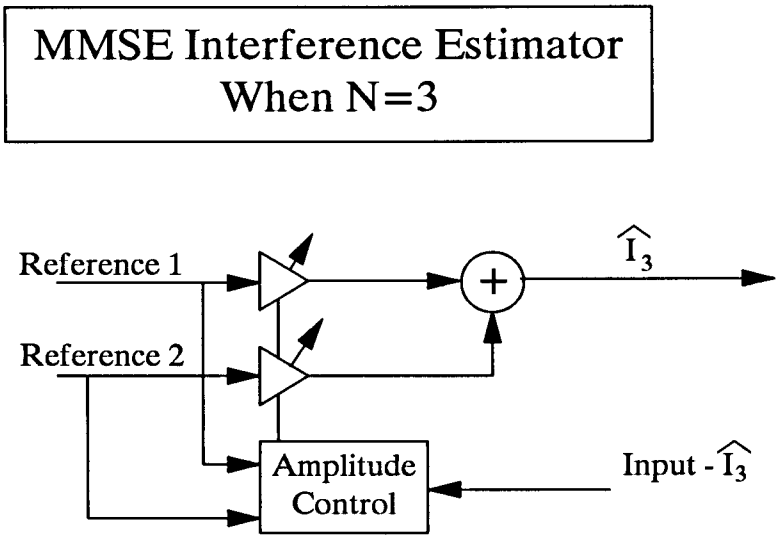

amplitude information from the incoming signal, and is generally assumed to correspond to the complex operation:

$$Output = Bandpass\left[e^{j\,\mathrm{Im}(\ln(Input))}\right].$$

Here Im(ln(*Input*)) denotes the imaginary part of the (natural) logarithm of the input signal, i.e., the phase of the complex input signal, and the pass bandwidth is assumed significantly smaller than the band center frequency. The action of the bandpass limiter on a single amplitude-modulated sinusoidal input is clearly to reproduce the carrier of the AM signal at a fixed amplitude. When dealing with FM inputs whose amplitudes are uncertain, the main virtue of this bandpass limiter is that given a wide enough passband, the phase function of the input is preserved almost exactly. The reproduction is inexact only in those frequency components outside the passband.

Evaluation of the bandpass-limiter output in the presence of multiple summed inputs, either interfering signals or noise, is difficult at best. Since the phase of the input signal (*Input* above) is a nonlinear function with memory, linear methods of evaluation of this function are not suitable. Expansions and analytical evaluations of the spectrum of the limiter output for certain interference and noise cases can, however, be found in many places in the extensive literature on FM interference, examples of which are in References 30 and 31. The analytical expansions are generally unenlightening, unfortunately. Additionally, they serve to confuse the nature of the output process by masking the fact that any small additive change in the input mix generally invalidates the analysis of the output processes by generating entirely new sets of intermodulation products.

In the detection of FM signals, the desired quantity is the derivative of the signal's phase function. Since the bandpass limiter leaves the phase of the resultant phasor sum of input signal components intact, it is sufficient to look at the derivative of the phase of the resultant input phasor prior to filtering. For the case of two interfering signals with constant but differing instantaneous frequencies (phase derivatives), the unfiltered derivative of the resultant phase function has asymmetrical peaks [30, 31]. In a simple sense these peaks can be viewed as the result of considering the angular velocity of a rotating phasor with a constant (tip) linear velocity but a time-varying magnitude. The rotating resultant phasor angular velocity will increase as the magnitude decreases, causing peaks in the phase

derivative. If the rotating phasor is actually the sum of two distinct rotating phasors, the overall average rotation will be that of the phasor with the larger magnitude, which gives the peaks their asymmetry. The peaks in the instantaneous frequency point towards the instantaneous frequency of the stronger signal and away from the instantaneous frequency of the weaker signal, as shown in Figure 12. The resultant time-average instantaneous frequency has been shown to be that of the stronger signal [30, 31]. In this way, capture was shown [30, 31] to result directly from the process of extracting the phase information of the input signal while discarding the amplitude information. For more practical FM interference situations, the instantaneous frequency of the input signals is not constant, and the instantaneous frequency can not be fully time-averaged. This results in a suppressed, but still present, distortion component that is due to the interference.

The bandpass limiter used in practice is often only an approximation to the ideal complex limiting operation. These limiters consist mainly of a zero-crossing detector, often just a high-speed digital logic buffer, followed by a bandpass filter (Figure 13). The actual function evaluated is:

$$Output = Bandpass\left[sgn\left(Input\right)\right]$$

where $sgn(x)$ is $+1$ for $x>0$, -1 for $x<0$ and 0 for $x=0$. As before, the pass bandwidth is significantly smaller than the passband center frequency. It is clear that the ideal (complex phase) and the practical (zero-crossing) operations are equivalent up to a gain constant when presented with a single sinusoidal input. The more complicated inputs present in FM interference situations do not, however, have such easily recognizable outputs. Computer simulations (see Figure 14) of the ideal and practical systems quickly verify that in general and also specifically for multiple summed FM sinusoidal inputs, the two nonlinear processes are not exactly equivalent, but are in many senses close in their capture properties. As might be expected, the two operations possess the same general quality of stripping the input signal of its amplitude information. Analytical computation of the time-domain output of bandpass limiters with summed signal and noise inputs is presented in [25], with the results showing strong signal improvement and weak signal suppression similar to that for the simplified, complex-limiting approximation. As a result, except when use of the direct implemented form of the bandpass limiter is explicitly required by the circuit topology, the complex limiting operation will be used in its place.

Figure 12

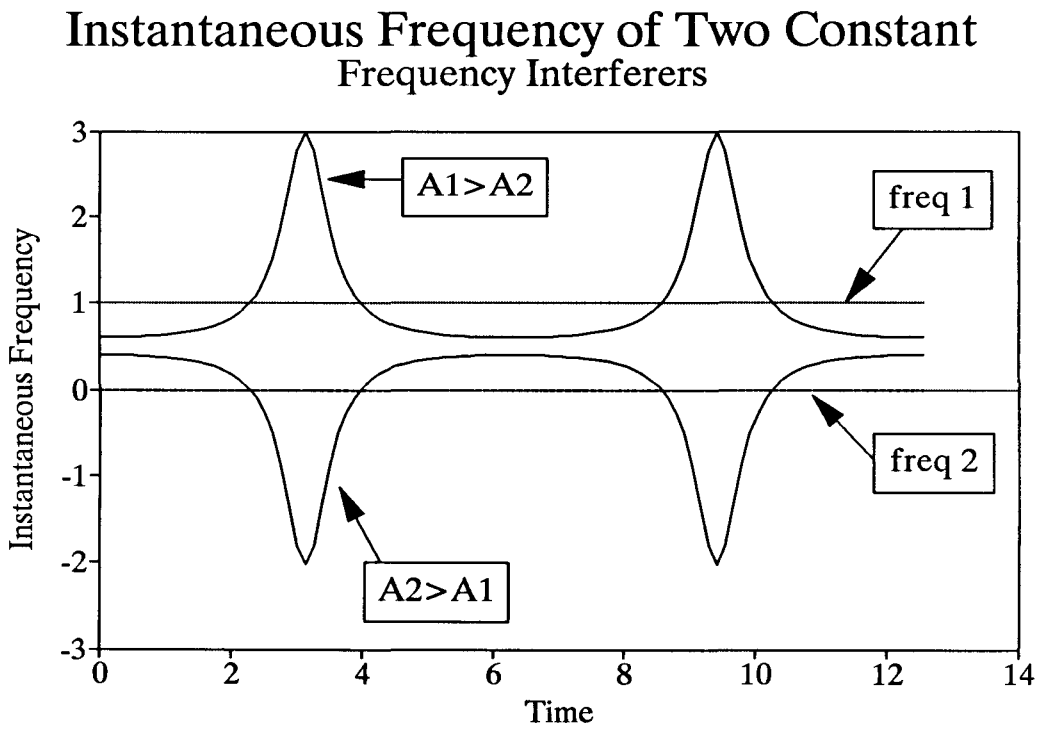
Instantaneous Frequency of Two Constant
Frequency Interferers
Instantaneous Frequency
Time
A1>A2
A2>A1
freq 1
freq 2
3
2
1
0
-1
-2
-3
0
2
4
6
8
10
12
14

Figure 13

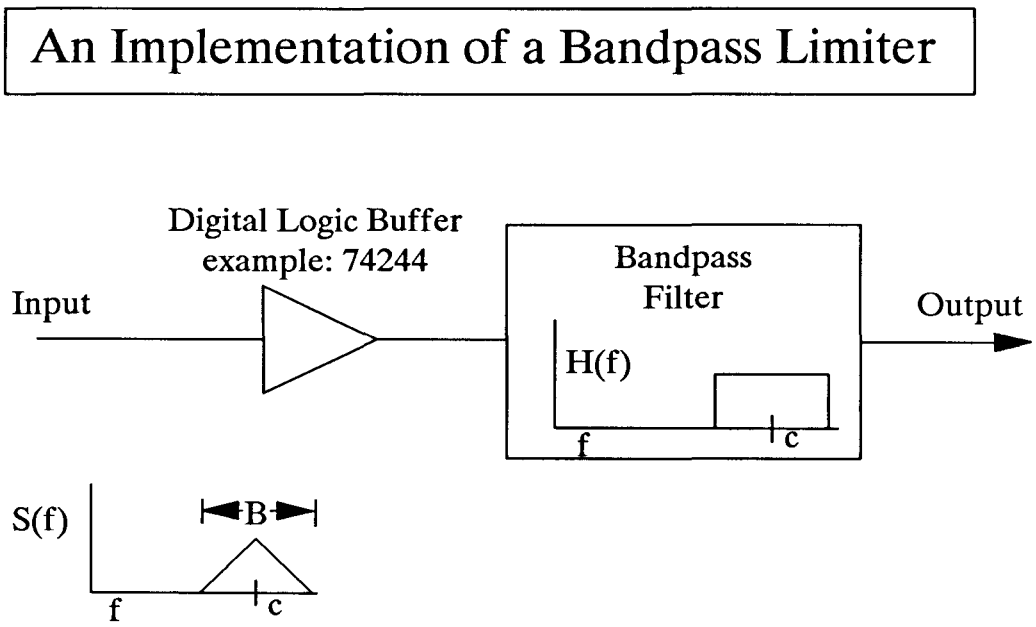
An Implementation of a Bandpass Limiter
Digital Logic Buffer
example: 74244
Input
Bandpass
Filter
Output
H(f)
f
c
S(f)
B
f
c

Figure 14

Response of Ideal and Practical Bandpass Limiters to Summed Sinusoidal Inputs

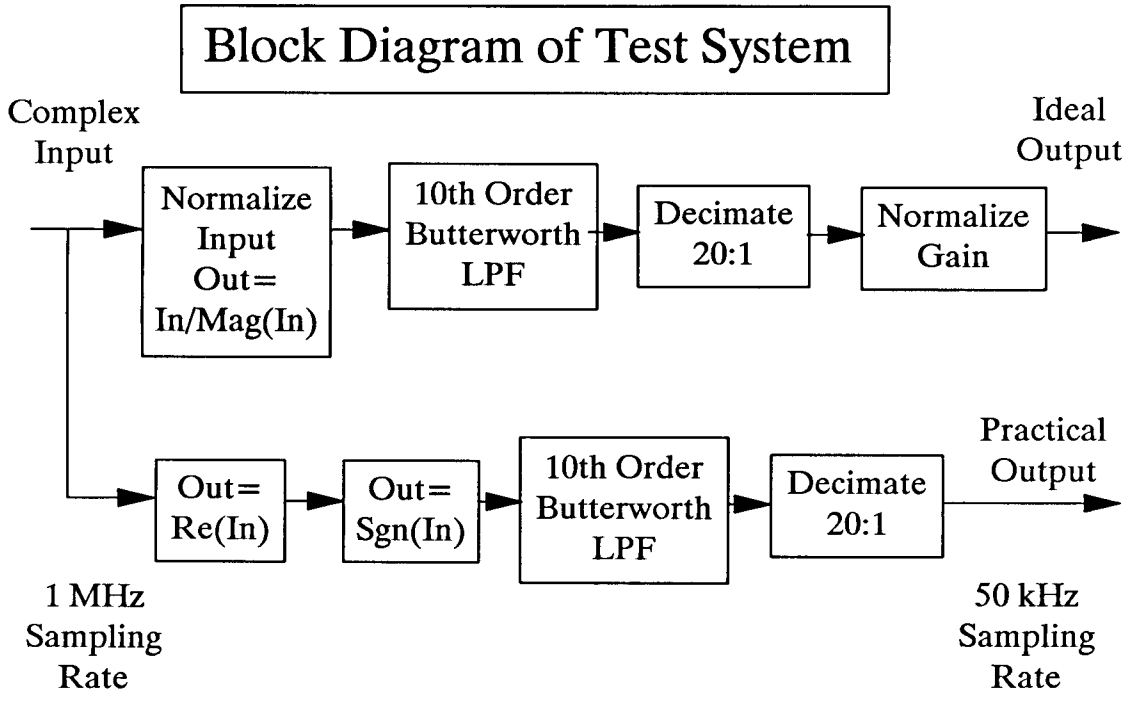

Figure 14 (continued)

Response of Ideal and Practical Bandpass Limiters to Summed Sinusoidal Inputs

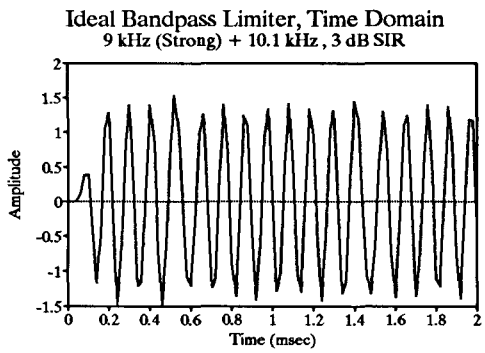

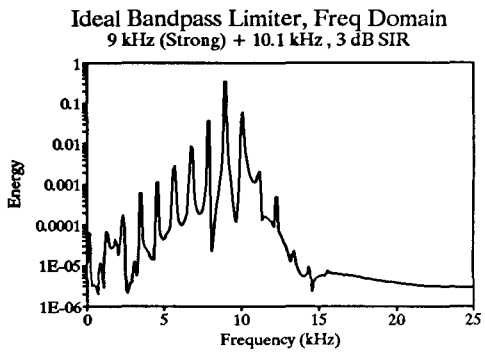

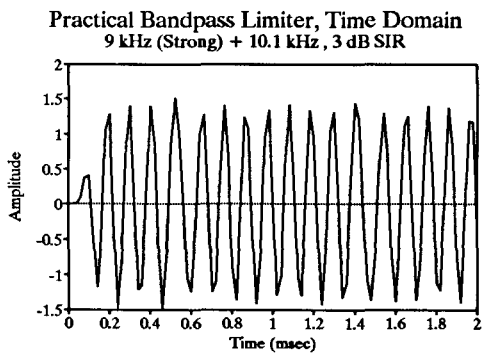

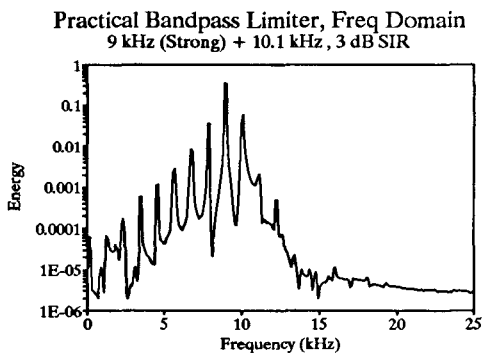

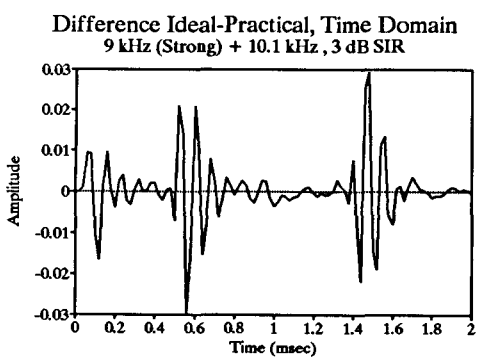

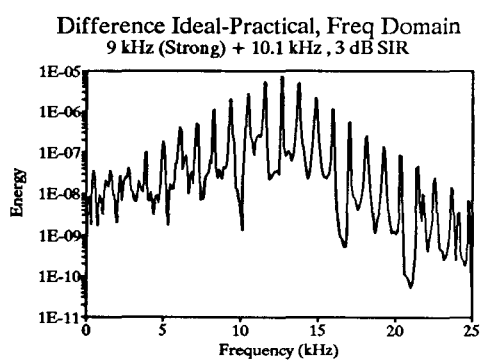

In considering the phased-locked loop (PLL) FM demodulator circuit topology, the following should first be noted. The PLL implemented in the common fashion, with a lowpass analog multiplier as the phase detector, is not, in general, an FM discriminator circuit by itself. Given the general input:

$$x(t) = A(t)\cos(\phi(t)),$$

the PLL will in general produce amplitude modulation to phase modulation (PM) conversion, resulting in an output different from $\frac{d\phi(t)}{dt}$. The trivial case where $A(t)$ is a constant, the one considered by all the texts on the subject, indeed results in the PLL's being an FM discriminator. However, because of the AM to PM conversion, this is not so in general. If the input to the PLL is of constant amplitude, then the PLL does operate as an FM discriminator, though. As a result, virtually all PLL-based FM demodulators built are built with a bandpass limiter preceding the actual PLL. If an amplitude-insensitive phase detector is used, the resulting system is equivalent to a bandpass limiter followed by a PLL. As in conventional limiter-discriminator receivers, the bandpass limiter produces the actual capture effect by performing what amounts to phase detection and remodulation of the incoming signal. The purpose of the following PLL discriminator is to estimate $\frac{d\phi(t)}{dt}$ from the input signal and to filter it to the loop's bandwidth.

For second-order loops, this bandwidth can be smaller than the incoming signal bandwidth since the loop must only follow the modulation. (For first-order loops, the 3-dB loop bandwidth should be about the same as the input signal bandwidth, since for first-order loops the 3-dB bandwidth is the same as the loop's lock range [1].) As a result of the decreased bandwidth, the PLL can operate on a smaller noise or interference bandwidth than a conventional discriminator (see [30] and [25]). For a given modulation index, the loop's capture-effect increase will be fixed. Any increase in capture would have to come from either a reduction in the loop's bandwidth by increasing its order, or by increasing the capture effect of the receiver's limiter configuration. The prior of these two alternatives makes lock acquisition difficult, and is unattractive for that reason. However, different limiter configurations have been explored in the past [30] with results of improved capture of the strongest input signal. The analysis presented in [30], shows that the signal-processing gain achieved by these devices comes mainly

from the improved filtering of the input signal, and the feedback-limiter devices generated, shown in Figure 15, operate similarly to a PLL in that they are sensitive to noise in a bandwidth centered around current instantaneous frequency [30]. The interference rejection properties of these feedback-limiter techniques are therefore based on the same principles as the PLL, and in some sense, preceding a PLL with such a device would be equivalent to using the VCO output of an initial PLL to feed a second PLL. Therefore, only the conventional bandpass limiter technique will be explored.

3.5. Effect of Phase and Amplitude Tracking Errors on CCPLL

The performance of any estimator-subtractor, interference-cancelling topology is relative to the required estimation accuracy. A preliminary analysis of this is followed by Roberts in [32], the approach of which is followed here with extensions based on the preceding analysis. Consider one signal component input to the CCPLL demodulator as:

$$s_1(t) = A_1(t)\cos(\omega_1 t + \theta(t)),$$

and let the estimate $\hat{s_1}(t)$ of $s_1(t)$ be:

$$\hat{s_1}(t) = r(t)A_1(t)\cos(\omega_1 t + \theta(t) + \varepsilon(t)).$$

The square of the envelope of the cancellation residual that is due to s_1 is:

$$R^2(t) = A_1^2(t)[1 + r^2(t) - 2r(t)\cos\varepsilon(t)].$$

When the phase error, $\varepsilon(t)$, is negligible, the uncancelled power is given simply by $A_1(1-r)^2$. As would be expected, this is the square of the error in the amplitude estimate.

Considering the estimation of the amplitude of the signal as a coherent AM reception problem, the mean-square error $E[A_1(1-r^2)]$ can be computed if we can find the appropriate model for the noise plus interference. The effective signal-to-noise ratio for AM demodulation is upper-bounded by the input SNR, considering true noise power only, $\frac{E[A_1^2(t)]}{E[N^2(t)]}$, where $N(t)$ is the true noise. The effective signal-to-noise ratio is lower-bounded by the ratio of the signal power to the noise plus interference, $\frac{E[A_1^2(t)]}{E[N^2(t)]+E[A_2^2(t)]}$, where $A_2(t)$ is the interfering signal, since in the worst case the entire interfering signal acts as noise.

Figure 15

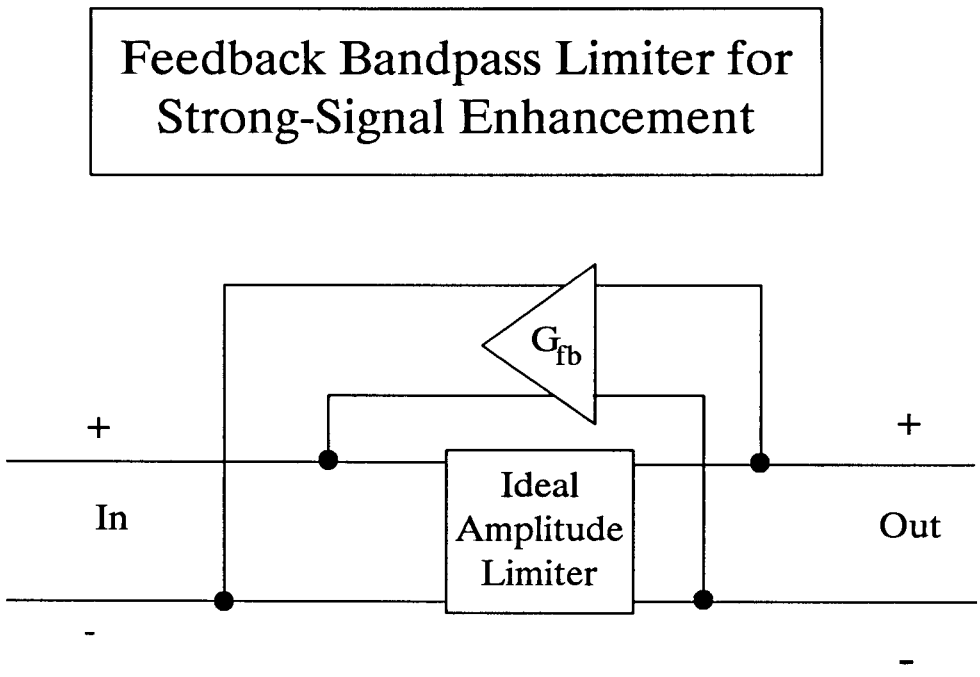
Feedback Bandpass Limiter for Strong-Signal Enhancement
G_{fb}
+
In
-
Ideal Amplitude Limiter
+
Out
-

In practice, the amplitude is of considerably smaller bandwidth than that of the entire FM signal. Let the bandwidth of the amplitude be W_A , and let the bandwidth of the FM signal be W. As an approximation to the mean effective noise for the amplitude estimation, take the sum of the true noise power in W_A and the fraction of the interferer power that would be in W_A if the interference power were uniformly distributed in its bandwidth:

$$N_{eff} \approx N_0 W_A + A_2^2 \frac{W_A}{W} .$$

The mean-square error of the amplitude estimate is A_1^2—SNR_D, where SNR_D is the coherently detected signal-to-noise ratio. As in Chapter II (2.1.5) the mean-square error is equal to the noise power in the bandwidth W_A . Therefore, with negligible phase error, the mean square of the amplitude estimate is:

$$E[R^2] \approx N_{eff} = W_A (N_0 + \frac{A_2^2}{W}) .$$

Since this error acts as noise to the reception of the second signal, the effective noise power for the second signal is increased by the above value when the estimate's phase error is small, giving the following an approximate signal-to-noise ratio at the input to the second receiver:

$$SNR_{2IN} \approx \frac{A_2^2}{(W + W_A)N_0 + \frac{W_A A_2^2}{W}} .$$

The effect of having both an inphase and a quadrature amplitude-tracking loop is that small, slowly varying phase offsets can be corrected with a smaller noise bandwidth than that required for tracking the signal's FM information. As can be seen above, amplitude-tracking loops operate on an equivalent noise bandwidth equal to that of the amplitude function. However, the addition of quadrature amplitude-tracking doubles the noise bandwidth of the amplitude estimate since the amplitude estimate is now essentially noncoherently derived. Therefore, with phase errors the noise power at the second receiver is increased by twice the value given for the negligible phase-error case, giving the SNR as:

$$SNR_{2IN} \approx \frac{A_2^2}{(W + 2W_A)N_0 + 2\frac{W_A A_2^2}{W}} .$$

3.6. Closely Related Interference-Cancelling Techniques

There is nothing magical about the implementation of the CCPLL interference canceller. In fact, by examining the basic analysis that led to the CCPLL system, new and simpler interference cancellers can be conceived. The resulting new interference cancellers presented here have simpler hardware implementations, and thus less complicated dynamics. One simplification is achieved through realization that tracking both inphase and quadrature amplitudes is equivalent to tracking the (slowly varying) phase of the signal. The implementation of a phase-locked loop operating with small phase error together with both inphase and quadrature amplitude-tracking loops is redundant. The simplification is based on a gradient-descent solution to the optimal MMSE amplitude-estimator equations for the special case of a negligible phase error in the reference, and it eliminates the quadrature amplitude-tracking loop.

Another, more important, simplification is based on a direct solution of the defining equations for the optimal amplitude equations. The direct solution to the optimal MMSE amplitude equations motivates a system with feedforward rather than feedback amplitude estimation. This system is defined by two coupled, nonlinear differential equations as opposed to the six defining equations of the CCPLL found in [18]. The resulting system has simpler dynamics that will be analytically shown below to restore perturbations in the tracked phase. The system is shown to have an unstable equilibrium when both PLL's capture the same signal component, providing some insight into the dynamics of signal acquisition. This simplified system is simulated, to further characterize its dynamics.

3.6.1. More Efficient Implementations of the CCPLL System

A re-examination of the optimal MMSE amplitude weights allows both direct implementation of the optimal estimator and a reduction in the hardware required for the implementation of the interference canceller. While the MMSE two-reference, two-weight estimator was examined in [18], important characteristics of the references were overlooked, resulting in an inefficient amplitude-estimator implementation. A new amplitude-estimation subsystem is developed here. Verification of its operation can actually be obtained from the results presented in [13] and [18].

3.6.1.1. Derivation of the Optimal MMSE Amplitude Estimate for the CCPLL System.

To begin, let the system be as depicted in Figure 16, with signal input to the system:

$$v(t) = s(t) + n(t),$$

where $n(t)$ represents both interfering signals and noise, all uncorrelated with the signal to be estimated, $s(t)$. Let the signal be modeled as:

$$s(t) = A(t)\cos(\theta(t)),$$

and let the reference inputs $x_1(t)$ and $x_2(t)$ from the VCO of the phase-locked loop that tracks $s(t)$ be:

$$x_1(t) = \cos(\theta(t) + \varepsilon(t))$$
$$x_2(t) = \sin(\theta(t) + \varepsilon(t)),$$

where $\varepsilon(t)$ is the phase-tracking error. The desired two-reference, two-weight estimator is given by:

$$\hat{s}(t) = w_1(t)x_1(t) + w_2(t)x_2(t)$$

with error: $e(t) = v(t) - \hat{s}(t)$. For the sake of clarity all the time variations will be dropped from the notation.

Using a vector form, where the reference is $\vec{x} = \begin{pmatrix} x_1 \\ x_2 \end{pmatrix}$, and the weight is $\vec{w} = \begin{pmatrix} w_1 \\ w_2 \end{pmatrix}$, the mean-square error is:

$$E[e^2] = E[v^2] - 2\vec{w}^T E[v\vec{x}] + \vec{w}^T E[\vec{x}\vec{x}^T]\vec{w}.$$

Let $\mathbf{R} = E[\vec{x}\vec{x}^T]$ and $\vec{r} = E[v\vec{x}]$, and complete the square of the terms dependent on $\vec{w}$:

$$E[e^2] = E[v^2] + \left((\vec{w} - \mathbf{R}^{-1}\vec{r})^T \mathbf{R} (\vec{w} - \mathbf{R}^{-1}\vec{r}) - \vec{r}^T \mathbf{R}^{-1}\vec{r}\right),$$

clearly giving at once the optimal two-reference, two-weight solution: $\vec{w}_{opt} = \mathbf{R}^{-1}\vec{r}$.

At this point it is common among those using adaptive techniques to throw up their hands and argue that estimating $\mathbf{R}$ and computing $\mathbf{R}^{-1}$ are both a lot of work [18, 28]. Yet in this case x_1 and x_2 are the cosine and sine of the same angle. As a result:

$$\mathbf{R} = 1/2\mathbf{I}, \rightarrow \mathbf{R}^{-1} = 2\mathbf{I},$$

where $\mathbf{I}$ is the two-by-two identity matrix. This allows the optimal weights to be computed directly:

$$\vec{w}_{opt} = 2\vec{r} = 2E\begin{pmatrix} v\,x_1 \\ v\,x_2 \end{pmatrix} = 2\left(E\begin{pmatrix} s\,x_1 \\ s\,x_2 \end{pmatrix} + E\begin{pmatrix} n\,x_1 \\ n\,x_2 \end{pmatrix}\right).$$

Figure 16

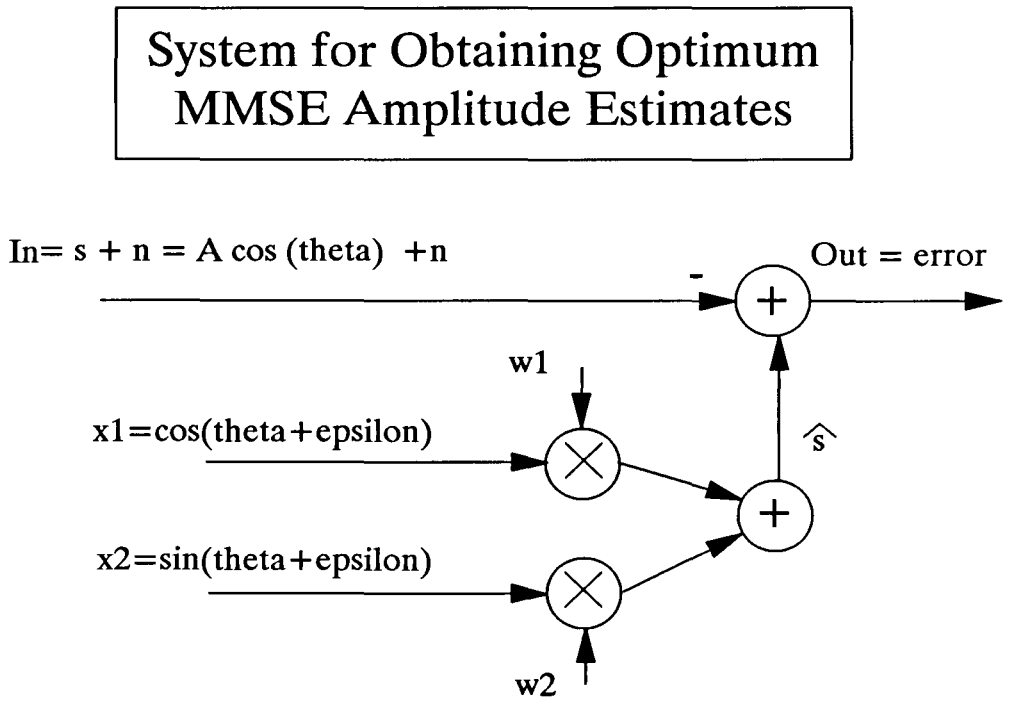
System for Obtaining Optimum MMSE Amplitude Estimates
In= s + n = A cos (theta) +n
Out = error
-
+
w1
x1=cos(theta+epsilon)
ŝ
+
x2=sin(theta+epsilon)
w2

Assuming that the correlation of $\vec{x}$ and the noise + interference term is negligible, as would be the case in a strong-signal capture environment, and using the model for $s(t)$ given before, the optimal weight becomes:

$$\vec{w}_{opt} \approx 2E\begin{bmatrix} A\cos(\theta)\cos(\theta+\varepsilon) \\ A\cos(\theta)\sin(\theta+\varepsilon) \end{bmatrix} = E\begin{bmatrix} A\cos(2\theta+\varepsilon) + A\cos(\varepsilon) \\ A\sin(2\theta+\varepsilon) + A\sin(\varepsilon) \end{bmatrix}.$$

For $\theta(t) = \omega_c t + \phi(t)$, where $\phi(t)$ is the frequency-modulating information and ω_c is the assigned center frequency, the double-frequency terms will average to zero. For second-order phase-locked loops, ε will be, in general, zero-mean. First-order loops are condemned to be phase followers, and therefore make ε nonzero-mean. Because of capture of the signal by its tracking phase-locked loop, for relatively high SNR environments and moderate SIR environments, the phase error will not only be zero-mean, but will be small as well. As a result, $E[A\sin(\varepsilon)] \approx 0$. This analysis suggests that one of the two quadrature branches of each amplitude-tracking loop in the traditional CCPLL implementation is nonfunctional. Indeed, the optimal weights become:

$$\vec{w}_{opt} \approx E\begin{bmatrix} A\cos(\varepsilon) \\ 0 \end{bmatrix}.$$

Examination of the amplitude tracks reported in [13] and [18] reveal that the quadrature weight, w_2 here, does indeed converge rapidly to zero, a fact that seems to have gone unnoticed until now. Additional simulation results verify that this weight goes to zero rapidly and that the tracking effect is entirely due to the inphase weight.

3.6.1.2. Simpler Amplitude Estimator Implementations

The utility of this proposal is that amplitude estimation for only the inphase portion of each signal should suffice, reducing the hardware of the CCPLL dramatically. Implementation of this system can be attempted either with a feedforward amplitude estimator using the form of the estimator above (Figure 17), or in a feedback loop form (Figure 18) by using the gradient-descent form of the optimal solution.

The direct form simplifies the dynamics of the system by replacing a feedback loop by a feedforward loop. In this case, the weight estimate is just the lowpass portion of the product of the original input signal (without any cancellation) and the inphase estimate. The lowpass filter should have a

Figure 17

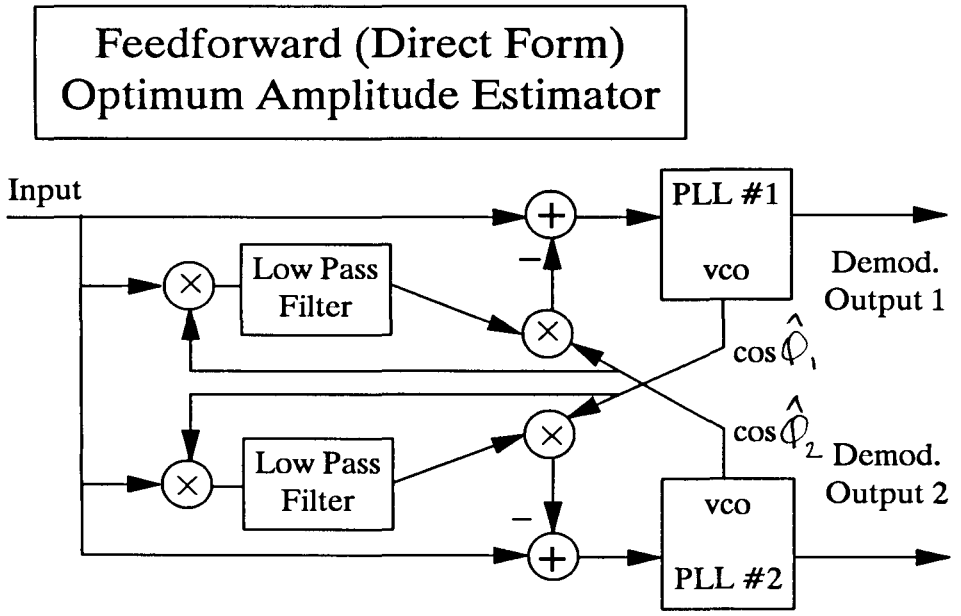

Figure 18

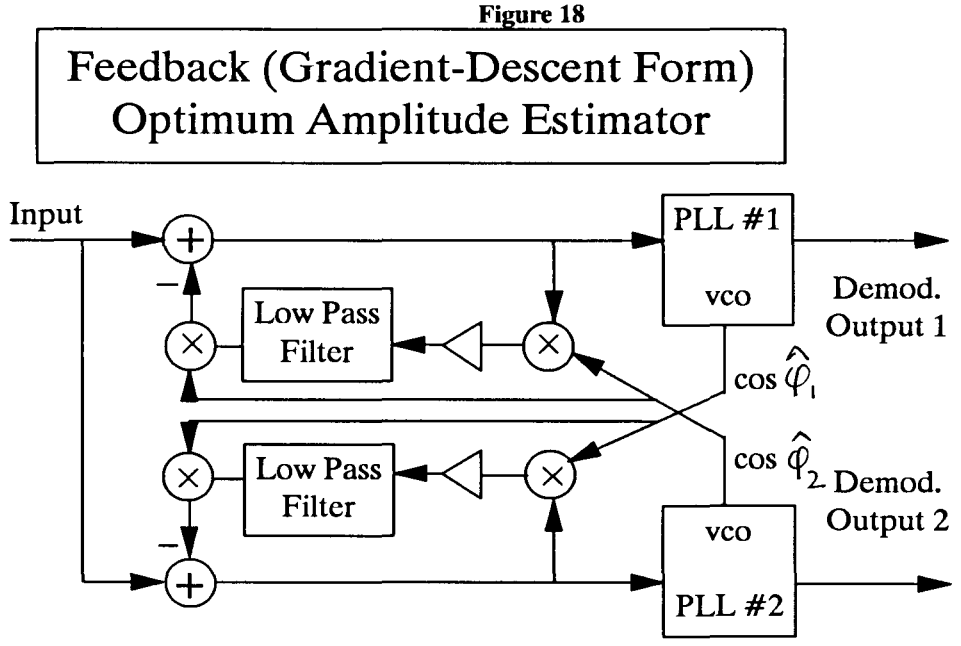

cutoff frequency high enough to pass the amplitude information, which is typically near the lower band edge of the modulating information. The estimator is a coherent AM receiver with the PLL's coherent phase reference as its coherent carrier reference. The coherent AM receiver thus tracks the amplitude of the FM signal just the same as if it were modulated on a constant-frequency carrier.

The gradient-descent solution has the form [28]:

$$\vec{w}_{k+1} = \vec{w}_k - \frac{\beta}{2}\frac{\partial}{\partial \vec{w}}(E[e^2]) \mid_{\vec{w}=\vec{w}_k} .$$

For the special case given here, the negative of the gradient is just $2E[x_1(v-w_1x_1)] = E[x_1e]$. Hence, the gradient-descent solution is just the inphase part of the amplitude-tracking loop given in the iterative CCPLL. However, the gradient-descent implementation form requires an integrator which the direct form does not require. On the other hand, the gradient-descent implementation is a proven hardware design, which stands in its favor.

Each implementation offers a reduction in both hardware and dynamical complexity, eliminating at least two of the six coupled differential equations from the original CCPLL. The original defining, coupled differential equations for the CCPLL with amplitude control are given in [18] for the case of negligible noise. These equations follow, with some reduction by trigonometric identities, from the implementation of the CCPLL shown in Figure 8. They do not contain a limiter prior to each PLL's input; however, for the steady-state case where the interfering signal is mostly cancelled, the limiter has almost no effect and the equations presented here are valid. The defining equations are, from [18]:

$$\begin{aligned}
\dot{x}_{1I} &= \beta_1[A_1\cos(\psi_1-\phi_1) + A_2\cos(\psi_2-\phi_1) - x_{1I}] * g_{1I} \\
\dot{x}_{1Q} &= \beta_1[A_1\sin(\psi_1-\phi_1) + A_2\sin(\psi_2-\phi_1) - x_{1Q}] * g_{1Q} \\
\dot{x}_{2I} &= \beta_2[A_1\cos(\psi_1-\phi_2) + A_2\cos(\psi_2-\phi_2) - x_{2I}] * g_{2I} \\
\dot{x}_{2Q} &= \beta_2[A_1\sin(\psi_1-\phi_2) + A_2\sin(\psi_2-\phi_2) - x_{2Q}] * g_{2Q} \\
\dot{\phi}_1 &= \alpha_1[A_1\sin(\psi_1-\phi_1) + A_2\sin(\psi_2-\phi_1) - x_{2I}\sin(\phi_2-\phi_1) - x_{2Q}\cos(\phi_2-\phi_1)] * h_{L1} \\
\dot{\phi}_2 &= \alpha_2[A_1\sin(\psi_1-\phi_2) + A_2\sin(\psi_2-\phi_2) - x_{1I}\sin(\phi_1-\phi_2) - x_{1Q}\cos(\phi_1-\phi_2)] * h_{L2} .
\end{aligned}$$

Here the input is of the form:

$$v(t) = A_1\cos(\omega_c t+\psi_1) + A_2\cos(\omega_c t+\psi_2) .$$

The first four equations specify the amplitude-control loops, while the last two specify the phase-locked loops. All the variables are real, with the amplitude estimates being represented by $x_{(1,2)\,(I,Q)}$ and the

phase estimates by $\phi_{1,2}$. The symbol * denotes convolution. The loop filters for PLL's 1 and 2 are, respectively, h_{L1} and h_{L2}, and the lowpass filters in the amplitude-control loops are g_{1I} , g_{1Q} , g_{2I} , and g_{2Q} . The PLL gains are α_1 and α_2, and the amplitude-control loop gains are β_1 and β_2 .

The addition of limiters would have a significant effect during signal acquisition by enhancing the strong and suppressing the weak signals. Since the amplitude-control loops are completely preceding the limiter, the limiter does not affect their operation except through its effect on the phase estimates. As a result, in a system with bandpass limiters, the first four differential equations above are unchanged. However, since the limiter nonlinearly mixes the additive signal components before they reach the PLL, the operations of the PLL cannot be distributed among the additive signal components as before. This is because the limiter has already distorted the linear combination of these components before they get to the PLL. Without the limiter the PLL's multiplication of its input by the VCO's output ($-\sin\phi_1$ or $-\sin\phi_2$) could be arithmetically distributed among the additive input components to form the product terms whose lowpass portions result in the sines and cosines of phase differences seen above.

With the limiter in place, however, this distribution and its corresponding trigonometric reduction and lowpass filtering to sines and cosines of phase differences cannot take place. The three operations, limiter, bandpass filter, and VCO multiplier are noncommutative, and therefore the combination prevents further reduction of the phase-tracking differential equations. With the limiter in place, the equations therefore take on the direct form of the implementation:

$$\dot{\phi}_1 = \alpha_1[\sin(\phi_1)BPLIM(A_1\cos\psi_1 + A_2\cos\psi_2 - x_{2I}\cos\phi_2 - x_{2Q}\cos\phi_2)]*h_{L1}$$
$$\dot{\phi}_1 = \alpha_1[\sin(\phi_2)BPLIM(A_1\cos\psi_1 + A_2\cos\psi_2 - x_{1I}\cos\phi_1 - x_{1Q}\cos\phi_1)]*h_{L2} ,$$

where $BPLIM(y)$ denotes the bandpass limiter's operation on y . The CCPLL equations with the limiter are not particularly enlightening in themselves, since they appear to offer no analytic reduction, and solving them numerically is equivalent to verifying acquisition performance by direct simulation. We will therefore consider the defining equations without the limiter, bearing in mind that they are valid only when significant cancellation of the interferer is taking place.

The gradient-descent form of the reduced solution, derived earlier and shown as Figure 18, follows by noting that its only difference to the system in [18] defined by the six equations above is that the quadrature amplitude estimates are set identically zero. The equations are therefore obtained by eliminating the terms multiplied by x_{1Q} and x_{2Q} and eliminating the equations for $\dot{x}_{1Q}$ and $\dot{x}_{2Q}$. Since there is now only one amplitude estimate per signal, the I , Q subscripts will be dropped. As a result, the reduced gradient-descent solution is governed by the simplified equations given below (again for negligible noise):

$$\dot{x}_1 = \beta_1[A_1\cos(\psi_1-\phi_1) + A_2\cos(\psi_2-\phi_1) - x_1] * g_1$$
$$\dot{x}_2 = \beta_2[A_1\cos(\psi_1-\phi_2) + A_2\cos(\psi_2-\phi_2) - x_2] * g_2$$
$$\dot{\phi}_1 = \alpha_1[A_1\sin(\psi_1-\phi_1) + A_2\sin(\psi_2-\phi_1) - x_2\sin(\phi_2-\phi_1)] * h_{L1}$$
$$\dot{\phi}_2 = \alpha_2[A_1\sin(\psi_1-\phi_2) + A_2\sin(\psi_2-\phi_2) - x_1\sin(\phi_1-\phi_2)] * h_{L2}\,.$$

The use of the direct feedforward form (Figure 17) of the optimal MMSE amplitude estimate simplifies the system even more, leaving just the two nonlinear equations for the phase-locked loops. In the direct feedforward form, amplitude estimates x_1 and x_2 are computed directly as follows:

$$x_1 = [(A_1\cos\psi_1 + A_2\cos\psi_2)\cos\phi_1]*g_1$$
$$x_2 = [(A_1\cos\psi_1 + A_2\cos\psi_2)\cos\phi_2]*g_2$$

where g_1 and g_2 are lowpass filters as before. Eliminating the double frequency terms gives:

$$x_1 = [A_1\cos(\psi_1-\phi_1) + A_2\cos(\psi_2-\phi_1)]*g_1$$
$$x_2 = [A_1\cos(\psi_1-\phi_2) + A_2\cos(\psi_2-\phi_2)]*g_2\,.$$

Substituting these expressions into the phase-locked loop equations for $\dot{\phi}_1$ and $\dot{\phi}_2$ results in the two differential equations that define the feedforward system:

$$\dot{\phi}_1 = \alpha_1[A_1\sin(\psi_1-\phi_1) + A_2\sin(\psi_2-\phi_1) - [(A_1\cos(\psi_1-\phi_2) + A_2\cos(\psi_2-\phi_2))*g_2]\sin(\phi_2-\phi_1)] * h_{L1}$$
$$\dot{\phi}_2 = \alpha_2[A_1\sin(\psi_1-\phi_2) + A_2\sin(\psi_2-\phi_2) - [(A_1\cos(\psi_1-\phi_1) + A_2\cos(\psi_2-\phi_1))*g_1]\sin(\phi_1-\phi_2)] * h_{L2}\,.$$

3.6.1.3. Phase Perturbation Analysis of the Feedforward Equations

It is instructive to consider a perturbation of the feedforward system from a steady-state solution. Let the input amplitudes A_1 and A_2 be constant, and let the driving input phase functions be:

$$\psi_1 = \omega_1 t \qquad\qquad \psi_2 = \omega_2 t + \varepsilon\,.$$

Since the phase-locked loops under consideration are second order or better ($h_{L1,2}$ each has at least

one pole), the loops will track the input phase rate (instantaneous frequency) as well as the input phase. We will consider a perturbation to the phase variable and consider the average phase rates tracked by the loops in order to remain in lock. In real systems this approach is further justified by the time constants associated with the loop lowpass filter, which are noted for their ability to "flywheel" the loop through relatively short noise bursts. Therefore, let the loop initial conditions be:

$$\phi_1 = \omega_1 t + \delta \qquad\qquad \phi_2 = \omega_2 t + \gamma .$$

Then the differential equations are:

$$\dot{\phi}_1 = \alpha_1[A_1\sin(-\delta) + A_2\sin(\Delta\omega t + \varepsilon-\delta) - [[A_1\cos(-\Delta\omega t-\gamma) + A_2\cos(\varepsilon-\gamma)]*g_2]\sin(\Delta\omega t+\gamma-\delta)]*h_{L1}$$
$$\dot{\phi}_2 = \alpha_1[A_1\sin(-\Delta\omega t-\gamma) + A_2\sin(\varepsilon-\gamma) - [[A_1\cos(-\delta) + A_2\cos(\Delta\omega t+\varepsilon-\delta)]*g_1]\sin(-\Delta\omega t-\gamma+\delta)]*h_{L2}$$

where $\Delta\omega = \omega_2-\omega_1$. Let g_1 and g_2 be narrowband filters so that they cut off below frequency $\Delta\omega$, as they would be for tracking amplitude functions whose bandwidths are less than those of the modulating information on an FM signal. The differential equations then simplify to:

$$\dot{\phi}_1 = \alpha_1[A_1\sin(-\delta) + A_2\sin(\Delta\omega t + \varepsilon-\delta) - A_2\cos(\varepsilon-\gamma)\sin(\Delta\omega t+\gamma-\delta)]*h_{L1}$$
$$\dot{\phi}_2 = \alpha_1[A_1\sin(-\Delta\omega t-\gamma) + A_2\sin(\varepsilon-\gamma) - A_1\cos(-\delta)\sin(-\Delta\omega t-\gamma+\delta)]*h_{L2} .$$

If $\Delta\omega$ is outside the passband of the lowpass loop filters h_{L1} and h_{L2}, the system displays the dynamics of ordinary, first-order phase-locked loops without any coupling. More importantly, the system behaves as if the interference were not present:

$$\dot{\phi}_1 = \alpha_1 A_1\sin(-\delta)$$
$$\dot{\phi}_2 = \alpha_2 A_2\sin(\varepsilon-\gamma) .$$

For small perturbations, ε , δ , and γ , the system can be linearized to:

$$\dot{\phi}_1 = -\delta\alpha_1 A_1$$
$$\dot{\phi}_2 = -(\gamma-\varepsilon)\alpha_2 A_2$$

which contains a sink at ($\delta = 0$, $\gamma=\varepsilon$). Since δ and $\gamma-\varepsilon$ are the instantaneous phase errors of ϕ_1 and ϕ_2, respectively, the response of the linearized system will be to correct the phase-error perturbation with an exponential decay according to the equations:

$$\dot{\phi}_1 = \alpha_1 A_1 (\psi_1 - \phi_1)$$
$$\dot{\phi}_2 = \alpha_2 A_2 (\psi_2 - \phi_2) .$$

Further examination of the two feedforward equations leads one to consider what happens if the phase tracks coincide ($\phi_1 = \phi_2$), especially in the case where both PLL's might momentarily acquire the same signal. In this case, it would appear that the system acts as if there were no cross-coupling at all, since the term that is due to the cross-coupling is multiplied by $\sin(\phi_1-\phi_2)$. Note that for a system with bandpass limiters, the nonlinear action of the limiter prevents the trigonometric reduction that results in the factor of $\sin(\phi_1-\phi_2)$. This term comes from the multiplication of the phase-locked loop's VCO with the subtracted estimate of the interference. In a system with a limiter, strong signal enhancement occurs prior to the PLL input. If the interference estimate is relatively close to the interference in frequency and phase, the nonlinear enhancement is based on the strength of the interference minus the estimate relative to that of the desired signal. As a result, if the phase tracks of the interferers were only to coincide momentarily ($\phi_1 = \phi_2$), the interference and its estimate together are suppressed at the input to the PLL, facilitating desired-signal capture and preventing the possibility of nullifying the effect of cross-coupling.

However, this examination of this case for the system without limiters is of interest during signal acquisition, specifically for the event where both loops capture the same signal. Consider a small perturbation of this case where $\phi_1 = \phi_2$. Let the input be:

$$\psi_1 = \omega_1 t \qquad\qquad \psi_2 = \omega_2 t + \varepsilon .$$

Let the initial conditions be:

$$\phi_1 = \omega_1 t + \delta \qquad\qquad \phi_2 = \omega_1 t + \gamma , \quad \gamma \neq \delta .$$

The differential equations are then:

$$\dot{\phi}_1 = \alpha_1[A_1\sin(-\delta) + A_2\sin(\Delta\omega t + \varepsilon-\delta) - [[A_1\cos(-\gamma) + A_2\cos(\Delta\omega t+\varepsilon-\gamma)]*g_2]\sin(\gamma-\delta)]*h_{L1}$$
$$\dot{\phi}_2 = \alpha_2[A_1\sin(-\gamma) + A_2\sin(\Delta\omega t + \varepsilon-\gamma) - [[A_1\cos(-\delta) + A_2\cos(\Delta\omega t+\varepsilon-\delta)]*g_1]\sin(\delta-\gamma)]*h_{L2} .$$

Assuming that $g_{1,2}$ and $h_{L1,2}$ remove the terms of frequency $\Delta\omega$, as before:

$$\dot{\phi}_1 = \alpha_1[A_1\sin(-\delta) - A_1\cos(-\gamma)\sin(\gamma-\delta)]$$
$$\dot{\phi}_2 = \alpha_2[A_1\sin(-\gamma) - A_1\cos(-\delta)\sin(\delta-\gamma)] .$$

By applying trigonometric identities and combining terms, the following equations are obtained:

$$\dot{\phi}_1 = \frac{\alpha_1 A_1}{2}[\sin(-\delta)-\sin(2\gamma-\delta)]$$

$$\dot{\phi}_2 = \frac{\alpha_2 A_1}{2}[\sin(-\gamma)-\sin(2\delta-\gamma)]\,.$$

Let the two loops be identical so that $\alpha_1 = \alpha_2 = \alpha$, and define $G = A_1\alpha$. For small perturbations, the system of equations can be linearized to:

$$\dot{\phi}_1 = -G\,\gamma \qquad\qquad \dot{\phi}_2 = -G\,\delta,$$

which by definition of ϕ_1 and ϕ_2 is the coupled system:

$$\dot{\phi}_1 = G\,(\psi_1 - \phi_2) \qquad\qquad \dot{\phi}_2 = G\,(\psi_1 - \phi_1)\,.$$

At this point we can consider the dynamics of the system. There are two cases to consider, one in which γ and δ are of the same sign , and one where they are of different signs. When the two errors are of the same sign, the linearization indicates that both errors will decrease in absolute value. However, since the rate of change of ϕ_1 is proportional to the phase error of ϕ_2 (γ) rather than to its own phase error δ , and ϕ_2 is likewise cross-controlled, the decrease will not return to an equilibrium at $\delta = \gamma = 0$. Without loss of generality, let $|\,\delta\,| < |\,\gamma\,|$. Because the initial absolute value of the phase error in ϕ_1 is less than that in ϕ_2 , and the rate of correction of ϕ_1 is greater than that in ϕ_2 , ϕ_1 will reach the point of zero phase error, while ϕ_2 still has nonzero phase error. At this point we have the following conditions for the rates of change and the phase errors:

$$\dot{\phi}_1 \neq 0 \qquad\qquad \dot{\phi}_2 = 0$$
$$\delta = 0 \qquad\qquad \gamma \neq 0\,.$$

Clearly, the phase error for ϕ_1 , δ , will cross over zero while the phase error for ϕ_2 , γ , is still on the original side of zero, giving us the perturbation case where δ and γ are of different signs.

When δ and γ are of different signs, the sign of $\dot{\phi}_1$ is the same as that of the error in ϕ_1 , δ , and hence the absolute value of the error, δ, will increase with time. Similarly, the absolute value of the error in ϕ_2 , γ, will increase with time, causing the rate of drift of both phase-locked loops to increase. This positive feedback will continue to accelerate the drift and shortly invalidates the linearization of the differential equations. Since the coupled differential equations increase the absolute value of small phase errors when the phase errors are of opposite sign, the equilibrium at $\phi_1 = \phi_2$, i.e., capture of the same signal by each loop, is unstable.

For the moment, consider the linearized dynamics of this drift away from the state where both loops are locked on the same signal. Without loss of generality let $|\delta| < |\gamma|$ initially. From the linearization above, since the rate of growth of $|\delta|$ is proportional to $|\gamma|$, and the rate of growth of $|\gamma|$ is proportional to $|\delta|$, the linearized system will tend to correct the imbalance in absolute value. Hence there are negative feedback dynamics in the growth of the absolute phase errors, tending to balance them so that $\gamma \approx -\delta$. These dynamics will continue to cause both $|\delta|$ and $|\gamma|$ to grow at the same increasing rate and value, until the linearization breaks down.

It is important to recall at this point our assumption that the average frequency of the phase-locked loops was constant. As both absolute phase errors begin not only to increase monotonically, but also to accelerate in opposite directions, this condition is violated. The oscillator frequencies of the two phase-locked loops begin to separate, one decreasing and the other increasing (Figure 19). The first parts of the linearization to break down are the linear approximations for $\sin(2\gamma - \delta)$ and $\sin(2\delta - \gamma)$. Assuming that $|\gamma| \approx |\delta|$ near the breakdown and using a standard cutoff for the linearization of the sine function to be $\frac{\pi}{6}$, the linearization is good for absolute phase errors $< \frac{\pi}{18}$. For a loop with a gain (G) of about 30,000 (loop lock range = 30 kHz) the linearized solution holds until the tracking frequency has drifted approximately 800 Hz. Since this presents a far wider frequency difference from the originally tracked input than the typical amplitude-tracking filter (g_1, g_2) bandwidths, these filters will begin to remove the originally tracked signal's component from the amplitude estimate.

Returning to the original equations for this perturbation and filtering out both components from the amplitude-control loops, the equations governing in this regime are:

$$\dot{\phi}_1 = \alpha_1[A_1\sin(-\delta) + A_2\sin(\Delta\omega t + \varepsilon - \delta)\,]^* h_{L1}$$
$$\dot{\phi}_2 = \alpha_2[A_1\sin(-\gamma) + A_2\sin(\Delta\omega t + \varepsilon - \gamma)\,]^* h_{L2}\,.$$

(Remember that δ and γ are time-varying functions.) These are also the equations governing the two phase-locked loops without any cross-coupling. At this point the loops begin to reacquire the signal as normal PLL's would since the entire assembly has lost lock on both the amplitude and the phase of either signal. There is one major difference, however, in that one of the loops' frequency estimates is biased toward the interfering signal, and one is biased away from it. The loop whose frequency is

Figure 19

Drift Away from State of Strong-Signal Lock by Both PLL's

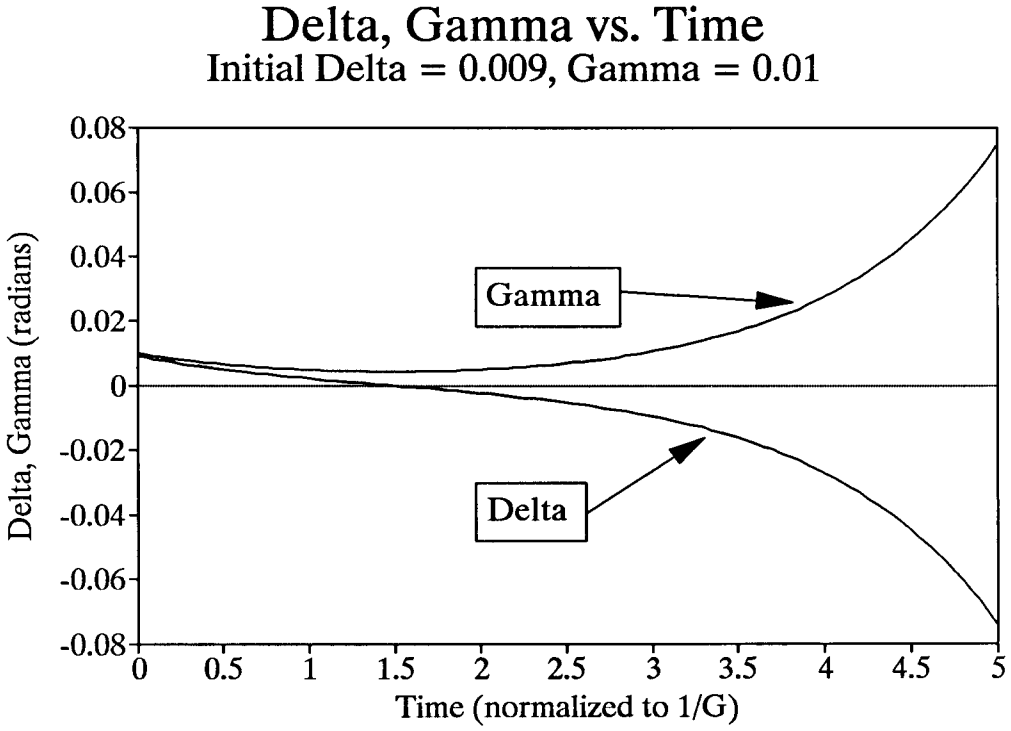

moving towards ω_2 will become less effective in filtering out that signal's power, and as a result, will be significantly slower in reacquiring the first signal. The cancellation of the first signal signal at this loop's input will have time to take hold, allowing the possible acquisition of the second signal.

3.6.1.4. A Difference-Amplitude Tracking Variation of the Feedforward Canceller

An examination of the feedforward canceller topology presented suggests that a major source of error in the amplitude estimates will be due to the VCO signal phase estimate's not being entirely uncorrelated with the undesired signal. For example, the stronger input signal may corrupt the weaker signal-tracking VCO estimate sufficiently to affect the amplitude estimate of the weaker signal. However, even with perfect capture by the PLL's, it is possible for the amplitude estimate to be corrupted by the undesired signal. This can easily occur when interfering FM signal inputs are momentarily close in instantaneous frequency, i.e., when their respective modulating signals are close in amplitude. When the instantaneous frequency difference falls within the passband of the amplitude-tracking lowpass filter, the amplitude estimate will be corrupted by the undesired signal. In fact, since nonideal lowpass filters are used, the undesired signal will have a corrupting effect, somewhat diminished, even when the instantaneous frequency difference is slightly outside the nominal passband of these filters. This unavoidable corruption of the amplitude estimate can be viewed as an undesired signal-leakage path into the interference-canceller reference, an effect that limits performance of the canceller as discussed in Section 3.3.1. It is therefore desirable to suppress any potential cross-leakage in generating the amplitude estimate.

One possible way of limiting such cross-leakage is to derive the amplitude estimate from as clean a source of the desired signal as is possible. The canceller topology already contains such a source during steady-state operation. The input to each limiter-PLL assembly has already had the estimate of the undesired signal subtracted from it, and it may therefore be a good source from which to produce the desired-signal amplitude estimate. In computing the amplitude estimate, one could multiply the VCO-produced signal estimate not by the overall canceller input signal $v(t)$, but rather by the input to its own limiter-PLL combination. The effect of leakage may be minimized in the canceller steady state by

doing so. This canceller topology is shown in Figure 20 and will be referred to as the **difference-amplitude-tracking topology.**

To examine this variation, we formally replace the terms for the amplitude estimates ($[A_1\cos(\psi_1-\phi_2) + A_2\cos(\psi_2-\phi_2)] * g_2$ and $[A_1\cos(\psi_1-\phi_1) + A_2\cos(\psi_2-\phi_1)] * g_1$) by a_2 and a_1, respectively, in the two defining differential equations for the feedforward system (page 51, just prior to Section 3.6.1.3). Now, from the topology defined in the previous paragraph and shown in Figure 20, the equations for a_1 and a_2 are:

$$a_1 = [A_1\cos(\psi_1-\phi_1) + A_2\cos(\psi_2-\phi_1) - a_2\cos(\phi_2-\phi_1)] * g_1$$
$$a_2 = [A_1\cos(\psi_1-\phi_2) + A_2\cos(\psi_2-\phi_2) - a_1\cos(\phi_1-\phi_2)] * g_2 .$$

Note that in the desired steady state, $\phi_1 \approx \psi_1$, $\phi_2 \approx \psi_2$, $a_1 \approx A_1$, and $a_2 \approx A_2$, so that these equations become:

$$a_1 \approx [A_1\cos(\psi_1-\phi_1)] * g_1$$
$$a_2 \approx [A_2\cos(\psi_2-\phi_2)] * g_2 .$$

Again consider the perturbation on the desired state. As before, let the input amplitudes A_1 and A_2 be constant, and let the driving input phase functions be:

$$\psi_1 = \omega_1 t \qquad\qquad \psi_2 = \omega_2 t + \varepsilon .$$

Let the loop initial conditions be a perturbation of the desired steady state:

$$\phi_1 = \omega_1 t + \delta \qquad\qquad \phi_2 = \omega_2 t + \gamma.$$

Then the loop differential equations are:

$$\dot{\phi}_1 = \alpha_1[A_1\sin(-\delta) + A_2\sin(\Delta\omega t + \varepsilon-\delta) - a_2\sin(\Delta\omega t+\gamma-\delta)]*h_{L1}$$
$$\dot{\phi}_2 = \alpha_2[A_1\sin(-\Delta\omega t-\gamma) + A_2\sin(\varepsilon-\gamma) - a_1\sin(-\Delta\omega t-\gamma+\delta)]*h_{L2} ,$$

with a_1 and a_2 being:

$$a_1 = [A_1\cos(-\delta) + A_2\cos(\Delta\omega t-\delta) - a_2\cos(\Delta\omega t+\gamma-\delta)] * g_1$$
$$a_2 = [A_1\cos(-\Delta\omega t-\gamma) + A_2\cos(-\gamma) - a_1\cos(-\Delta\omega t+\delta-\gamma)] * g_2 .$$

With some trigonometric substitution to combine terms of the same frequency, the amplitude terms a_1 and a_2 become:

$$a_1 = [A_1\cos(-\delta) + (A_2-a_2\cos(\gamma)+a_2\sin(\gamma))\cos(\Delta\omega t-\delta)] * g_1$$
$$a_2 = [(A_1-a_1\cos(\delta)+a_1\sin(\delta))\cos(-\Delta\omega t-\gamma) + A_2\cos(-\gamma)] * g_2 .$$

Figure 20

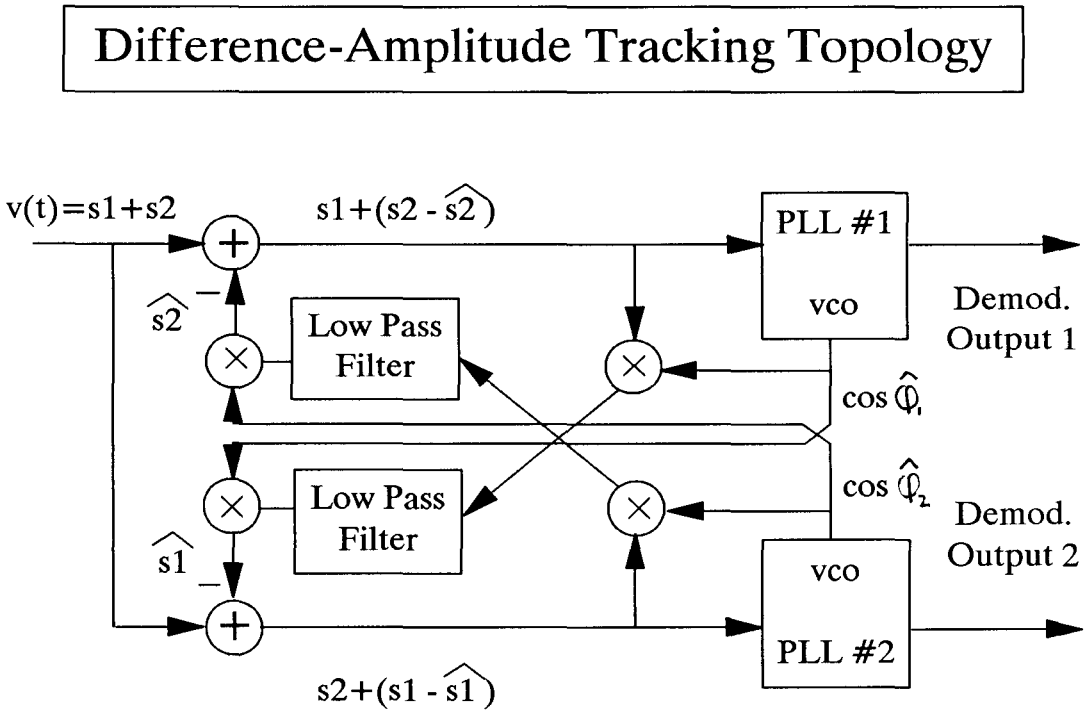
Difference-Amplitude Tracking Topology
v(t)=s1+s2
s1+(s2 - ŝ2)
PLL #1
vco
Demod.
Output 1
ŝ2
Low Pass
Filter
cos φ̂1
cos φ̂2
Low Pass
Filter
Demod.
Output 2
ŝ1
vco
PLL #2
s2+(s1 - ŝ1)

As seen above, any leakage of the undesired signal through the amplitude lowpass filter will be significantly attenuated for small δ and γ. After filtering out the amplitude terms with frequency $\Delta\omega$, the perturbation is reduced to the same system studied earlier after the amplitude filtering (Section 3.6.1.3, intermediate equations on page 52):

$$\dot{\phi}_1 = \alpha_1[A_1\sin(-\delta) + A_2\sin(\Delta\omega t + \varepsilon-\delta) - A_2\cos(\varepsilon-\gamma)\sin(\Delta\omega t+\gamma-\delta)]*h_{L1}$$
$$\dot{\phi}_2 = \alpha_2[A_1\sin(-\Delta\omega t-\gamma) + A_2\sin(\varepsilon-\gamma) - A_1\cos(-\delta)\sin(-\Delta\omega t-\gamma+\delta)]*h_{L2}\,.$$

The advantage of the difference-amplitude-tracking topology over the regular feedforward topology is as we foresaw: the extra attenuation of the undesired signal in the amplitude estimate even when the instantaneous frequencies are close.

Consider now what happens to the difference-amplitude-tracking topology when the two loops start tracking the same signal. As before, let the driving phase be:

$$\psi_1 = \omega_1 t \qquad\qquad \psi_2 = \omega_2 t + \varepsilon,$$

and let the initial conditions be:

$$\phi_1 = \omega_1 t + \delta \qquad\qquad \phi_2 = \omega_1 t + \gamma\,, \quad \gamma\neq\delta.$$

The equations for the amplitude estimates are then:

$$a_1 = [A_1\cos(-\delta) + A_2\cos(\Delta\omega t+\varepsilon-\delta) - a_2\cos(\delta-\gamma)] * g_1$$
$$a_2 = [A_1\cos(-\gamma) + A_2\cos(\Delta\omega t+\varepsilon-\gamma) - a_1\cos(\delta-\gamma)] * g_2\,.$$

Filtering the $\Delta\omega$ frequency terms and letting δ and γ be small, these equations become:

$$a_1 \approx A_1 - a_2$$
$$a_2 \approx A_1 - a_1\,.$$

Since the two amplitude equations above are linearly dependent, the two amplitude estimates are underdetermined, and hence they can vary widely in relation to the signal amplitude, A_1, while still satisfying the defining equation. When no interfering signal is present, the amplitude estimates are free to wander, possibly producing unstable behavior. In a practical system this effect would be dealt with by disabling the canceller when no significant interference is present, as indicated by the residual power level after the desired signal has been removed.

The free wandering of the amplitude estimates in the undesired equilibrium indicates that the dynamics of the difference-amplitude canceller may be different from those of the previously examined

feedforward canceller. This difference can be easily checked in the differential equations by considering a_1 and $a_2 = A_1 - a_1$ fixed, as is justified by the much longer time constants of the amplitude-estimation filters in comparison with the PLL's. The defining differential equations are then :

$$\dot{\phi}_1 = \alpha_1[A_1\sin(-\delta) + A_2\sin(\Delta\omega t + \varepsilon-\delta) - a_2\sin(\gamma-\delta)]*h_{L1}$$
$$\dot{\phi}_2 = \alpha_2[A_1\sin(-\gamma) + A_2\sin(\Delta\omega t + \varepsilon-\gamma) - a_1\sin(-\gamma+\delta)]*h_{L2}\,.$$

Substituting $a_2 = A_1 - a_1$ and filtering out the $\Delta\omega$ frequency terms gives :

$$\dot{\phi}_1 = \alpha_1[A_1\sin(-\delta) - (A_1-a_1)\sin(\gamma-\delta)]$$
$$\dot{\phi}_2 = \alpha_2[A_1\sin(-\gamma) + a_1\sin(\gamma-\delta)],$$

which, for small δ, γ linearizes to :

$$\dot{\phi}_1 = -\alpha_1[a_2\gamma + a_1\delta]$$
$$\dot{\phi}_2 = -\alpha_2[a_2\gamma + a_1\delta]\,.$$

By substituting for δ and γ, $\psi_1 - \phi_1$ and $\psi_1 - \phi_2$, respectively, we obtain :

$$\dot{\phi}_1 = -\alpha_1 A_1\left[\psi_1 - \frac{1}{A_1}\left(a_2\phi_2 + a_1\phi_1\right)\right]$$
$$\dot{\phi}_2 = -\alpha_2 A_1\left[\psi_1 - \frac{1}{A_1}\left(a_2\phi_2 + a_1\phi_1\right)\right].$$

The behavior of this cross-coupled system is clearly dependent on the amplitude-estimate values. The equations above appear to verify the intuitive solution that the PLL with an amplitude estimate close to A_1 will be properly corrected, while the PLL farther away will be cross-coupled in its phase correction in a manner similar to the simpler feedforward system examined earlier. Further examination of these equations within the framework of the linearization does not appear to be enlightening at this time. However, before leaving the perturbation example it is important to note that the behavior of the difference-amplitude system around the undesired equilibrium does serve to demonstrate not only that its dynamics tend to be more complicated than the simpler feedforward canceller, but also that they tend to be more sensitive to initial conditions. The initial conditions of the amplitude estimates greatly affect the perturbation dynamics. In some sense this would imply that the difference-amplitude canceller is more chaotic than the simple feedforward canceller. The instability of the undesired steady-state equilibrium and the improved cancellation in the desired steady-state equilibrium have been verified in simulation results, to be presented in the next section.

3.6.2. Simulation Results

The new feedforward interference cancellers were simulated on an IBM PS/2 Model 70/386 personal computer in order to verify their dynamics and to demonstrate their ability to separate co-channel interfering FM signals. The simulations were written in the C language and used direct-form discrete-time representations of the interference cancellers. Simulation sampling rates were much greater than Nyquist for the input signals (at least 10 times oversampled), so that simulated loop parameters resembled those of analog systems. Although the oversampling serves to reduce the differences between simulation of a continuous time system via the first-order Euler method and simulation of a sampled data system, these simulations are in fact still discrete-time sampled data systems. As such, these simulations stand as proof of concept for digital, or more generally sampled, implementations of FM interference cancellers, while prior work [18] proved the concept of continuous analog interference-canceller implementation. Hence, both analog and digital technologies are viable methods for implementing these cancellers in hardware.

The loop parameters used for these simulations were drawn from the recommendations in [18]. The PLL's were second-order designs with integral-plus-proportional loop filters, as in [18]. Loop parameters were calculated from modulation parameters as given in [18]:

Loop filter (both loops) Laplace Transform : $1 + \frac{K_{1,2}}{s}$

Strong-signal tracking loop :

Loop gain $\alpha_1 \approx \sqrt{5 f_{dev\,1} W_1}$

Integral gain $K_1 \approx \alpha_1$

Weak-signal tracking loop :

Loop gain $\alpha_2 \approx \frac{A_1}{A_2}\sqrt{8 f_{dev\,2} W_2}$

Integral gain $K_2 \approx \frac{\alpha_2}{2}$

where the maximum frequency deviation and modulation bandwidth of signal i are $f_{dev\,i}$ and W_i respectively.

It should be noted that for a given channel with specific modulation characteristics, the loop parameters could have been optimized. This was not the focus of these simulations. In addition, the recommendations of [18] are strongly based on conventional, single-user PLL-receiver design, and it is possible that multiuser receiver forms like the CCPLL and its variants developed here could have slightly different optimum-parameter formulations. A discussion of optimum loop parameters would require extensive knowledge of the specific receiver application, something that is beyond the scope of this chapter and these simulation studies. In the case of Chapter IV where the interference cancellers are applied to the cellular telephone channel, the measure of performance, call quality, is somewhat subjective. Therefore, determination of optimal loop parameters is beyond the scope of the simulations of Chapter IV as well. The recommendations of [18] are therefore taken with the knowledge that in practice, performance of the interference cancellers might be improved by additional specialization of the design.

The following interference-canceller forms were tested :

1. an inphase and quadrature amplitude-tracking feedforward canceller,
2. an inphase-only amplitude-tracking feedforward canceller,
3. an inphase and quadrature difference-amplitude-tracking feedforward canceller, and
4. an inphase-only difference-amplitude-tracking feedforward canceller.

3.6.2.1. Acquisition Characteristics

Figure 21 shows the acquisition behavior of each of the four cancellers under constant-frequency inputs. The input signals to be separated were both of constant amplitude and were separated in frequency by 1 kHz. Although this is one of the simpler separation problems, this is perhaps the most difficult acquisition problem since the signals never cross in frequency. The weak-signal to strong-signal power ratio was -8 dB. These loops were designed for acquiring the two constant-frequency signals rather than by using the FM tracking design rules given above. The weak-signal loop had a loop gain of 6000 (6 kHz bandwidth) and an integrator gain of 1000, while the strong-signal loop had a loop gain of 2000 and an integrator gain of 100. Both had 100 Hz second-order Butterworth amplitude-

Figure 21

Comparative Acquisition of Interference Cancellers: Constant Frequency Inputs

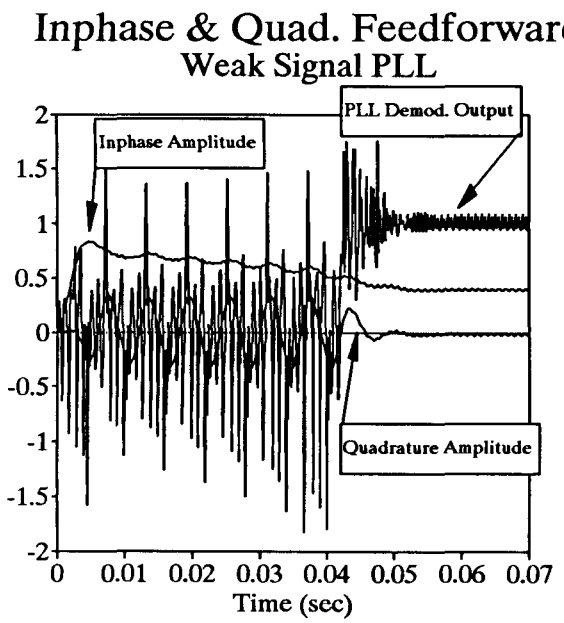

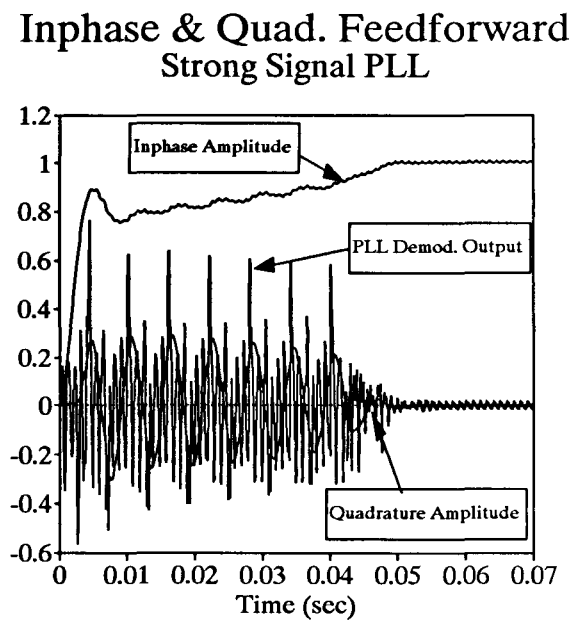

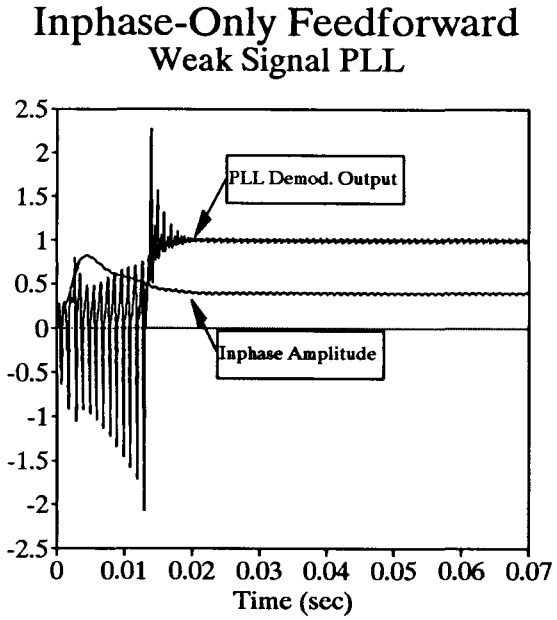

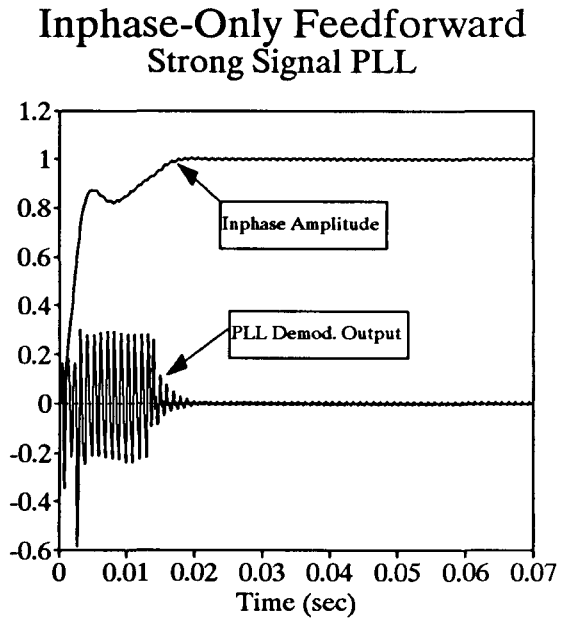

Figure 21 (continued)

Comparative Acquisition of Interference Cancellers: Constant Frequency Inputs

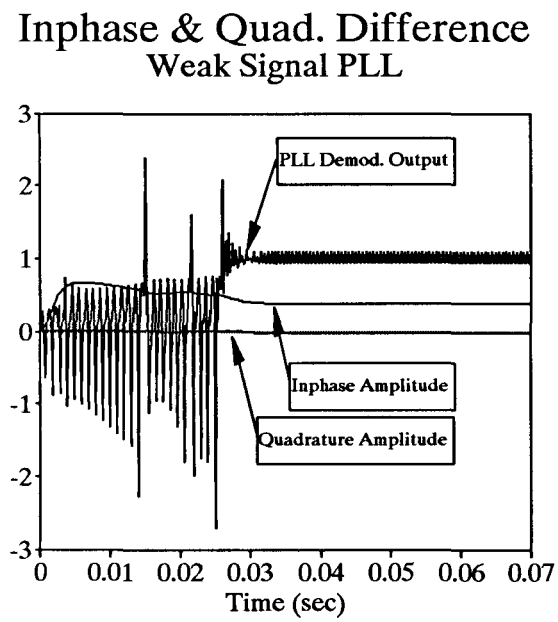

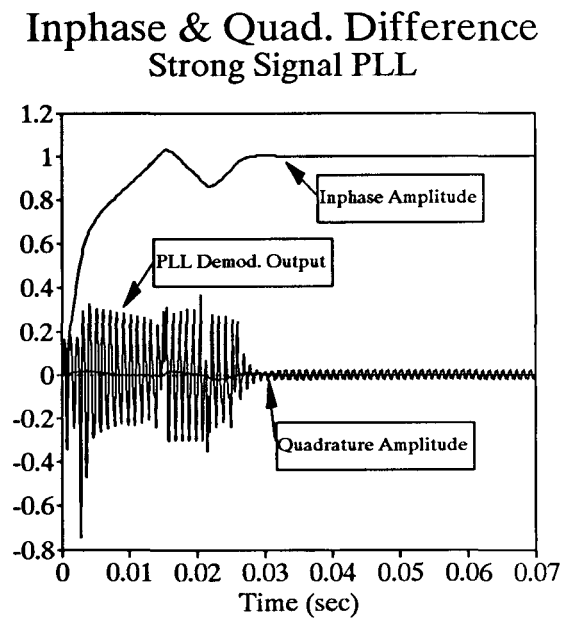

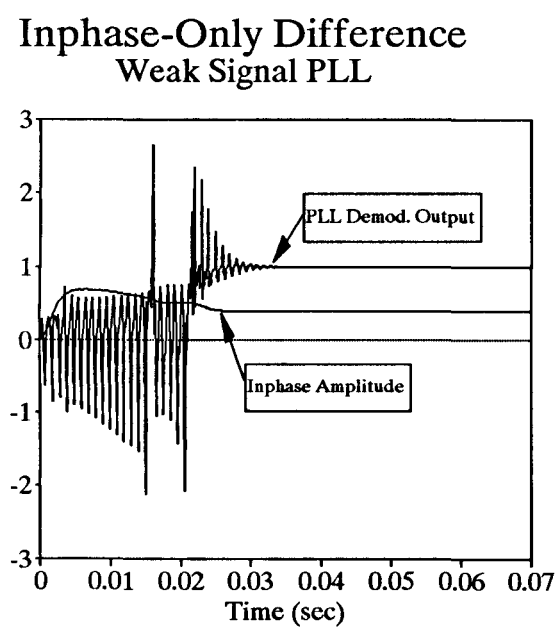

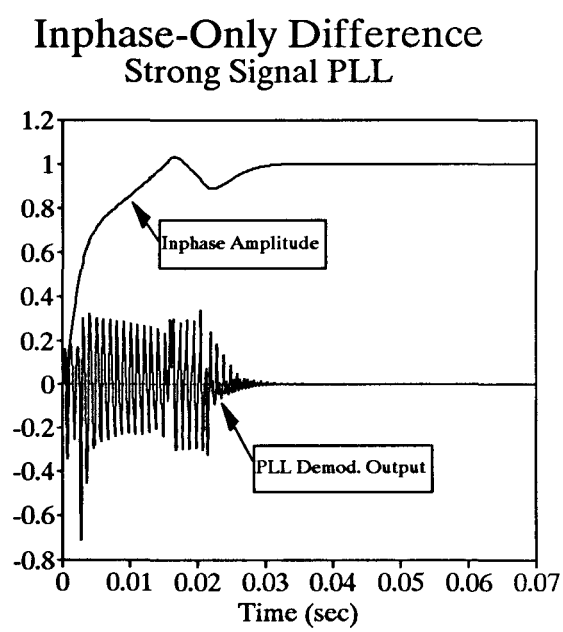

tracking filters. Both PLL's were started out locked on the stronger of the two signals, which corresponded to a PLL output level of 0.0.

Several observations can be made from the constant-frequency acquisition responses in Figure 21. The first is that for signals that do not cross in instantaneous frequency, the acquisition response is dominated by the amplitude-estimator response time. The time constants for the PLL's are on the order of 10^{-3} seconds, while the weak-signal acquisition time and the amplitude-estimation filter time constants are both an order of magnitude greater. Capture of the weak signal cannot occur until the strong-signal amplitude estimate has developed. A second observation is that the inphase and quadrature amplitude-tracking forms have a distinctly longer acquisition time than the inphase-only forms. Examination of the amplitude estimates suggests that the extra degree of freedom provided by the quadrature amplitude-tracking loop provides enough additional error to prevent acquisition at the earlier times taken by the inphase-only forms.

In addition, the more complicated amplitude dynamics of the difference-amplitude-tracking forms cause them to acquire later than the other feedforward cancellers; however, the difference-amplitude cancellers provide better cancellation after acquisition. This better interference suppression is due to their inherently cleaner amplitude estimates. It is important to notice that in all the cancellers, strong-signal demodulation is significantly improved after weak-signal acquisition, indicating the important role that interference cancellation can play even for situations where the strong signal is desired.

Figure 22 shows the acquisition behavior of the cancellers when the weaker signal is FM modulated. The power difference is still 8 dB, and the weaker signal is modulated by a 300 Hz sinusoid with a 6 kHz peak frequency deviation. In order to make this more indicative of FM separation dynamics, the strong-signal loop is designed for more wideband response than before, with a loop gain of 15000 and an integrator gain of 10000. The second loop is designed for an interferer with 3 kHz modulation bandwidth, since this is the bandwidth of voice channels that will be used later. From these studies, we can see that acquisition is no longer dominated by the amplitude-estimation response, but occurs at an earlier time when the FM signal instantaneous frequency crosses the strong signal frequency. The

Figure 22

Comparative Acquisition of Interference Cancellers: FM and Constant Frequency Input

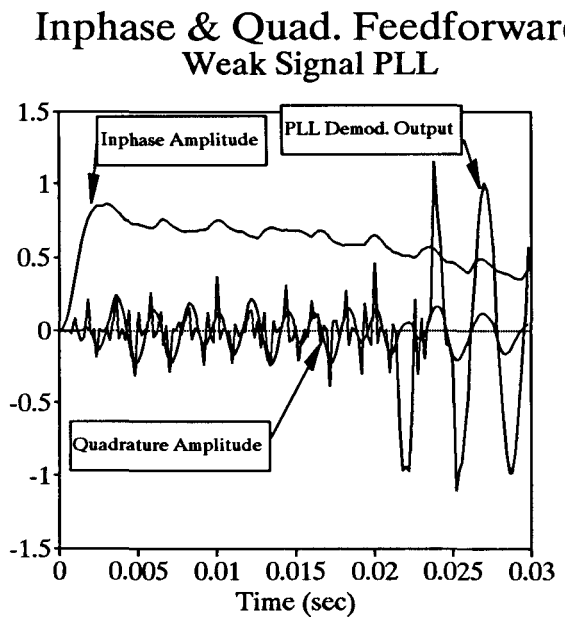

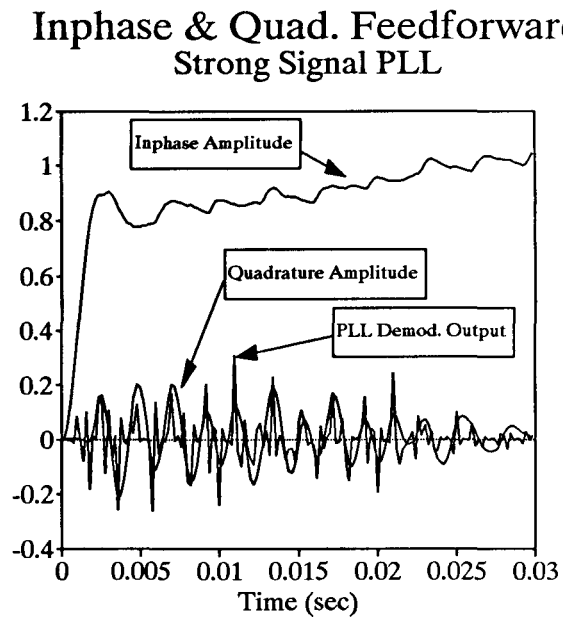

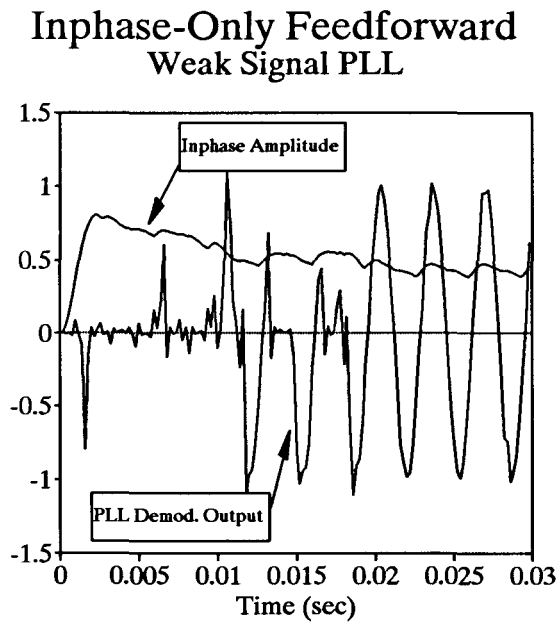

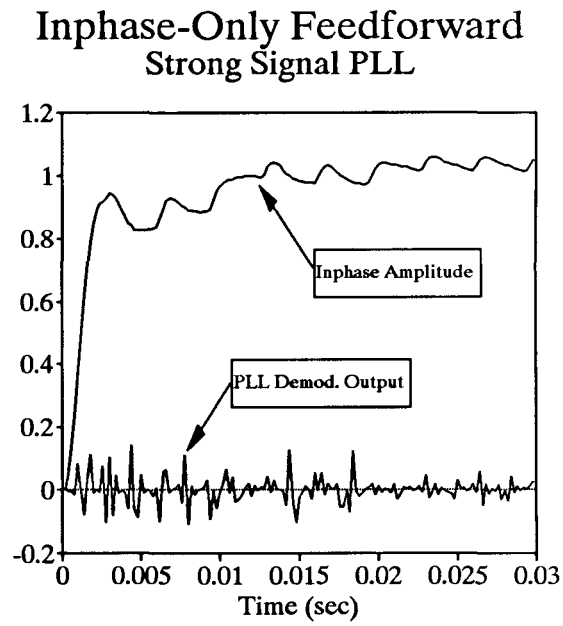

Figure 22 (continued)

Comparative Acquisition of Interference Cancellers: FM and Constant Frequency Input

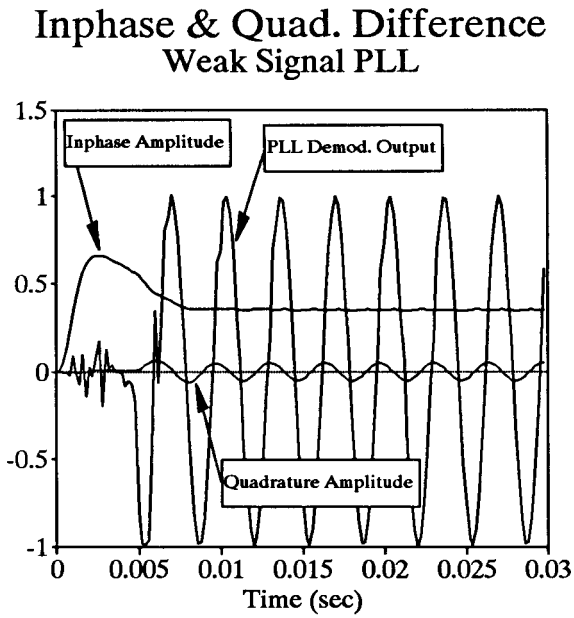

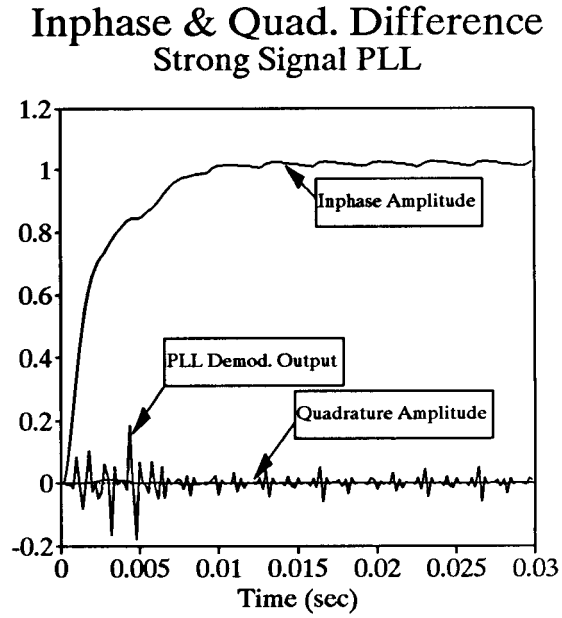

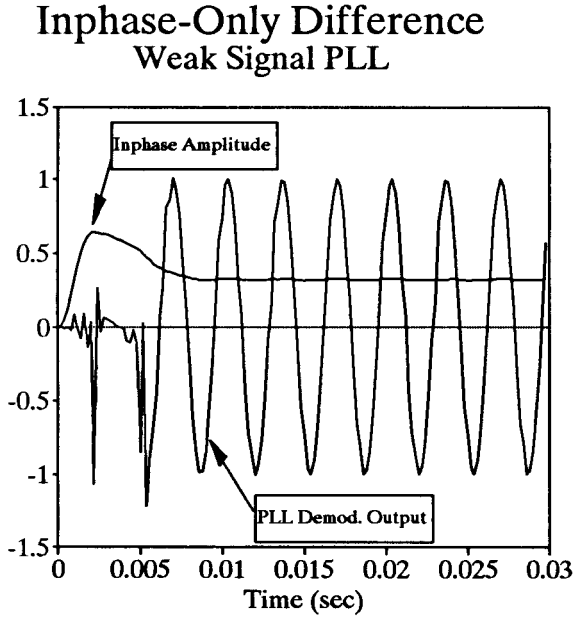

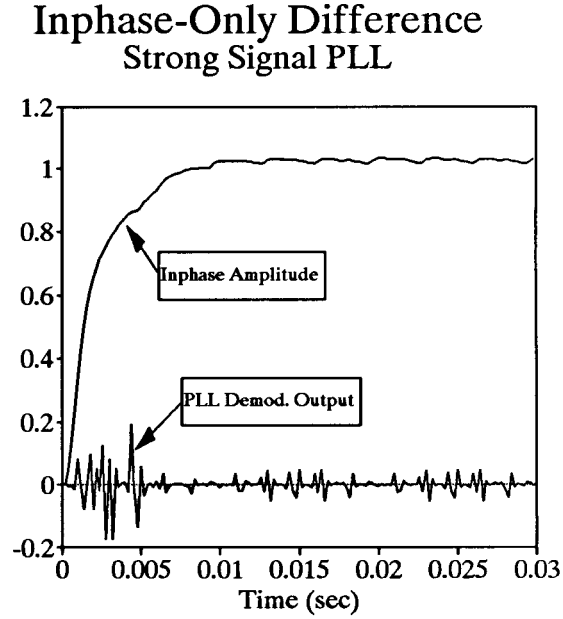

required level of strong-signal cancellation for weak-signal acquisition is less than the constant-frequency interference case because the weak signal crosses into the PLL's passband and can be acquired without as large a change in the PLL's phase and frequency estimates. In this case as well, the difference-amplitude forms exhibit better cancellation than the simpler cancellers, without any signs of instability. One major difference is that since the amplitude-estimation process no longer dominates acquisition, the inphase and quadrature amplitude-tracking forms no longer take significantly longer to acquire the signal than the inphase-only forms do.

3.6.2.2. Steady-State Behavior

Figure 23 shows an example of a "signal switching" behavior found in all the cancellers. This behavior is characterized by the two PLL's exchanging which of the two interfering signals they track. This phenomenon appears to occur when the interfering signals cross in instantaneous frequency, but it is also more common when the signals are close in amplitude. This makes sense in light of the fact that the signals are being separated precisely by tracking their amplitudes, phases and instantaneous frequencies. When the "distance" provided by these parameters becomes small, i.e., when the parameters of the two signals are momentarily close, confusion of the two signals becomes more likely. This hypothesis is supported by the FM weak-signal acquisition behavior described above and shown in Figure 22. If the receiver can identify the demodulated output of the two interfering signals, this effect is not damaging. Identification could be easily accomplished by placing a different tone in each potential interferer. Such identification would probably be implemented in a practical system anyway, as a means of detecting whether the desired-signal-to-interference ratio was adequate.

Figure 24 shows sample outputs for constant-amplitude FM signals. The strong signal is frequency-modulated with simulated voice. The voice simulation was based on a three-pole model with three formants at 500 Hz, 1000 Hz, and 2700 Hz.[2] Peak frequency deviation was 12 kHz. The strong-to-weak signal-power ratio was +6 dB, and the weak signal modulated by a sinusoid with the same FM parameters to make evaluation easier. As can be seen from Figure 24, both the strong and the weak

[2] I thank Professor Lloyd Welch of the University of Southern California for this voice simulator.

Figure 23

Signal-Switching Behavior of Interference Cancellers

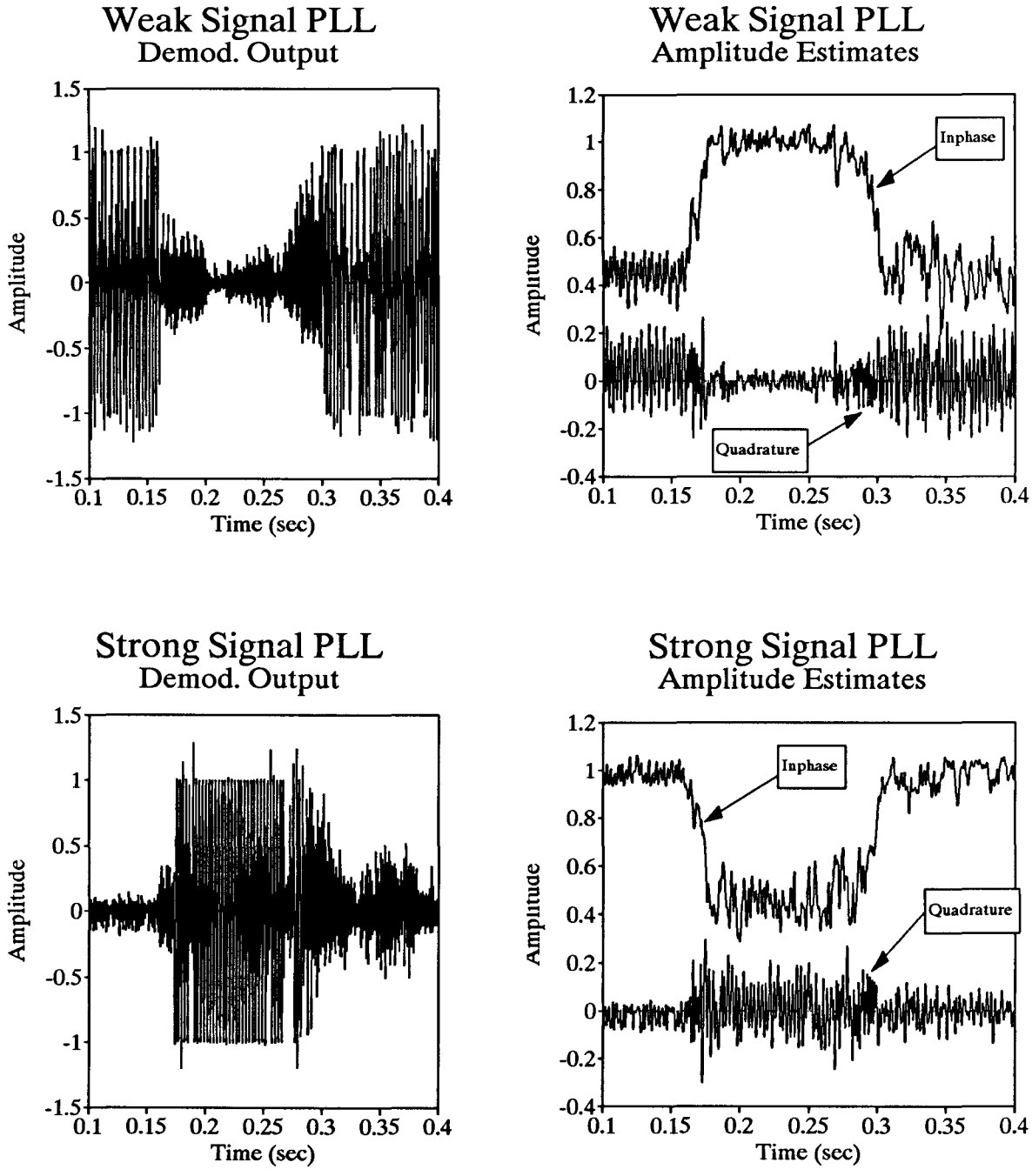

Figure 24

Sample Output Spectra for Interference Cancellers

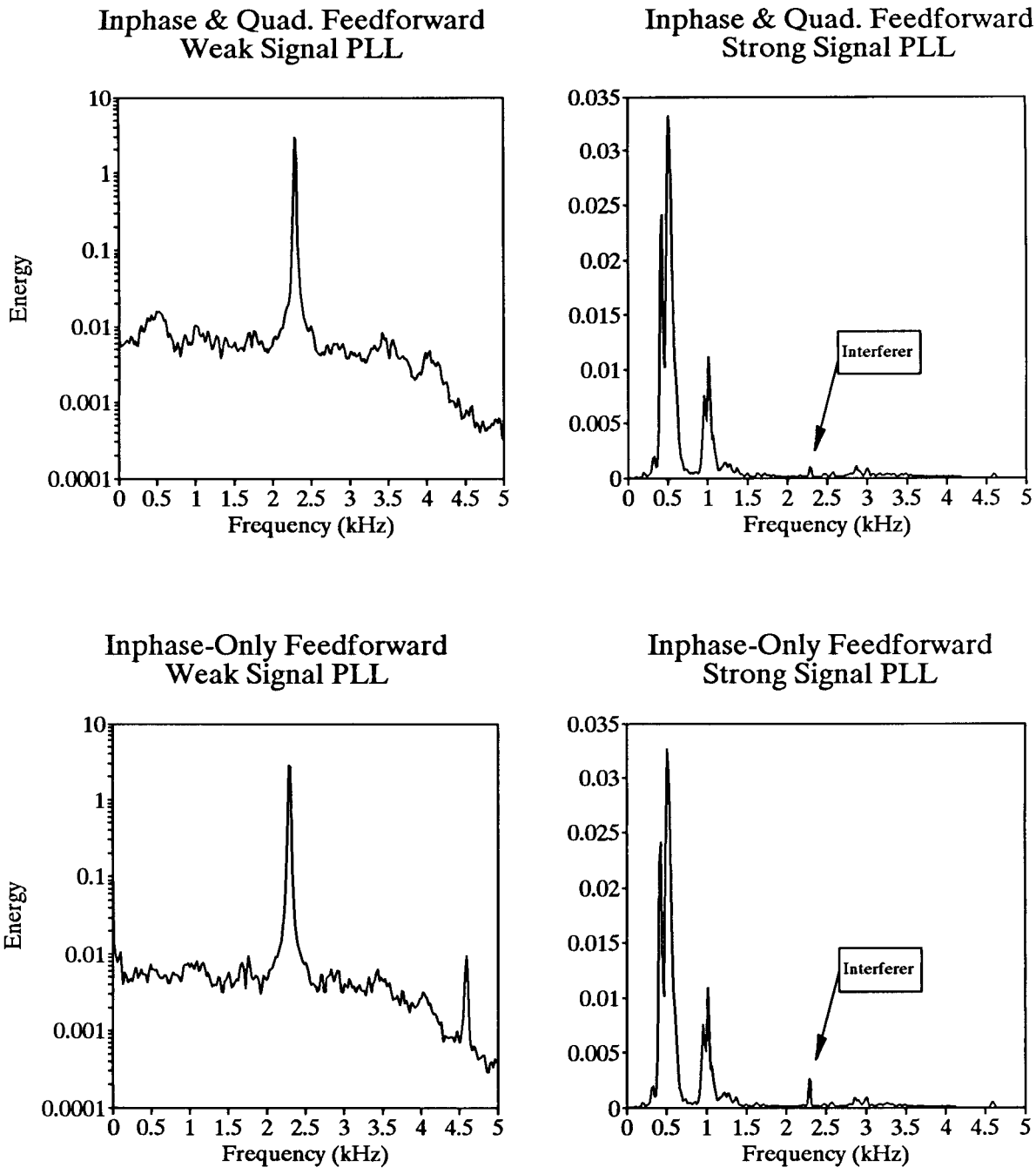

Figure 24 (continued)

Sample Output Spectra for Interference Cancellers

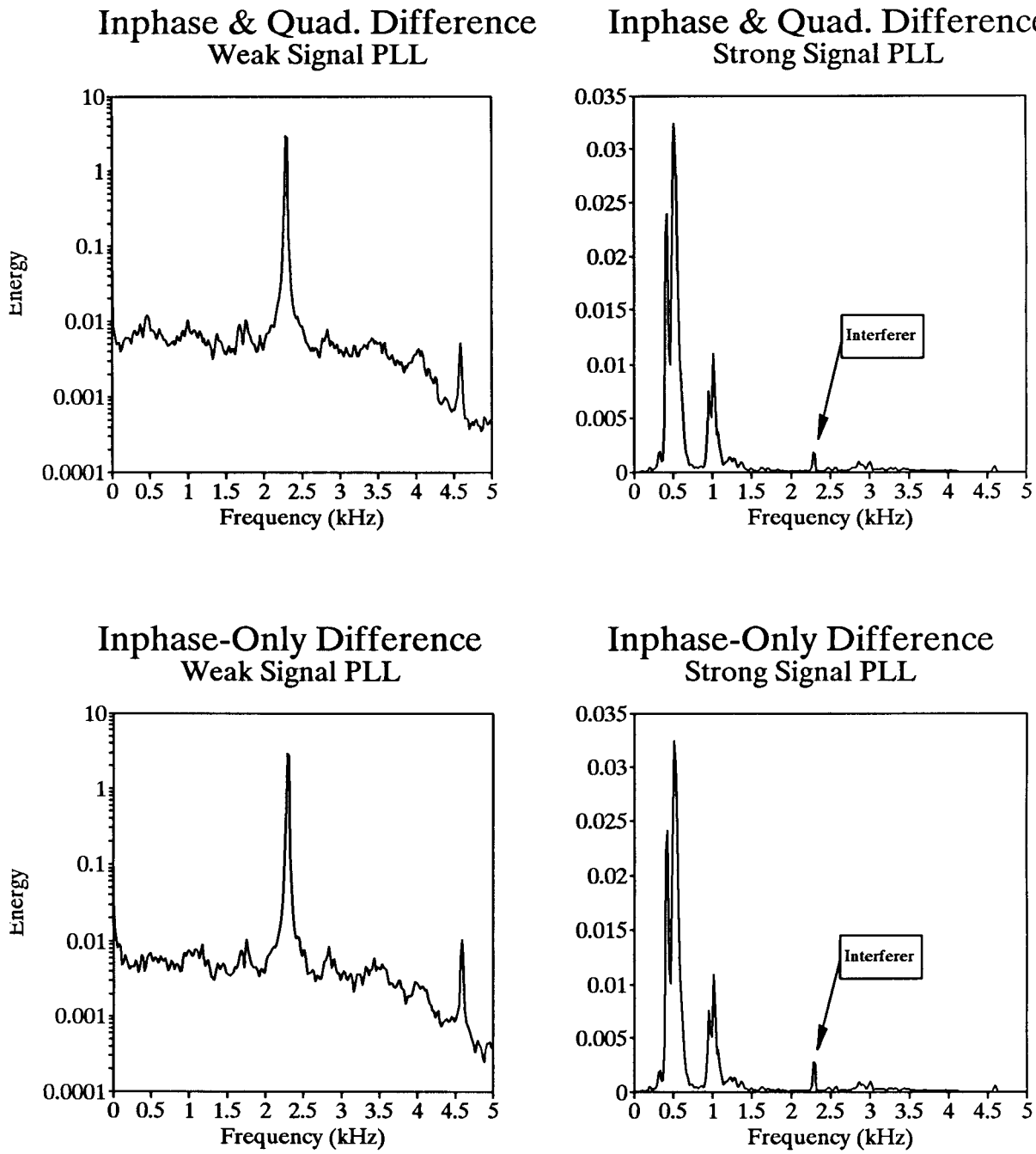

signals were demodulated with little residual interference in the demodulated products. PLL parameters were set according to the recommendations in [18]. The simulation results suggest that the difference-amplitude cancellers perform slightly better than the simpler forms, at least on constant-amplitude signals. However, their more complex dynamics may affect their behavior on channels with amplitude variation.

Further experimentation on these amplitude-preserving channels demonstrated good cancellation at a wide range of strong-to-weak signal-power ratios. However, since specific channel parameters will undoubtedly affect canceller performance, further experimentation on this somewhat ideal channel will not be discussed here. These results are meant to demonstrate the feasibility of applying the cancellers to real communications channels. They are intended not only to shed some light on the canceller dynamics, but also to motivate the experiments in Chapter IV on the cellular telephone channel.

3.7. Summary of CCPLL Improvements

Improvements to the basic CCPLL system based on the optimal MMSE amplitude estimator have been presented. A feedforward amplitude-estimation procedure results from direct solution of the MMSE amplitude equations. This simplifies the resulting system dynamics by reducing the number of defining differential equations from six to a maximum of four for both inphase and quadrature tracking. The tracking of the amplitude as a complex value is shown to provide little cancellation gain since the PLL generally tracks close in phase. The tracking loop for the quadrature-amplitude component not only increases the hardware requirements but also increases the amplitude-tracker noise bandwidth. In some simulation cases, we saw that the additional degree of freedom that was due to complex amplitude tracking increased weak-signal acquisition time. As a result, forms of the feedforward canceller that tracked only the inphase component of the amplitude were developed, further reducing the number of defining differential equations from four to two.

The reduction in differential equations made it possible to show that the system has a stable equilibrium at the desired steady state of tracking both signals. Furthermore, it was shown that the equilibrium of both loops tracking the strong signal is unstable. The perturbation analysis revealed that

the bandwidth of the amplitude-tracking loops, since it is generally less than the bandwidth of the PLL loop filter, was important relative to the instantaneous frequency difference of the two signals. The strong signal amplitude will corrupt the weak-signal amplitude estimate if a difference frequency term can pass the amplitude filters.

To minimize this source of corruption, a variation of the feedforward system was developed which develops the amplitude estimates from the input signals to the PLL - limiter assemblies, allowing the interference cancellation to reinforce the desired steady state. This variation, the difference-amplitude-tracking topology, was shown to possess the same stable equilibrium as the inphase-tracking feedforward system, but with greater immunity to periods when the instantaneous frequency difference is within the bandpass of the amplitude-estimation filter. However, the difference-amplitude-tracking topology was predicted to have more complicated dynamics than the simpler feedforward cancellers, with a potential for instability in the presence of no interference.

Simulation verified the above results, showing successful separation and demodulation of each of two co-channel interfering FM modulated signals by all four feedforward interference-canceller topologies (inphase and quadrature amplitude-tracking, inphase-only amplitude-tracking, inphase and quadrature difference-amplitude-tracking, and inphase-only difference-amplitude-tracking). The next chapter will examine the potential for application of these interference cancellers to the cellular telephone channel. All four cancellers will be tested on a simulation of the cellular telephone environment.

Chapter IV

Applications to the Cellular Telephone Channel

The cellular telephone channel is an important example of a multiuser channel since it uses the natural geographic attenuation of signals to allow a limited number of frequency slots to be reused across small "cell" areas. Rules for determining when a frequency may be reused are determined by tolerable interference levels; hence by allowing an increase in the level of interference that can be tolerated, frequencies may be reused more often within a given fixed geographical area. This would increase the cellular system's spectral efficiency, allowing more communications to take place over the existing limited spectrum allocation. The basic characteristics of the cellular telephone channel are described here along with a measure of the current spectral efficiency. The multipath fading property of this channel is examined and is presented as a major factor in interference-related call degradation. The problem to be addressed with interference cancellers is defined, along with estimates of the potential for frequency reuse gains. The interference cancellers of the preceding chapter are tested on a simulation of the multipath fading cellular channel, with encouraging results, and some of the practical economic aspects of a receiver hardware upgrade are discussed.

4.1. Overview of the Cellular Telephone Channel

The frequency-allocation of the cellular telephone channel in the United States, like that of other radio communications channels, is the product of much administrative regulation, and as such, can be administratively defined [33,34]. Since cellular voice transmission is full duplex as opposed to push-to-talk, the cellular channel is naturally divided into mobile-to-base and base-to-mobile frequency sets [33]. Because of the requirement for having competing cellular systems available in each metropolitan area, the available bandwidth in each set is then halved between two competing carriers. The individual channel spacing in the United States is set at 30 kHz, and voice transmission is FM with pre-emphasis and a maximum peak frequency deviation of ± 12 kHz [35].

Propagation in the individual channels has been modeled as an inverse fourth-order law [36,37]. Moreover, in more microscopic detail, the channel is plagued by multipath, resulting in short time-scale

Rayleigh fading and large-scale average lognormal shadowing [21]. Since the shadowing is highly geographically dependent and occurs in an average (long-term) signal level sense, it will not be dealt with further here. While shadowing may provide some relief from interfering signals, the Rayleigh fading devastates the on-average capture effect [21]. Fades of from 10 to 40 dB with durations on the order of one to ten milliseconds occur at rates from 1 to 100 per second [35]. However, it should be remembered that capture can be observed on the time scale of the FM channel bandwidth, or at least the tracking loop bandwidth for PLL's, a minimum of ±3 kHz. As a result, demodulator outputs can and do actually show signal capture during the relatively long time between fades.

Use of the cellular telephone system in the United States has grown at an unexpectedly rapid rate. Judging from continuing sales of new units, the demand is not yet saturated, even though the costs of use and subscriber equipment are still relatively high, with even the least expensive mobile phone units priced at over three hundred dollars. The technical challenge of serving such a large traffic volume over a limited frequency-allocation is the main one facing the growing cellular telephony industry. To help towards a solution, new multiaccess modulation and coding schemes are being generated elsewhere [7]. For them, implementation is still a long time off, partly because of the administrative process of obtaining a frequency-allocation, and partly because of the substantial subscriber investment in the existing cellular system. As a result, the discussion here is constrained to only those approaches using the current cellular telephone modulation and coding schemes.

4.1.1. FM Voice Modulation Parameters

The cellular telephone channel has 24 kHz allocated for voice transmission. Voice is syllabically companded (companded with a time constant on the order of 20 milliseconds), pre-emphasized and frequency-modulated [35]. The peak frequency deviation is 12 kHz, maintained by amplitude clipping if necessary [35]. The rms frequency deviation is 2 kHz, with f_{rms}^2 log normally distributed with standard deviation of about 5 dB [35].

4.2. Utilized vs. Available Channel Capacity

Evaluation of potential gains in spectral efficiency in voice channels is complicated by the relatively low information rate of speech. Improvements in source coding techniques such as vocoders can achieve significant reductions in the required transmission bandwidth. Since the focus here is on the spectral efficiency of modulation parameters, we desire a measure that is independent of source coding techniques. One such measure for evaluating the spectral efficiency of FM-based schemes can be generated by comparing the capacity of the received demodulated AWGN channel to the capacity of the wideband transmission channel.

For first-order Butterworth pre-emphasized FM transmission in Gaussian noise operating above threshold, the detected SNR is given by [1]:

$$SNR_D = \left(\frac{f_d}{f_3}\right)^2 \overline{m}^2 \frac{P_T}{N_0 W},$$

where N_0 is the noise power spectral density, W is the demodulated bandwidth, P_T is the signal power, while f_3 , f_d , and $\overline{m}$ are the 3 dB pre-emphasis frequency, the peak frequency deviation, and the average message amplitude, respectively. Noting that $(f_d\overline{m})^2$ is the mean-square frequency deviation (f_{rms}^2), and letting $\gamma = \frac{B_T}{W}$ be the bandwidth expansion ratio, the detected SNR becomes:

$$SNR_D = \gamma \left(\frac{f_{rms}}{f_3}\right)^2 SNR_T,$$

where SNR_T is the transmitted SNR.

For the continuous additive white Gaussian channel, the detected capacity is then given by:

$$C_D = \frac{B_T}{\gamma} \log(1 + \gamma \left(\frac{f_{rms}}{f_3}\right)^2 SNR_T).$$

Define the **capacity usage ratio** U_C as the ratio of the total available capacity C_T to the single-user detection capacity C_D:

$$U_C = \frac{C_T}{C_D} = \gamma \left[\frac{\log(1 + SNR_T)}{\log(1 + \gamma \left(\frac{f_{rms}}{f_3}\right)^2 SNR_T)}\right].$$

U_C represents the maximum number of independent users, each of rate C_D, that the transmission

channel could potentially support within its capacity limitation C_T. Any potential multiaccess protocol cannot provide a total information rate across all the users on a given frequency that is greater than the transmission channel capacity (see Chapter II, Section 2.3.3).

The bandwidth expansion coefficient in the cellular case is $\gamma = \frac{24kHz}{3kHz} = 8$. We see from the above equation that the capacity usage ratio for the additive white Gaussian model increases to 8 for large SNR_T. A plot of the capacity usage ratio U_C vs. SNR_T is shown as Figure 25.

The argument above suggests that at least in the additive white Gaussian model, the cellular channel might be able to support up to 8 users for large SNR_T. Proper use of the channel requires that the users be noninterfering, or that they transmit with sufficient information-theoretic redundancy that the effects of interference can be removed. It should be noted that as the SNR decreases to the FM threshold (about +8 dB for the modulation parameters of cellular telephone [36]), the approximate equations used for detected SNR become increasingly erroneous. So-called threshold-extension FM demodulators (such as phase-locked loop and frequency-compressive feedback FM demodulators) lower the threshold value and thus improve the performance in low SNR (or deep fades).

We now turn to examine what modifications to the capacity model would be required for the fading channel. As a simple model, consider the fading channel as a "block interference" channel [37] having two possible states. (A more realistic approach would give greater available capacity by considering the actual statistics of the fading channel, and calculating its capacity directly.) In the first state, the channel is approximated by the additive white Gaussian noise (AWGN) channel with signal-to-noise ratio equal to SNR_T. In the second, faded, state, which occurs with probability p, the channel is useless and can carry no information. Furthermore, let the amplitude track of the received desired signal provide the side information necessary to determine if the channel is in the useless state by setting some threshold value on the amplitude. Then the capacity of this interference channel, from [38], is simply the average of the two individual channel capacities:

$$C_T = (1-p)B_T\log(1+SNR_T) \ .$$

Treating the fades as erasures in the detection process, we get a similar expression for the limiting

Figure 25

Capacity Usage Ratio vs. SNR_T for the Cellular Channel (AWGN case)

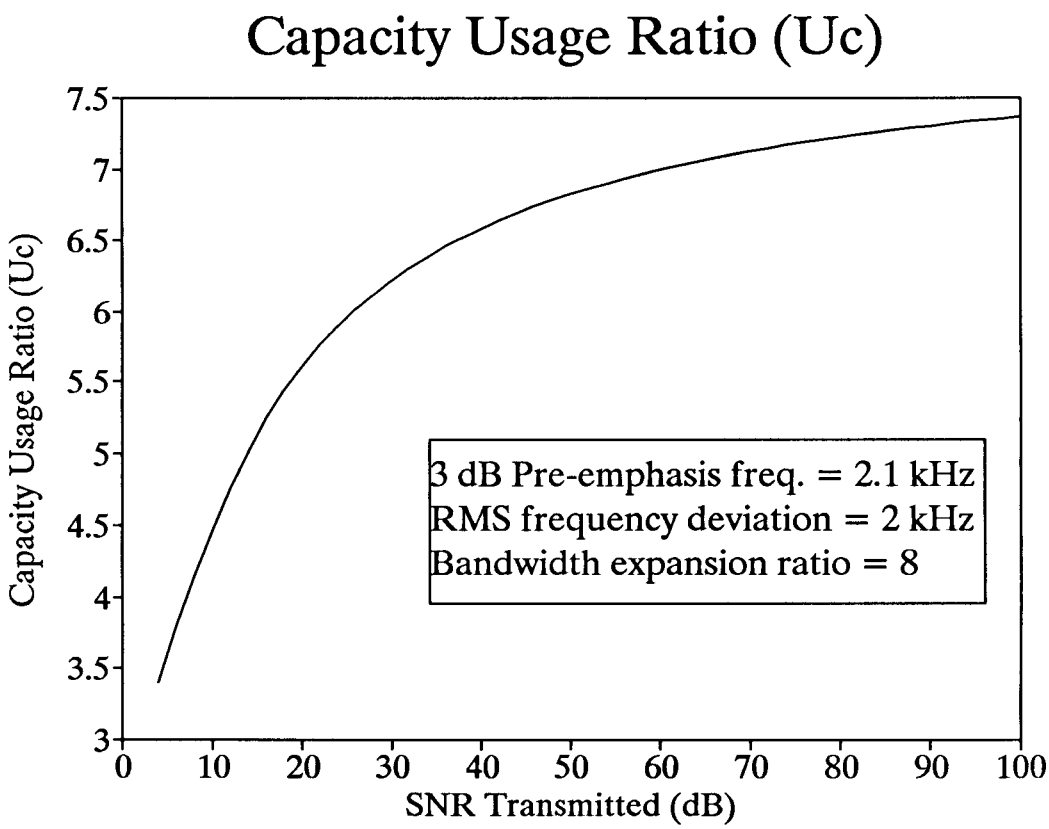

detected capacity:

$$C_D = (1-p)\frac{B_T}{\gamma}\log\left(1+\gamma\left(\frac{f_{rms}}{f_3}\right)^2 SNR_T\right),$$

so that the capacity usage ratio, U_C , is unchanged. The detected capacity here is a limiting capacity, assuming a receiver with sufficient complexity to interpolate the continuous modulating signal over the fades. For FM voice transmission, such a receiver might be considered as a vocoder that makes its estimate of the speech during the fades based on the prior speech. Current cellular receivers are far less complex than this, and, in fact, cannot reliably even detect fades, rather allowing short bursts of interference.

The current cellular system assigns only one user to each frequency-allocation slot in a given cell with inter-cell co-channel assignment spacing designed so that the average total signal-to-interference ratio is never less than about 18 dB [7]. Considering the interference as noise while using SNR_T as 18 dB, and using a standard 2100 Hz cutoff for Butterworth pre-emphasis [21], the current cellular system would have a capacity usage ratio of about 5.4 within a given cell. (Note that current coding and modulation support less than one user on a given frequency per cell. A given frequency is assigned a maximum of one time in any cell, and the same frequency cannot be assigned to every cell in a region under any reported assignment rule. Hence the usage ratio is only an upper bound to the number of such users that the channel could potentially support.) If the interference could be completely removed from the noise, the capacity usage ratio within a given cell might be increased up to the limiting 8, provided that the SNR that was due to noise alone were sufficiently high. This would allow 48% more users to be serviced in the channel-capacity-limited case for the FM modulation process in one limited geographic area. The larger number of users permitted by the higher usage ratio could be accommodated in practice by allowing decreased spacing for assigning the same frequencies, i.e., increasing tolerable levels of interference, until the detected signal-to-interference-plus-noise ratio after interference cancellation is equivalent to that for the original 18 dB.

4.3. Current Receiver Hardware

The current FM cellular telephone receiver is a simple limiter-discriminator demodulator. While the limiter-discriminator based receiver is inexpensive and simple to produce, advances in analog integrated circuits continually make more complex receiver designs practical. Entire loop-based FM receivers integrated on a chip can be purchased by consumers for under 5 dollars (e.g., Radio Shack TDA7000). At this cost, the cellular telephone receiver, the main element responsible for call quality in a cellular phone costing several hundred dollars or more, can certainly afford to have some money spent on improved performance, especially to increase the traffic capacity.

4.4. Multipath and Call Degradation

The signal that the cellular telephone receiver must demodulate has been characterized as one plagued by multipath fading. The facts that the mobile is in motion and that there are several received signal paths combine to produce a received signal whose amplitude is Rayleigh distributed and with >5 dB signal fades occurring at rates of 50 - 100 Hz. Larger fades (>10 dB) can occur more frequently than 1 per second ([35], [21]). The fading errors come in bursts of duration inversely proportional to vehicle speed, with the 10 dB fades lasting an average of 10 milliseconds at vehicle speeds of 20 mph [35]. This severe multipath environment presents the main problem in FM mobile communications.

Because of this rapidly varying environment, the FM signal must be strong enough to overcome the more frequent fading, and must be fairly robust in the presence of deeper fades. For data communications, the situation is a problem that can be solved by appropriate burst-error-correction codes, but they will not be considered here. Instead, only the problem of voice channel degradation is considered.

From the standpoint of information theory, we have seen that discarding amplitude information is a lossy process. At worst, an amplitude track can at least provide a figure of confidence for the frequency estimates taken at the same time to be used as side information in further filtering processes. At best, the amplitude tracks can be used to feed a received-signal environment model in an effort to separate the signal of interest. As an example, consider the case of an angle-modulated signal in addi-

tive Gaussian noise. Clearly, the angle information will be corrupted the most when the received amplitude is near its mean, and the received information will be the least corrupted when the amplitude is nearest its maximum and minimum (Figure 26), except in the case of origin encirclements. These can be more easily detected with amplitude information, since a time track of the amplitude will decrease at the same time as the instantaneous frequency is increasing. By using the amplitude information inherent in the received signal, a joint estimation (amplitude and phase) approach has been shown to produce reception with 5 dB better output signal-to-noise ratio than more conventional PLL-based receivers [22].

4.5. Interference Power and Call Quality

For high-traffic cellular systems, the interference power is usually significantly greater than the background noise power [21]. Frequency allocation schemes must meet the requirement that the minimum mean signal-to-interference ratio be +18 dB [7], in the current scheme. At first glance this seems more than a little conservative, considering the FM capture effect. However, the basis for the SIR requirement is derived not from considering a signal of constant power, but from the maximum tolerable losses under multipath fading [36,38]. For speech systems, tolerable variations in maximum acceptable probability of loss that is due to multipath fades vary from .1 as the highest acceptable value for speech down to 0.01 for a high-quality speech system [36]. The problem for the interference canceller is then to reduce the level of interference sufficiently so that track of the desired signal can be maintained through a fade without loss. Because tracking through the time evolution of a fade is the important parameter, the fading characteristic of the cellular channel will have to be accurately simulated not just in its time-average Rayleigh statistics but also in its time-evolving behavior. Such simulators inevitably are based on direct simulation of the physical environment, combining multiple paths with different phase and doppler shifts to produce a fading resultant. This kind of simulator is used in the next section.

4.6. Cellular Channel Simulator

Figure 26

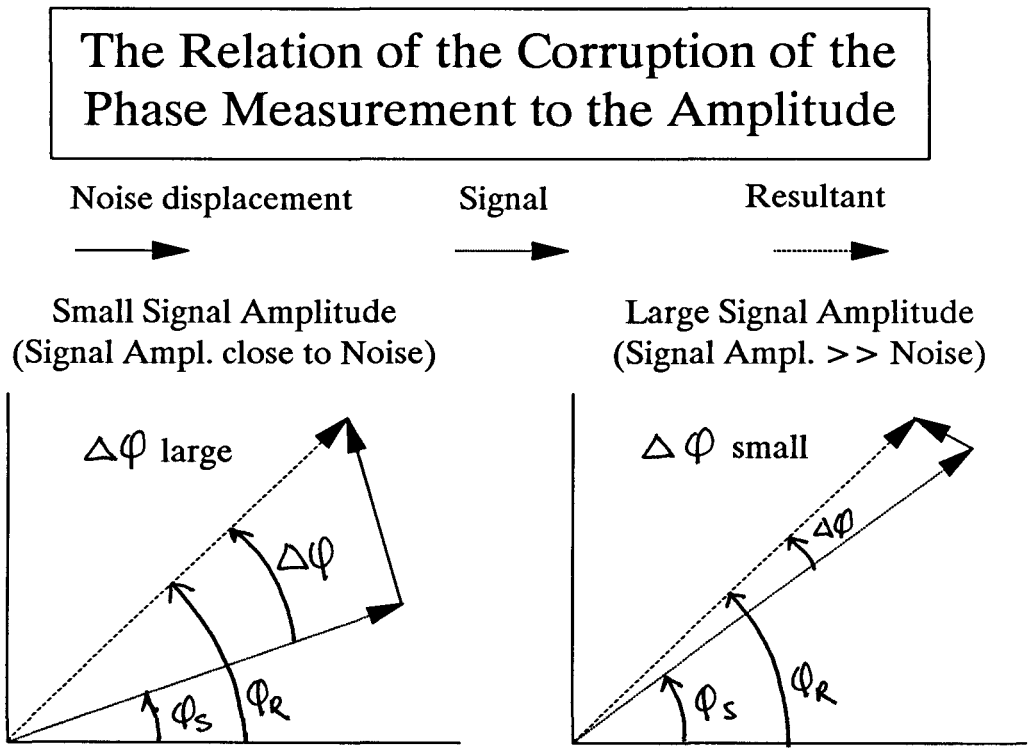
The Relation of the Corruption of the Phase Measurement to the Amplitude
Noise displacement
Signal
Resultant
Small Signal Amplitude
(Signal Ampl. close to Noise)
Large Signal Amplitude
(Signal Ampl. >> Noise)
Δφ large
Δφ
φs
φR
Δφ small
Δφ
φs
φR

The interference canceller was evaluated in the cellular telephone environment by using the multipath simulation form proposed by Jakes in [21]. The large-scale effects of lognormal shadowing present in the cellular channel were left out of that model, since they can be easily modeled as a decrease in the average SIR. In this method N paths, equally distributed in angle of arrival and randomly (uniformly) distributed in phase, are summed to produce the inphase and quadrature AM components. Symmetric paths are lumped together so that there are only $N_0 = \frac{1}{2}(\frac{N}{2} - 1)$ complex signals to sum. The differing angles of arrival produce different doppler shifts for the individual paths. The maximum doppler shift of a path, ω_m , is a parameter for the simulation. The maximum doppler shift used was 90 Hz, corresponding to a speed of about 70 miles per hour at 800 MHz. The inphase and quadrature components of the envelope, both approximately Gaussian, were computed as:

$$A_I(t) = 2\sum_{n=1}^{N_0} \cos\beta_n \cos\omega_n t + \sqrt{2}\cos\alpha\cos\omega_m t \ ,$$

$$A_Q(t) = 2\sum_{n=1}^{N_0} \sin\beta_n \cos\omega_n t + \sqrt{2}\sin\alpha\cos\omega_m t \ .$$

Here the doppler and phase shifts of the n th path are denoted by ω_n and β_n, respectively, and α represents the phase shift of the channel with the maximum doppler shift. The resulting signal-amplitude statistics for $N_0 = 8$ showed the desired lowpass Rayleigh fading characteristics, an example of which is shown in Figure 27.

4.7. Improving the Cellular System

The ultimate goal of interference cancellation on the cellular channel is to allow reception limited only by the signal-to-noise ratio in all the available bandwidth in all regions, and without capacity reduction from interference. It seems unlikely that with only receiver changes but without a change in modulation or coding techniques, interference can be so completely mitigated. We therefore must find intermediate measures of improvement against which proposed systems can be evaluated. One such measure is improvement of the minimum mean SIR for toll-quality speech reception, when using the current modulation specification. A successful application of interference cancellation would tolerate a lower mean SIR level. This would clearly allow a single-user frequency assignment (30 kHz) to be

Figure 27

Cellular Channel Simulator Statistics

FADESIM parameters:

Sample rate : 20 kHz
Maximum Doppler : 90 Hz
Number of angle components (N_0):8

Summary inphase statistics: Maximum = 8.81, Minimum = -10.33, Avg = -0.0104

Histogram of inphase amplitude:
(bin 0 is minimum, bin 100 is maximum, bins are equally spaced)

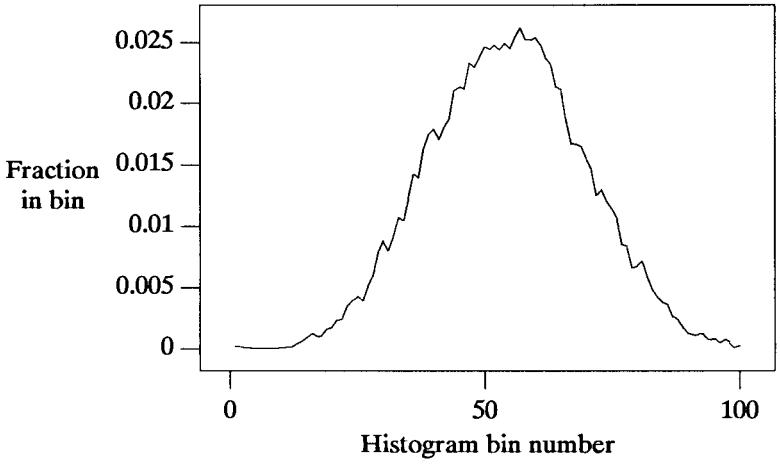

Summary quadrature statistics: Maximum = 8.71, Minimum = -11.06, Average = -0.00208

Histogram of quadrature amplitude:
(bin 0 is minimum, bin 100 is maximum, bins are equally spaced)

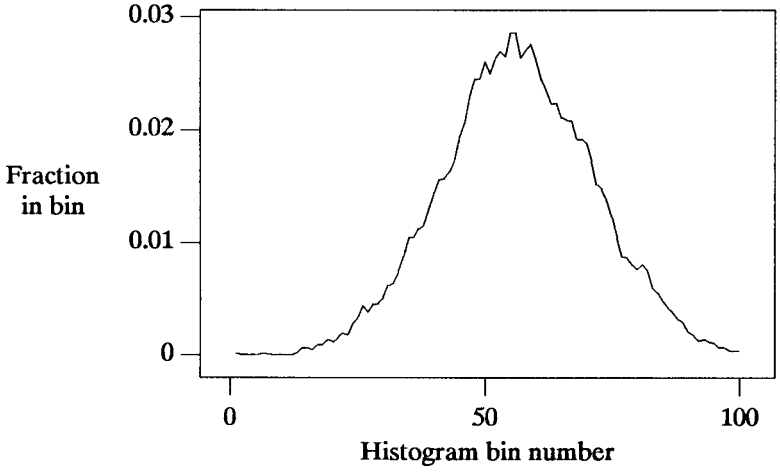

(Results were normalized for unit average power prior to use in simulations)

reused more closely than is currently possible.

Whether predetermined fixed-frequency assignments or dynamically allocated frequency assignments are used in a cell to allocate the spectrum among users, the efficiency with which the spectrum is used is limited by the minimum spatial separation between two assignments. In a nonfading environment, the minimum separation between two assignments could be calculated directly from the minimum mean SIR by using the measured propagation law. In a multipath fading environment, this separation must be derived from the minimum tolerable SIR that can be taken on an instantaneous basis during a fade, considering the maximum allowable dropout probability. The minimum mean SIR is not the key parameter here. For example, a minimum tolerable SIR of 0 dB would still not allow reuse of a signal within its own cell. According to [36], the minimum tolerable SIR in FM systems usually requires empirical derivation, since it is highly dependent on the particular receiver in use. For these purposes a reasonable minimum tolerable SIR value for current receiver technology is given as +8 dB [36].

4.8. A One-Dimensional Model for Estimating Frequency-Reuse Distance Improvements

In [36], the probability that the fading signal will be above the minimum tolerable SIR (used as a measure of call quality) is derived for a one-dimensional system as an easily calculated function of the separation between a receiver and two transmitters (one desired and the other interfering). The transmitters are positioned at points on a line with the desired-signal transmitter at 0 and the interfering transmitter at 1. The receiver's position along the line is denoted by x. Analysis of this interference case assumes that one interferer contributes most of the interference power. Based on a fourth-order propagation law and a Rayleigh fading environment, the probability that the fading signal will be above the minimum tolerable SIR a^2 is

$$P = \frac{(1-x)^4}{a^2x^4 + (1-x)^4}.$$

This approaches zero as a approaches infinity, and is equal to 1 at a equal to zero, as must be.

From [36], a high-reliability voice system would have a one-percent probability of a fade below minimum tolerable levels. Data communications would require a much lower fade probability and

would require burst correction; however, since the focus of these studies is on voice communications, we will accept the voice value of one percent. Substituting this value of 0.01 (-20 dB) for 1-*P*, we obtain a fourth-order polynomial, the roots of which in the interval between zero and one give the maximum reception distance away from the desired-signal transmitter:

$$(.01 - a^2)x^4 - 4x^3 + 6x^2 - 4x + 1 .$$

The roots of this equation can be easily found for a given value of a, which gives the maximum fractional distance, x, that a receiver can be away from its desired transmitter in this simple model without unacceptable levels of interference. Because the area in which the frequency can be used determines coverage in a land-based system, spectral efficiency is related to x^2, the square of the radius within which the frequency can be used with acceptable interference [38]. By reducing the minimum tolerable SIR, a , as in FM threshold-extension receivers such as PLL's and frequency-compressive feedback receivers [1], the allowable transmitter-receiver separation can be increased. (Interference-cancelling receivers do not exactly fit the FM threshold-extension receiver definition, since they do not extend performance against noise. However, they do extend the tolerable levels of interference, the parameter of interest here.)

Solutions for the roots of the polynomial above are tabulated in Table I for some values of the minimum tolerable SIR. The areas relative both to the use radius for a system where adjacent cells can use the same frequency ($x = 0.5$, $SIR_{\min}$ = -20 dB) and to a system with minimum tolerable SIR of + 8 dB (from Section 4.7) are computed in Table I.

Table I represents the potential gains achievable by reducing the minimum tolerable SIR; however, they do not represent actual minimum-use radii since they allow for only one interferer. Even for a requirement of SIR greater than or equal to +18 dB, the results above are liberal with respect to current, fixed-frequency-allocation rules. For example, the current fixed-frequency-assignment rule for seven channel sets requires at least 2 cells between cells using the same frequencies [33]. The requirement of at least 2 cells between cells using the same frequencies translates to a maximum-use distance of x = 0.17. According to Table I for a minimum tolerable SIR of +18 dB, which achieves maximum use distance of x = 0.26, one cell diameter would fit between the two cells using the same frequency,

Table I : One-Dimensional Maximum Frequency Use Distance versus Minimum Tolerable SIR

SIR_{min} (dB)	x	x^2	Area rel. to $x = 0.5$	Area rel. to 8 dB area
18	0.261	0.0682	0.2728	0.4766
15	0.295	0.0870	0.3481	0.6083
12	0.331	0.1092	0.4369	0.7634
9	0.366	0.1343	0.5372	0.9386
8	0.378	0.1431	0.5723	1.0000
6	0.401	0.1609	0.6435	1.1244
3	0.432	0.1867	0.7467	1.3048
0	0.457	0.2089	0.8358	1.4603
-3	0.475	0.2257	0.9027	1.5773
-6	0.486	0.2367	0.9467	1.6542
-9	0.493	0.2432	0.9728	1.6997
-12	0.497	0.2468	0.9871	1.7248
-15	0.499	0.2487	0.9947	1.7380
-18	0.500	0.2496	0.9985	1.7448

which is a 56% larger cell radius, and 143% larger cell area than the seven-channel, fixed-frequency-assignment rule. This shows that the frequency is being used with acceptable quality over a larger region. However, under conditions where only a small number of interferers are dominant, dynamic frequency-allocation schemes might actually perform similarly to the model above. Dynamic assignment algorithms would potentially make better use of the reduction in minimum tolerable SIR than fixed-frequency assignments because they can take advantage of smaller changes in the allowable interference power.

The results tabulated in Table I can also be used to demonstrate the potential gains in spectral efficiency by reducing the minimum tolerable SIR. Assuming that the use area in a more realistic case would be proportional to that computed here, we can consider improvements in proportion to the +8 dB minimum tolerable SIR use area. Reduction from the +8 dB minimum SIR level to the 0 dB level, for example, would increase the service area covered by one frequency by 46 %. Since the interference canceller must be able merely to receive the weaker signal in order to cancel it, reduction of the minimum tolerable SIR below 0 dB is not unrealistic. This same principle implies the possibility of overlapping regions of reception where either of the interfering signals can be received, as in the information-theoretic results of Chapter II. Without considering overlapping, a decrease in the minimum SIR level to the -18 dB level would give a 75 % increase in the serviceable area. This same decrease would allow for adjacent cells to reuse the same frequency in the one-dimensional model above.

4.9. CCPLL Operation in the Multipath Channel

In previous attempts to apply CCPLL interference-cancellation techniques to multipath channels [18], the canceller was intended only to remove the self-interference that produces the Rayleigh fading envelope. A single desired-signal path would be demodulated as the desired signal, with other paths of the same signal being cancelled as interference. In theory this would enable the canceller to eliminate the Rayleigh fading envelope imposed on the desired signal by the combination of many different signal paths with different time delays and doppler shifts. In practice, however, the paths were too highly

correlated for independent amplitude estimation [18], and hence the multipath cancellation failed. In the preceding chapter we saw that the amplitude estimate for a given signal component, in this case a given signal path, is corrupted by an amount related to its separation in frequency from the other signal components. For doppler shifts that are small relative to the modulation bandwidth, many signal paths will pass through the amplitude-estimate filters into each single path's amplitude estimate. If the amplitude-estimate filter bandwidths could be made arbitrarily small, this problem might be avoided; however, such narrowing of the amplitude-estimate filters would proportionally increase both acquisition time and the time it takes to adjust to small changes in the reception environment. Therefore, we chose a different approach to interference cancellation on the multipath channel.

As we learned in Chapter III, the effectiveness of the interference cancellers is related to the frequency difference between the two signals to be cancelled. Since different paths are shifted only by their relative doppler, which is small in proportion to the modulation bandwidth (a maximum of $\pm$ 90 Hz as calculated in Section 4.6), separation of paths should not be particularly effective. Hence we apply the interference canceller in such a way as to make use of the difference in instantaneous frequency between uncorrelated, co-channel interfering FM signals. The application of interference cancellers here will be directed at receiving both the stronger and the weaker of two signals. This approach, motivated by the information-theoretic results of Chapter II, is quite different from the earlier approach in [18], which was really more an attempt at channel equalization than interference cancellation.

The interference canceller must be able to track signals with time-varying amplitudes. This was not done in the previous chapter. In an effort to track the Rayleigh fading envelopes of the signals with minimal delay, the amplitude-estimation filters are chosen to be first-order Butterworth filters with cutoff frequencies larger than the bandwidth of the amplitude modulation. In order to force a desired PLL to be the first to acquire a signal, the amplitude-estimation filter was made wider on one loop than on the other. The amplitude loop bandwidths were 400 Hz for the weak-signal estimator and 200 Hz for the strong-signal estimator. The cellular channel simulator described in Section 4.6 provided the amplitude fading paths. Representative snapshots of the fading-power time sequence are shown in

Figure 28.

The PLL's must be able to separate signals with the same general modulation characteristics but with widely varying instantaneous power levels. Without the Rayleigh fading, the loop parameters would be proportional to the power ratio as suggested in [18]. The fading channel makes determination of the exact power ratio to be used difficult, but it is reasonable to design the loops for the mean-power ratio. In a practical application the mean-power ratio could be estimated or controlled in order to get the best response, but for this test case we will choose a fixed value. For these simulations, since the ultimate goal is to separate interferers with close mean-power levels for frequency reuse in the same cell, the loops are designed for a mean-power ratio close to one. Again, as in Chapter III, no attempt was made at optimizing the loop parameters for the expected modulation characteristics. The PLL's were designed using the rules from [18] for 3 kHz modulation bandwidth at 12 kHz peak frequency deviation and a weak-to-strong amplitude ratio of 0.85 (1.4 dB SIR, strong to weak). Experimental results in [18] indicate that performance is improved by matching the power level to the "weak" signal loop parameters. As a result, performance may suffer slightly at signal-to-interference ratios away from 0 dB.

One advantage of designing around a power ratio close to one is that the bandwidths of both loops are kept small. This permits cleaner phase tracking of both signals in any case, since both PLL's now see a smaller instantaneous bandwidth. Both the fading, which shifts the signal phase as well as its amplitude, and the small loop bandwidths required for operation at a mean-power ratio close to one predictably make the instantaneous loop phase errors larger. The error will degrade the performance of the inphase-only amplitude-tracking interference cancellers relative to the inphase and quadrature tracking forms, which can correct for loop phase error in the amplitude estimates.

In addition to expecting better performance from the inphase and quadrature amplitude-tracking forms, we also expect the difference-amplitude-tracking configurations to perform better than the feed-forward configurations. This is because the fading channel requires amplitude tracking at a bandwidth close to the lower edge of the modulation bandpass. More interfering signal power can come through the amplitude filters, causing corruption of the amplitude estimate. As we saw in Chapter III, the main

Figure 28

Close-up View of Channel Fading

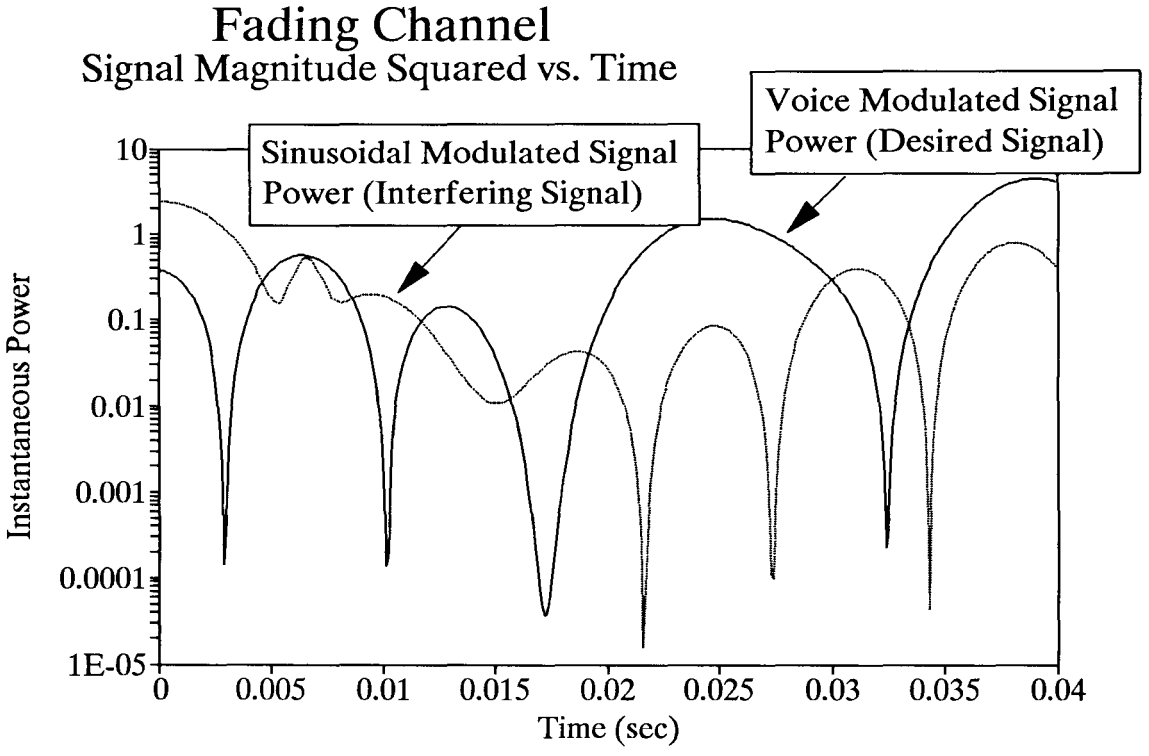

advantage of the difference-amplitude configurations is the reduced corruption of amplitude estimates by the interference. In a system where the amplitude-tracking filters are wider, this factor should become important in determining performance.

4.9.1. Small Time-Scale (order of 10 msec) Performance

Figure 29 shows a close-up view of acquisition of two fading signals at several mean SIR's for the inphase and quadrature difference-amplitude canceller. The envelope traces given before in Figure 28 correspond to the demodulated outputs in Figure 29. The modulation on the strong signal is simulated voice, as in Chapter III. In order to make the evaluation of interference in the demodulated outputs easier, the weak-signal modulation in Figure 29 is a sinusoid (840 Hz) with the same FM modulation parameters as the voice. The voice has not been companded, nor has it been pre-emphasized as in the cellular system. The application of the operations of companding and pre-emphasis was omitted so that the contribution of the interference canceller could be easily evaluated. However, the application of the two operations would probably improve performance, since both are known for reducing the effects of interference. The companding process is, for example, noted to suppress FM "click noise" [35]. Short bursts of interference getting through the canceller would indeed manifest themselves as click noise. The compander would attenuate the interference that passed through the canceller, making it difficult to determine how much interference suppression was due to the canceller. Pre-/de-emphasis would likewise suppress high-frequency interference.

Figure 29 shows the relatively fast acquisition of both signals even in the fading environment. At 0 dB SIR, both signals are acquired within 2 msec, a time commensurate with the amplitude-estimation filter bandwidth of 400 Hz. Even at +13 dB SIR, the weak interfering signal is acquired within 10 msec. Secondly, comparing the results of Figure 29 with the input fading-power levels shown in Figure 28, it is clear that the amplitude estimates do not follow the fades, but rather seem to acquire a time-averaged estimate. This is somewhat surprising since the bandwidths of the amplitude-estimation filters are certainly wide enough to respond to the fades; however, in this coupled system, the PLL's, with their faster time constants, could be responding to the fades by adjustments to their instantaneous

Figure 29

Close-up View of Interference-Canceller Outputs

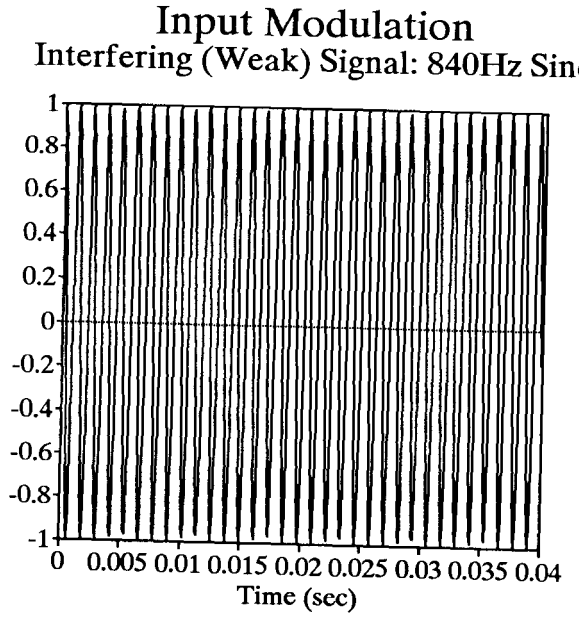

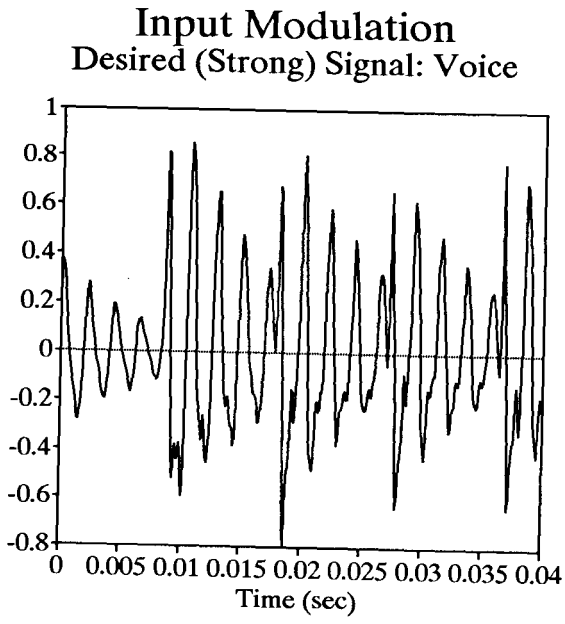

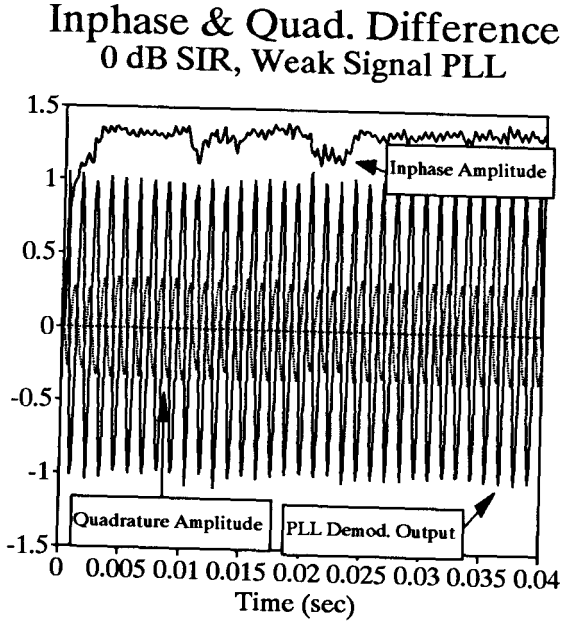

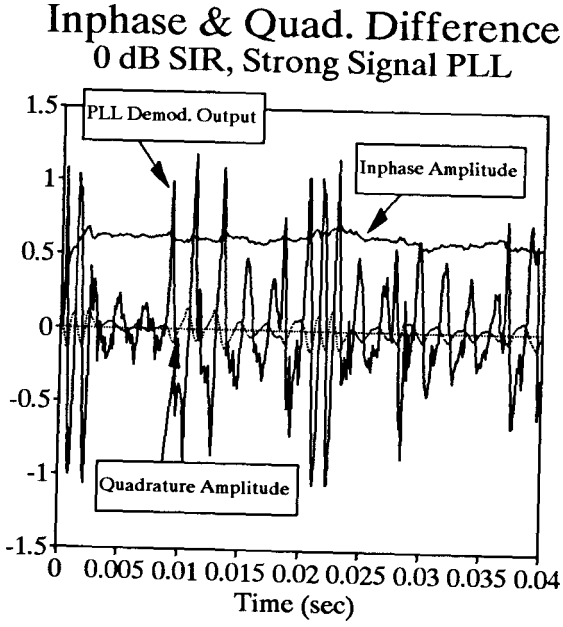

Figure 29 (continued)

Close-up View of Interference-Canceller Outputs

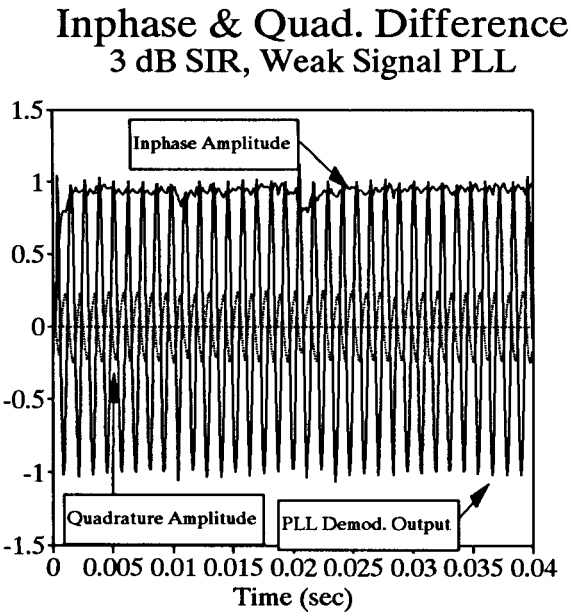

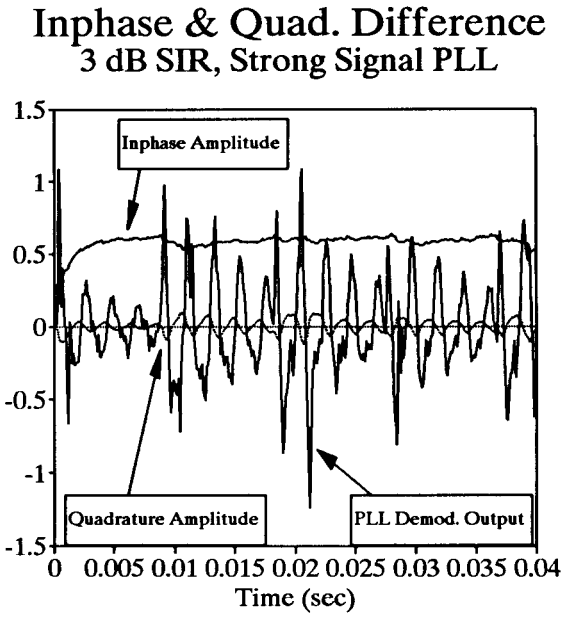

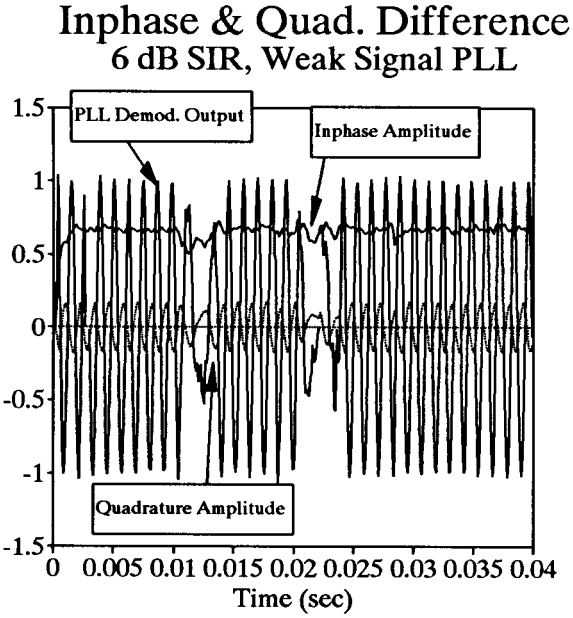

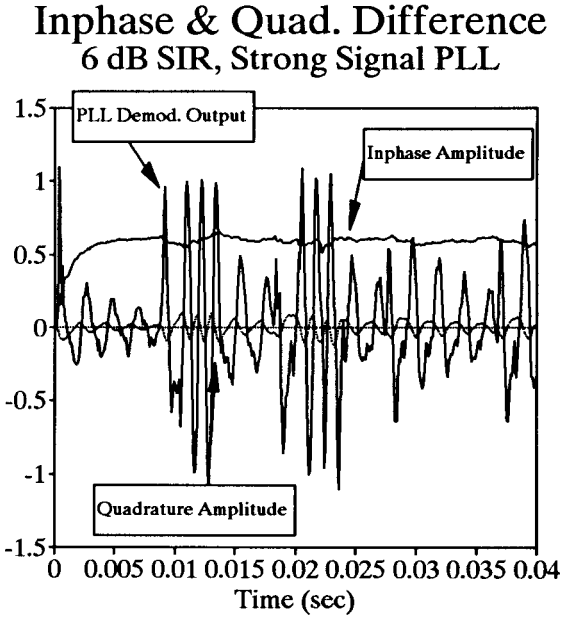

Figure 29 (continued)

Close-up View of Interference-Canceller Outputs

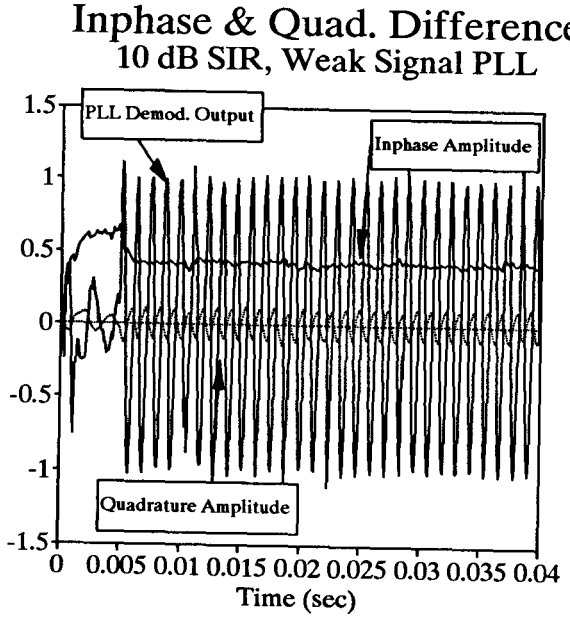

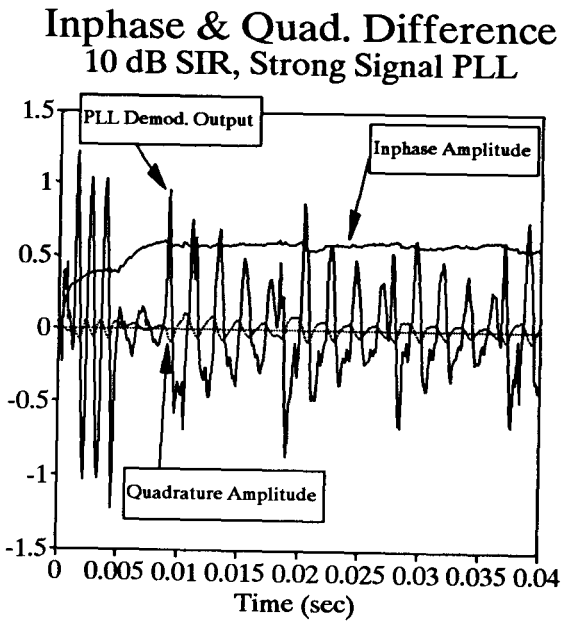

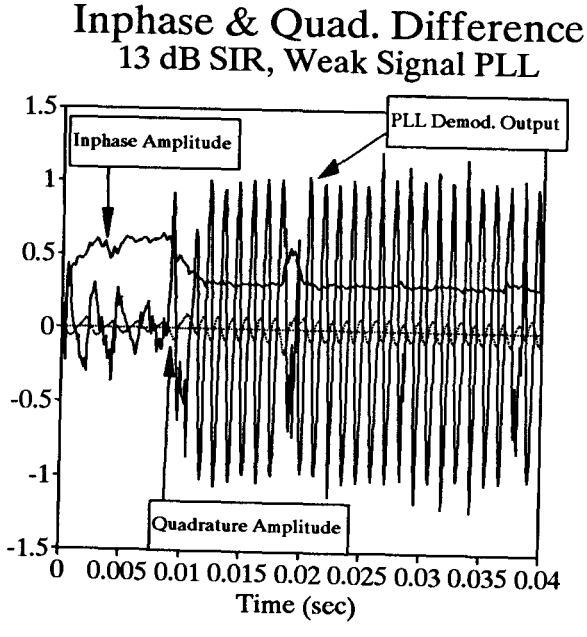

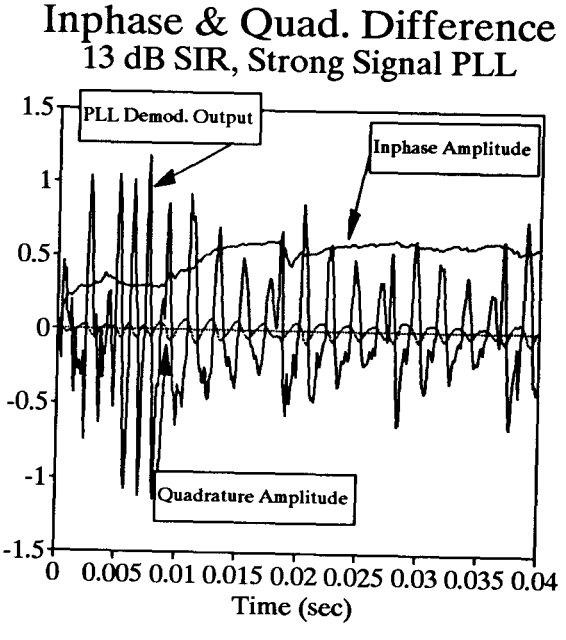

phase offsets. Figure 29 shows the system remaining in lock with both signals, despite the fading channel, at SIR's of +3 dB and 0 dB. As we foresaw, performance away from the designed operating SIR is degraded. Lock on the weak interfering signal is temporarily lost during fades at SIR's below +3 dB; however, except for a few incidences of signal-switching behavior like that reported in Chapter III, the strong signal does remain unaffected.

4.9.2. Longer Time-Scale Performance

Figure 30 shows the results of a full second of simulation. The first thing to notice is that the behavior of the inphase and quadrature difference-amplitude-tracking configuration is superior to the other forms, as we foresaw. The narrow loop bandwidths have contributed significantly to the phase error, as is evidenced by the activity in the quadrature-amplitude estimates. If the loops were tracking the signals with small phase error, the quadrature-amplitude estimates should be negligible. As a result of the phase error, the inphase-only tracking forms were able to cope effectively with the interference only at mean SIR levels of +13 dB, still a 5 dB gain over the current mean SIR requirements [7]. As expected with the wide amplitude-estimation filters, the difference-amplitude-tracking forms significantly outperformed the other forms. All the cancellers were tested with the same design parameters. It is important to remember that the performance of the other cancellers may be improved by optimization of these parameters for each particular design, but for now we see that we can select the inphase and quadrature difference-amplitude (IQDIF) configuration as the best performer.

Initial analysis of the results in Figure 30 indicates that at 0 dB mean SIR, the IQDIF canceller suppressed the sinusoidal modulation by almost 27 dB. This figure is calculated by taking the total energy in the sinusoid modulation and dividing it by the energy at the 840 Hz sinusoid frequency in the voice-signal demodulated output. The original voice signal did not have any appreciable energy at that frequency, and examination of the spectrum does not reveal much in the way of intermodulation products. Since the sinusoid is always present in the interfering signal, suppression by 27 dB corresponds to a probability of interference capture of 0.002. This appears to be much better than the 1 percent

Figure 30

Interference-Canceller Results, FM-Voice + FM-Sinusoid

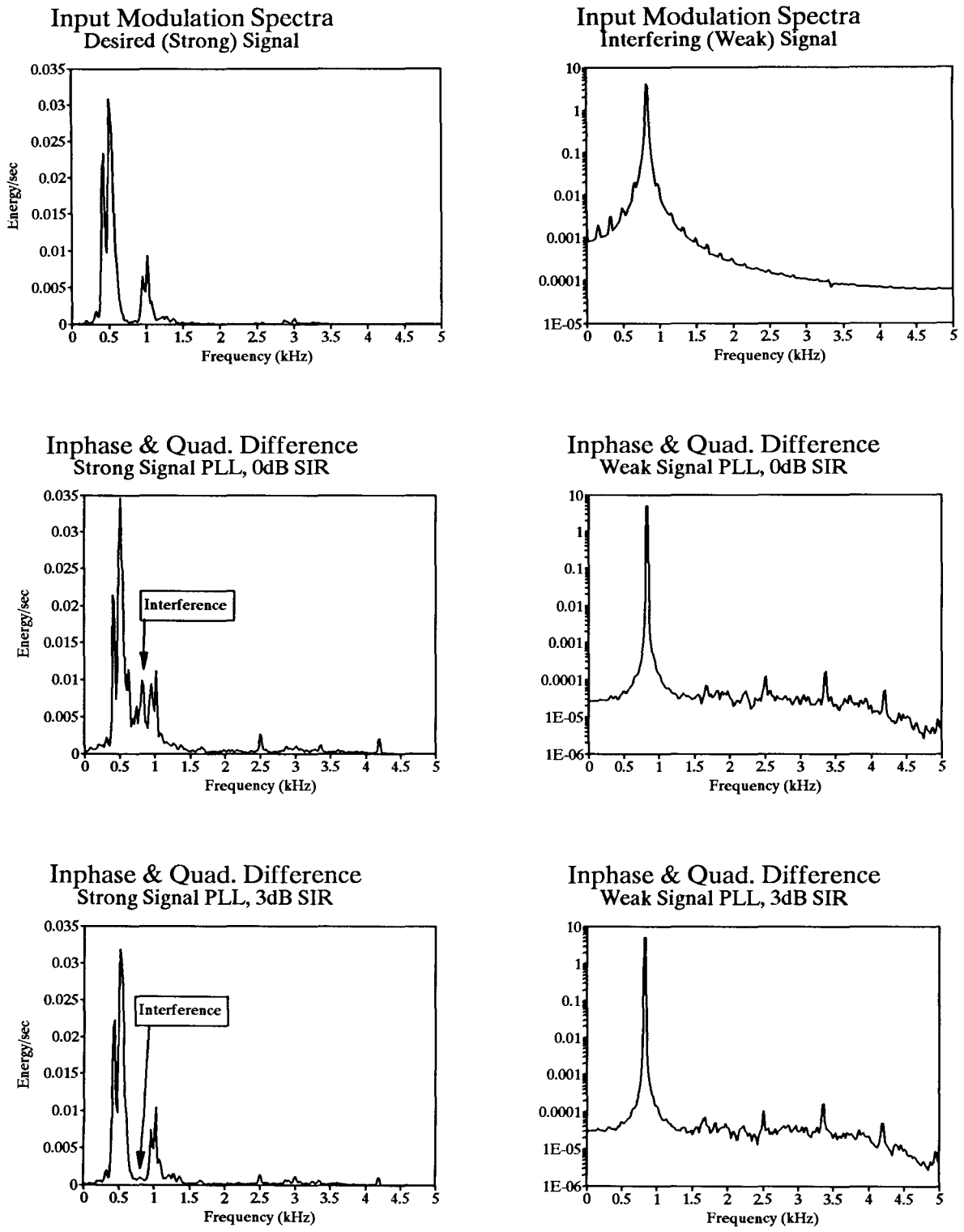

Figure 30 (continued)

Interference-Canceller Results, FM-Voice + FM-Sinusoid

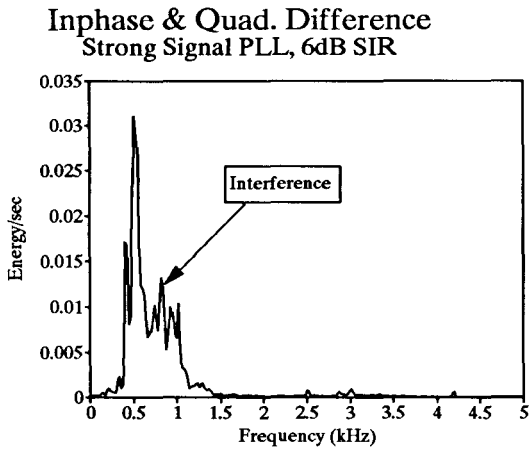

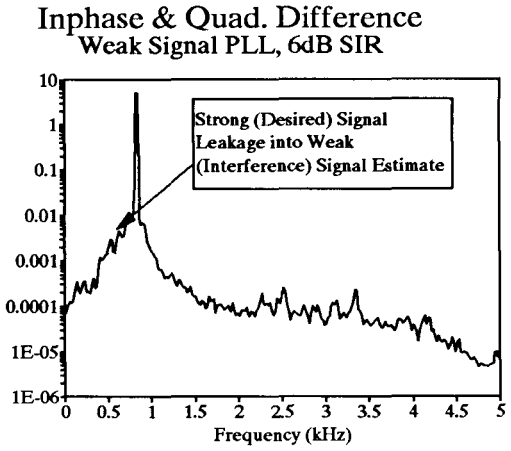

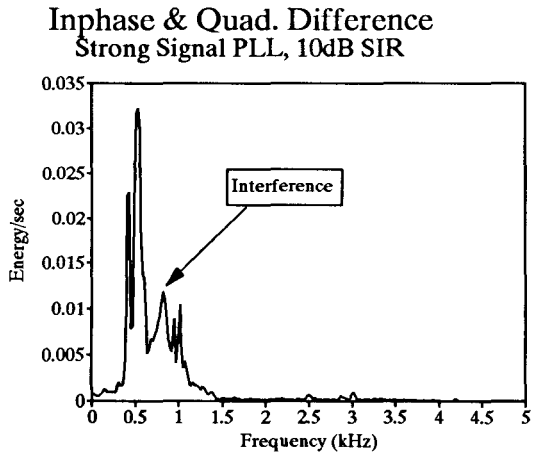

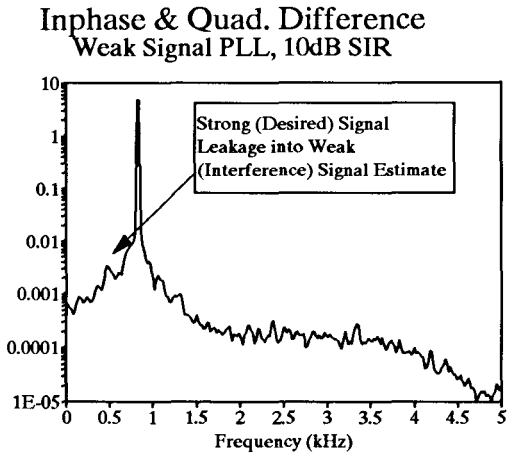

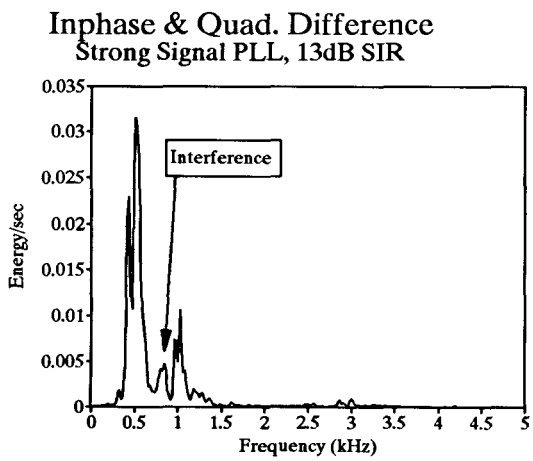

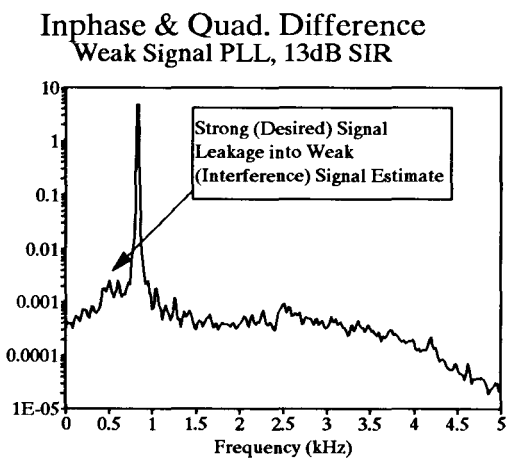

Figure 30 (continued)

Interference-Canceller Results, FM-Voice + FM-Sinusoid

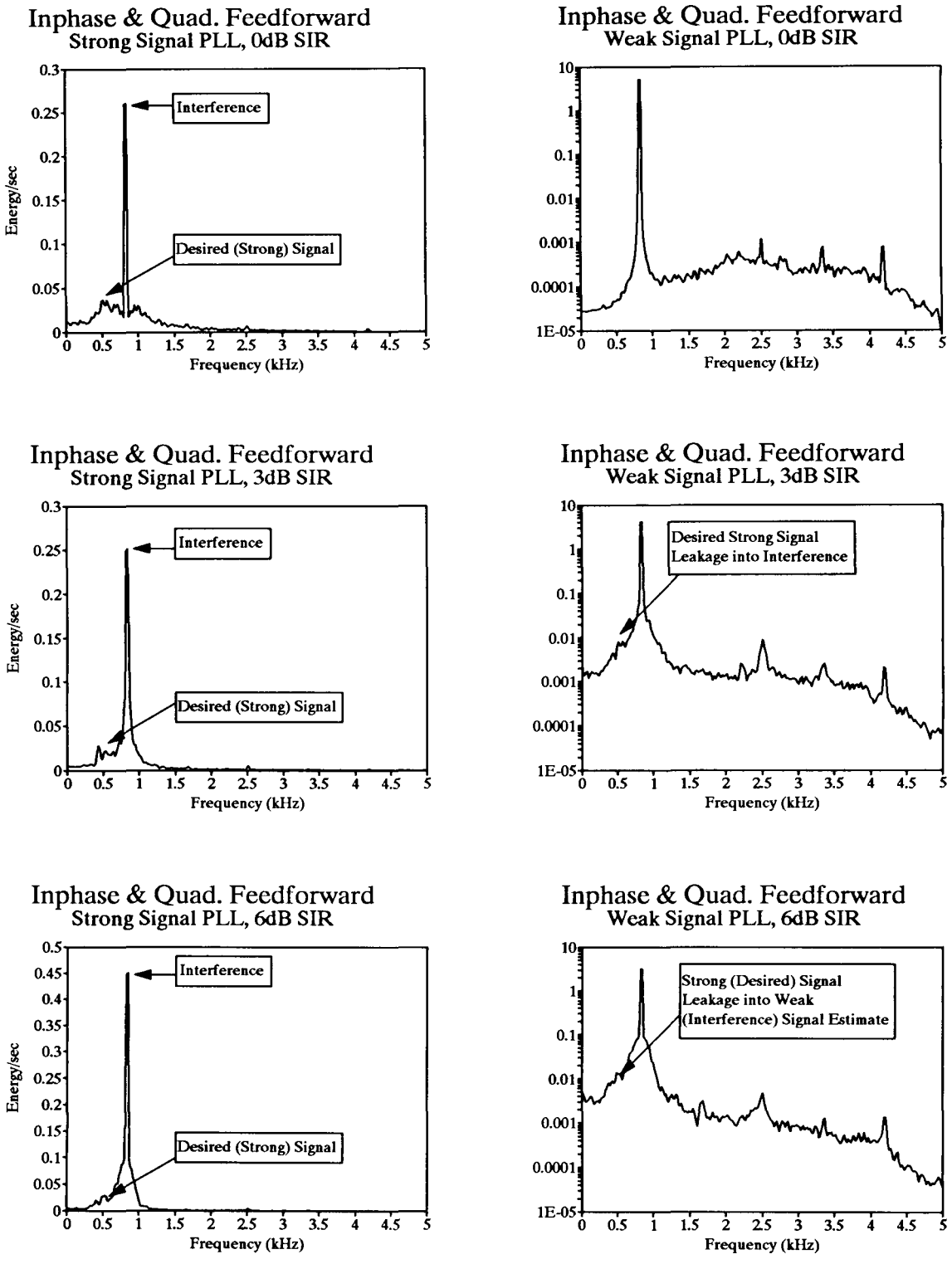

Figure 30 (continued)

Interference-Canceller Results, FM-Voice + FM-Sinusoid

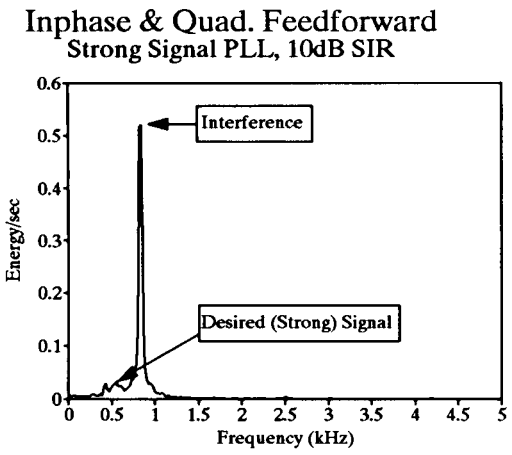

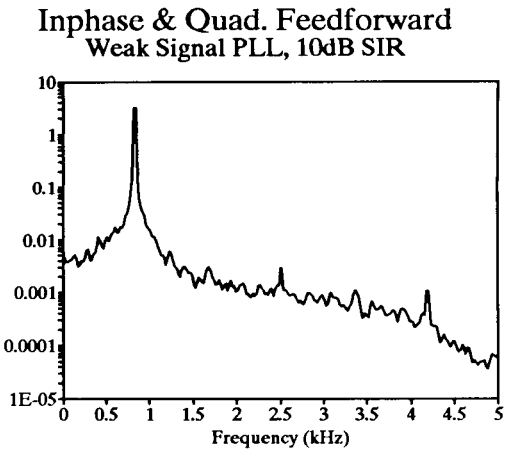

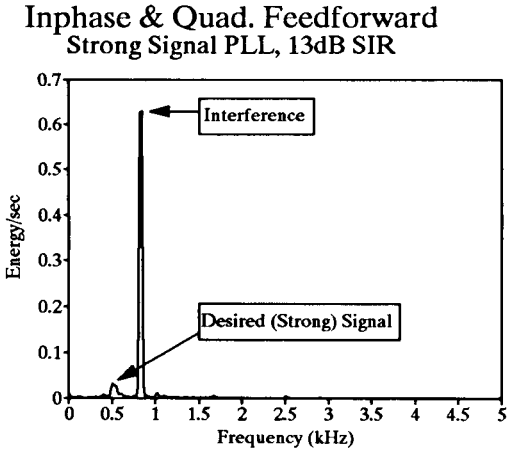

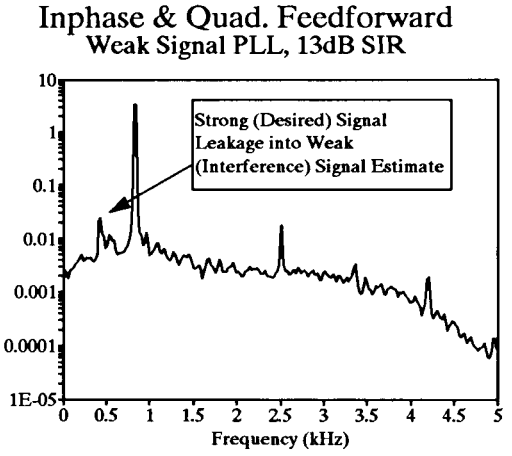

Figure 30 (continued)

Interference-Canceller Results, FM-Voice + FM-Sinusoid

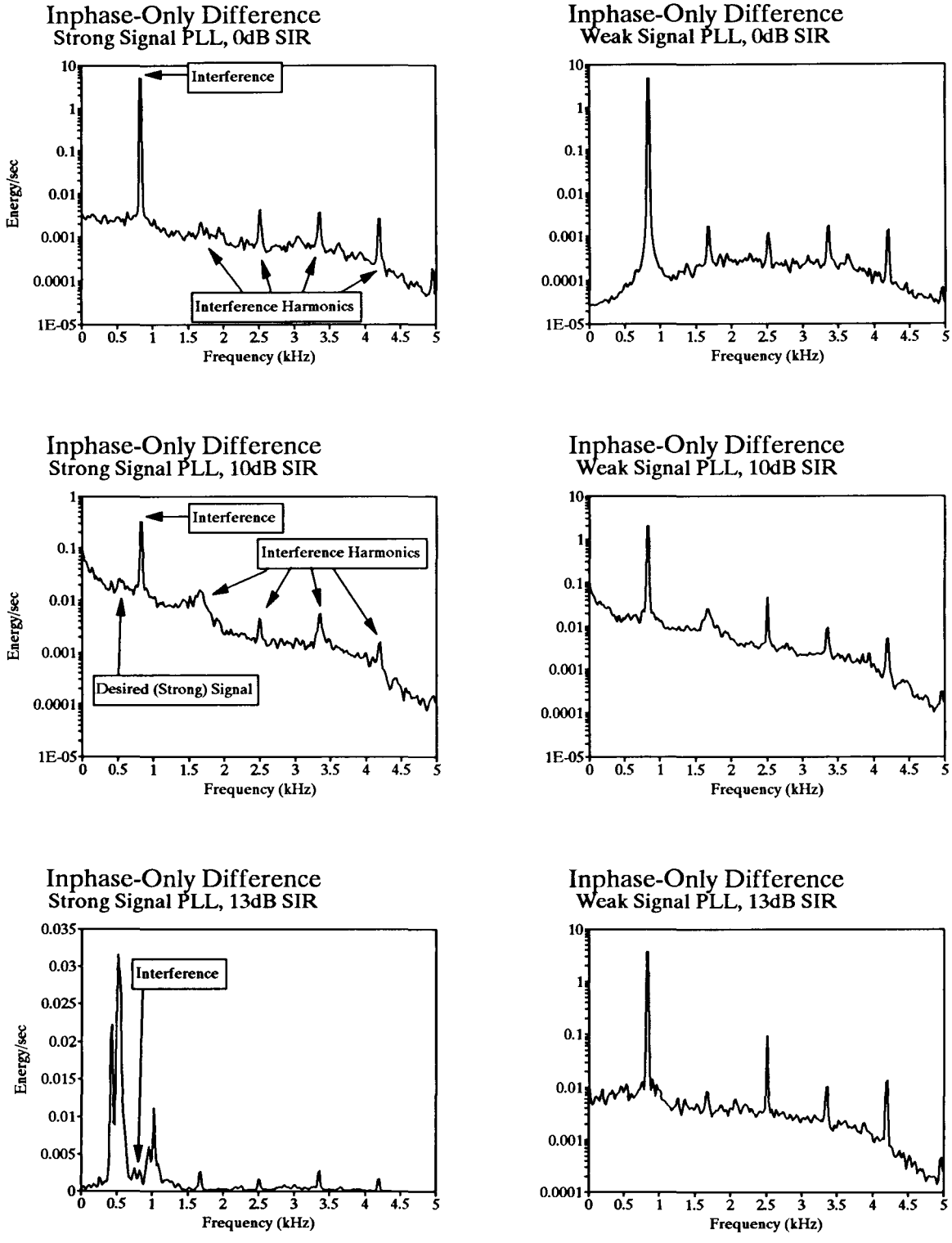

Figure 30 (continued)

Interference-Canceller Results, FM-Voice + FM-Sinusoid

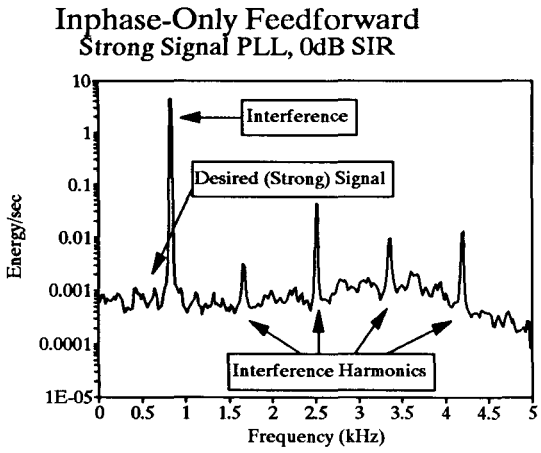

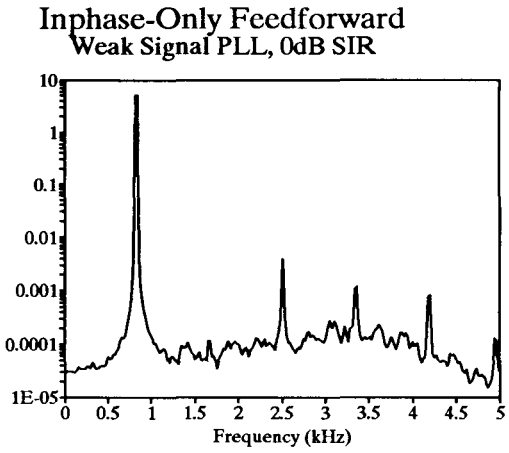

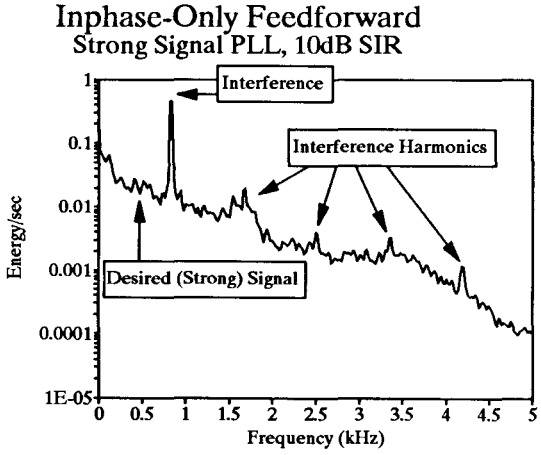

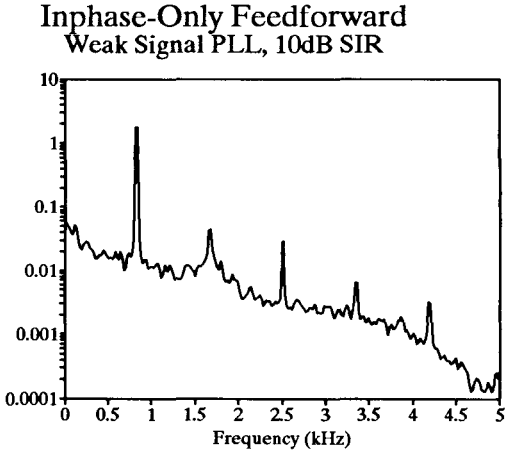

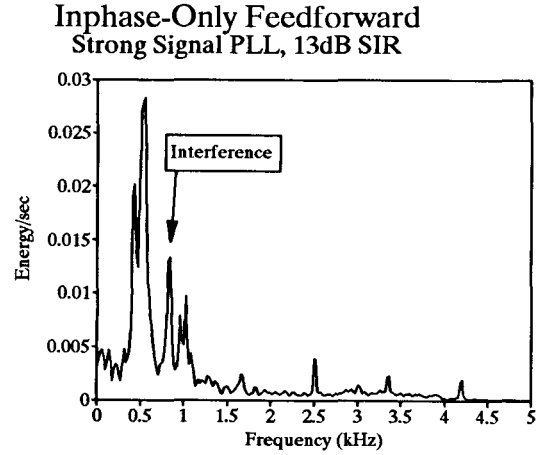

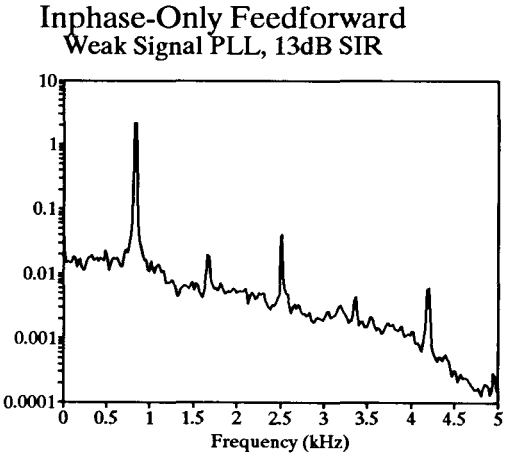

Figure 30 (continued)

Interference-Canceller Results, FM-Voice + FM-Sinusoid

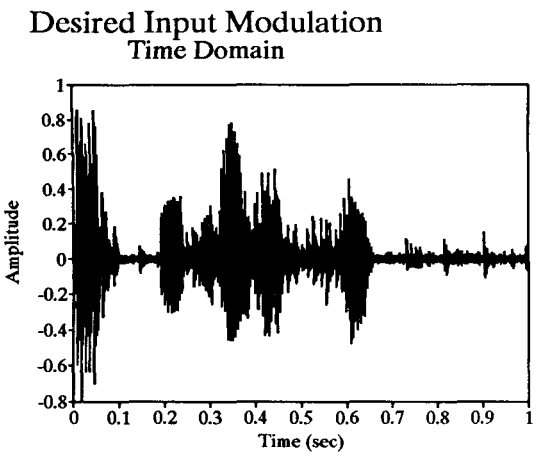

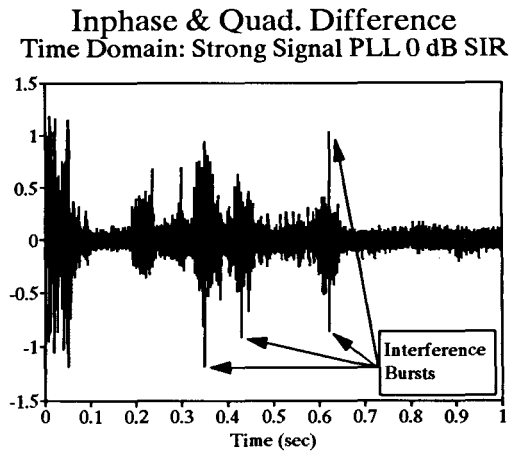

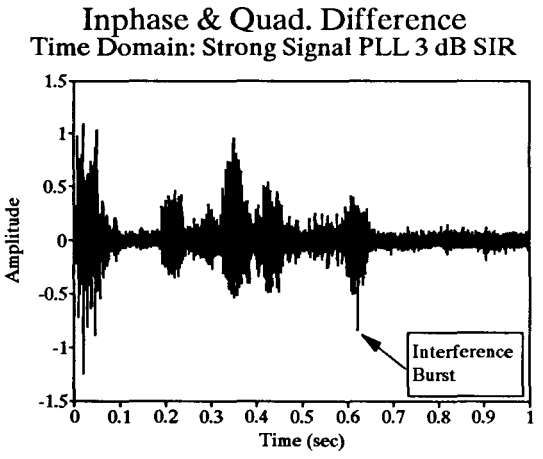

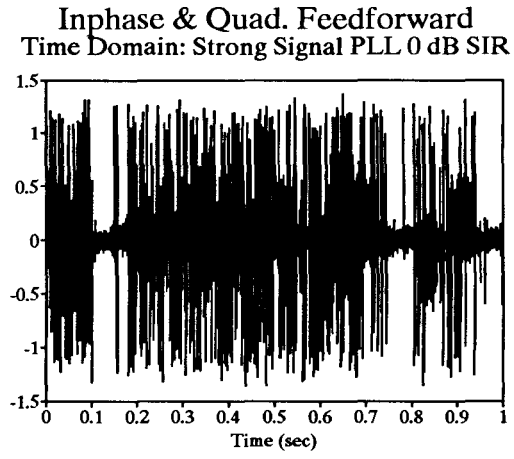

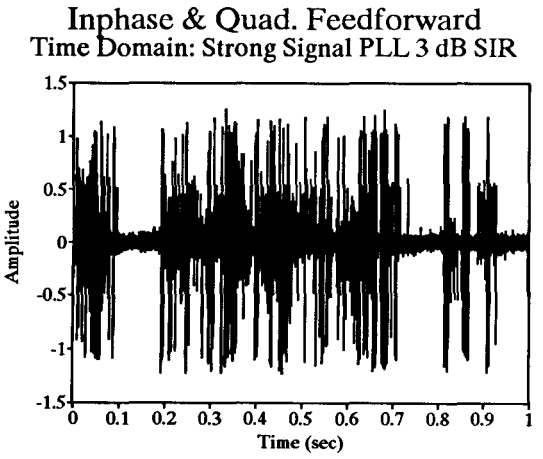

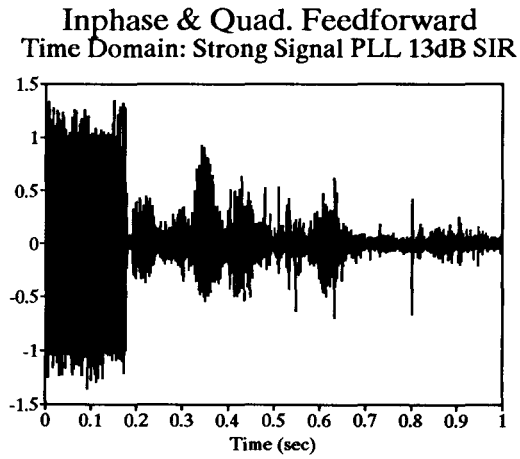

probability of dropout that is due to fade given by [36] as a requirement for a high-reliability voice system. A quick look at the demodulated time sequence of the voice output, also in Figure 30, confirms this result. Bursts of interference appear as short-duration, high-amplitude spikes and are obviously rare events for the IQDIF canceller.

The sinusoid used for modulation of the interferer in Figures 29 and 30, however, is not very representative of the typical voice interferer. To remedy this unrealism, experiments were done to demonstrate the separation of two voice-modulated signals with the IQDIF canceller. Figure 31 shows some results of these experiments. The time sequence and the spectra of the modulation are shown prior to the canceller results. Figure 32 shows time histories of the spectral components in both the original voice and the demodulated outputs of the cancellers for the 0 dB SIR and 3 dB SIR cases. From these graphs and the spectra in Figure 31, it is clear that there has been little leakage between the two received signals. Exact determination of call quality should, however, be done with human listeners, and is beyond the scope of this study. These simulations do seem to indicate, though, that a proper application of interference cancellers in cellular telephony, such as variations of the IQDIF canceller form, could provide not only closer reuse of a given frequency than is currently possible, but reuse of a frequency even perhaps within the same cell.

4.10. Some Considerations of the Improvement of Existing Systems

The most difficult part of any system upgrade is often the details of its implementation. Upgrading the existing cellular system is no exception. In upgrading an existing system, especially one in which a substantial amount of hardware is owned by and distributed throughout the public, it is important that upgrades be small and self-contained. Any subscriber-equipment receiver upgrade cannot be much more than a single integrated circuit design. It seems indeed possible to implement the inphase and quadrature difference-amplitude interference canceller as a single integrated circuit design. The production of two PLL's on a single chip is certainly within current technology. An example of a chip with the equivalent of two PLL's plus interface and control circuitry is the Quallcomm (Q2234), a dual direct digital synthesizer [7]. In addition to the two PLL's that make up most of the canceller, the

Figure 31

Interference-Canceller Results, FM-Voice + FM-Voice

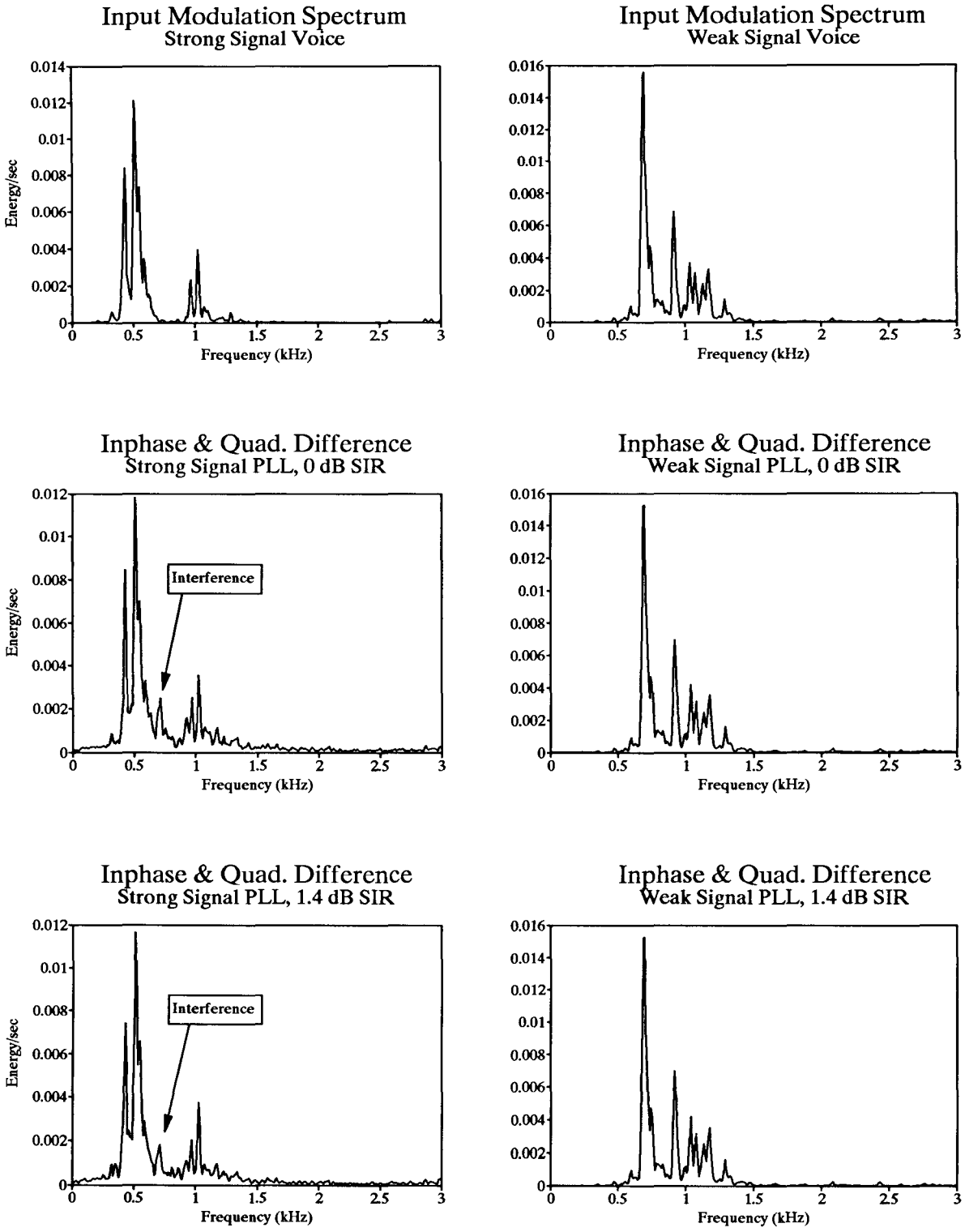

Figure 31 (continued)

Interference-Canceller Results, FM-Voice + FM-Voice

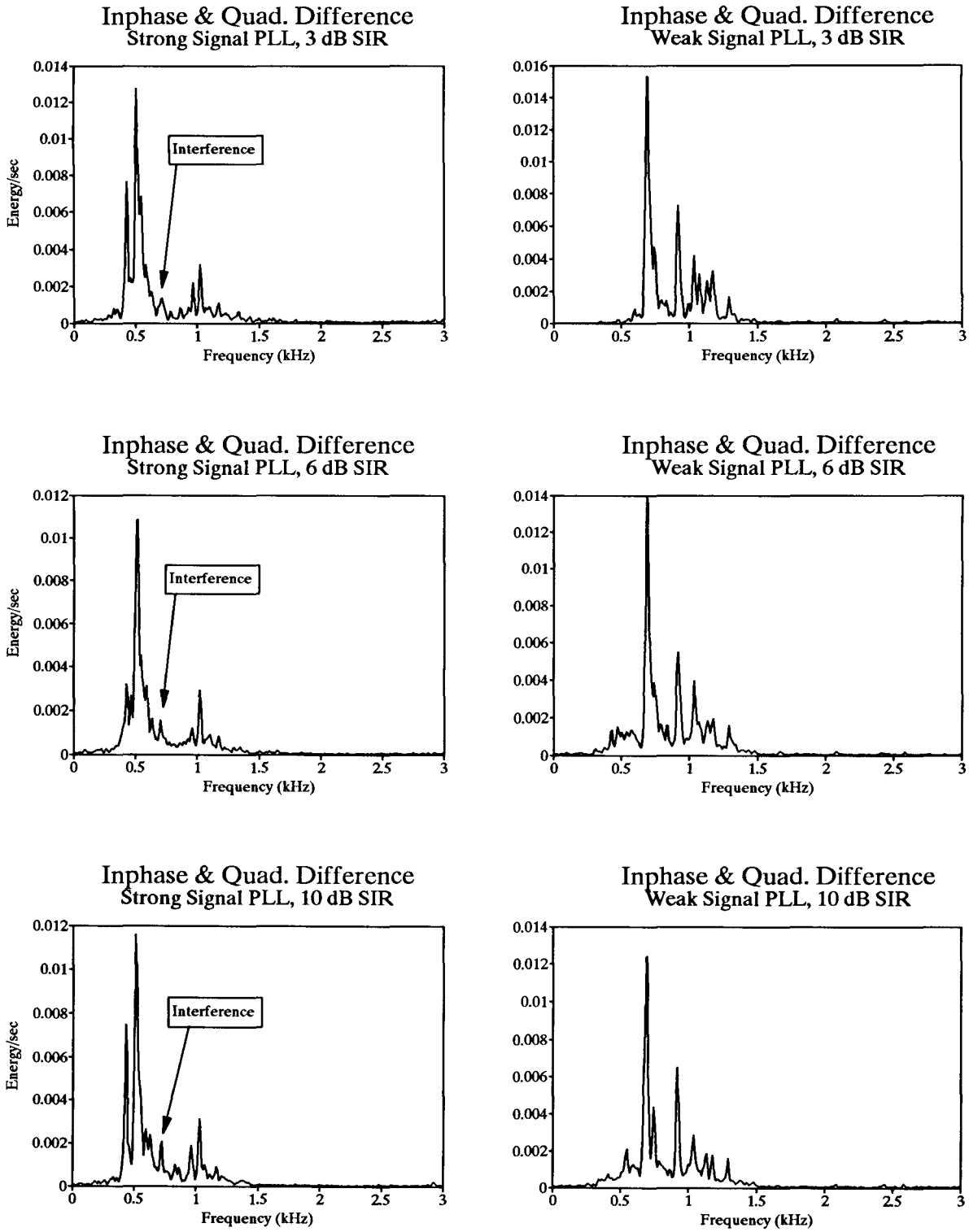

Figure 31 (continued)

Interference-Canceller Results, FM-Voice + FM-Voice

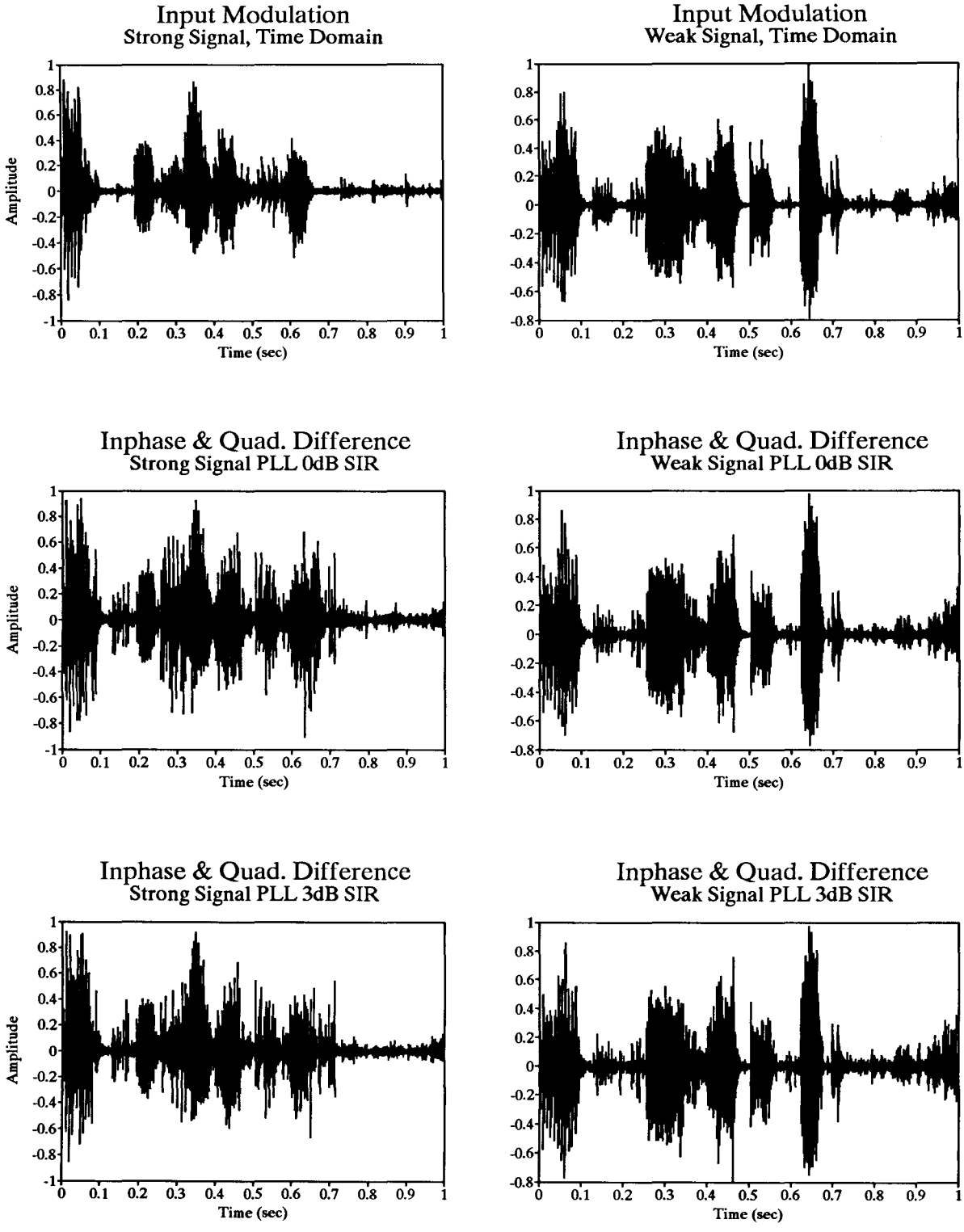

Figure 32

Interference-Canceller Spectral Time Histories, FM-Voice + FM-Voice

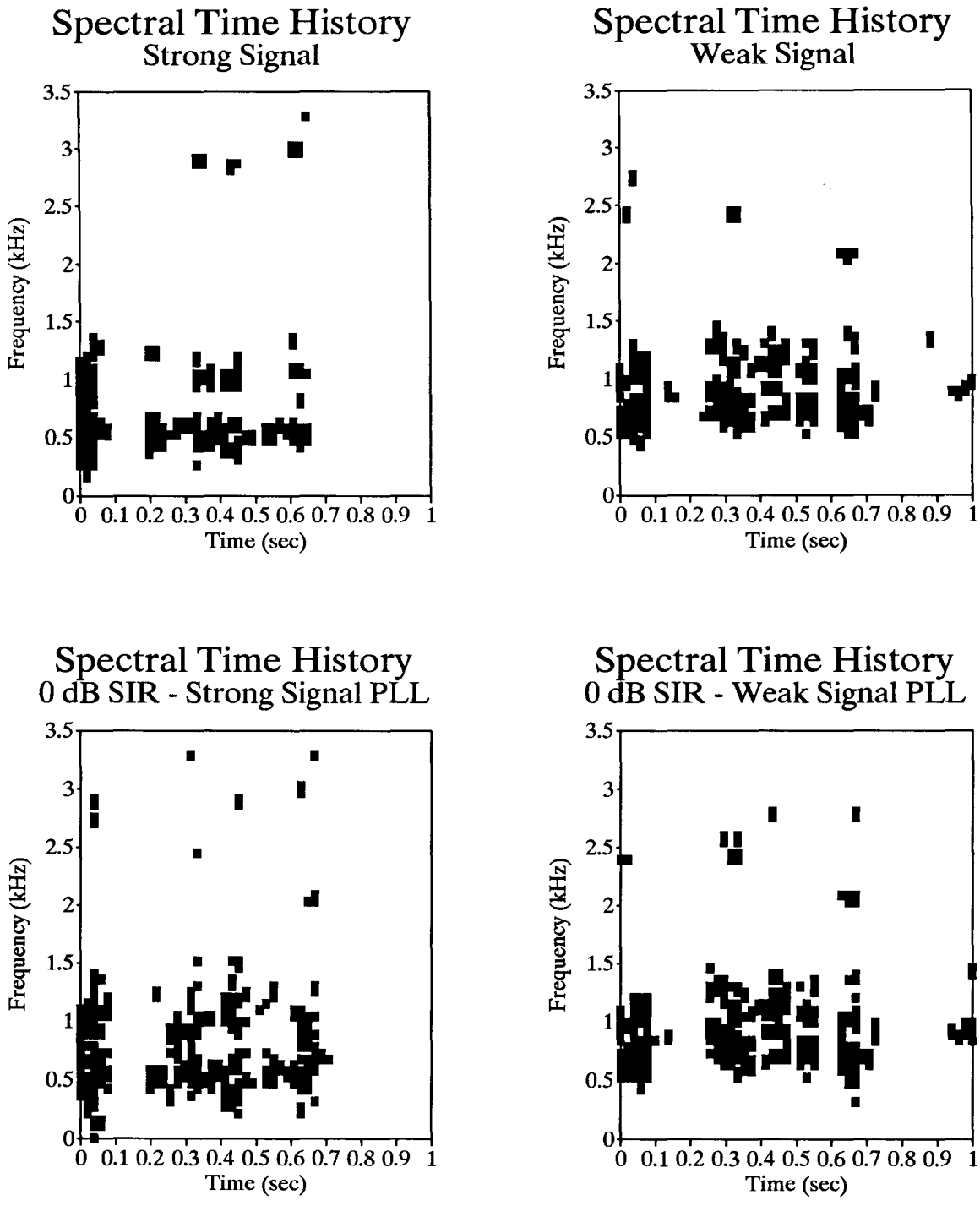

Figure 32 (continued)

Interference-Canceller Spectral Time Histories, FM-Voice + FM-Voice

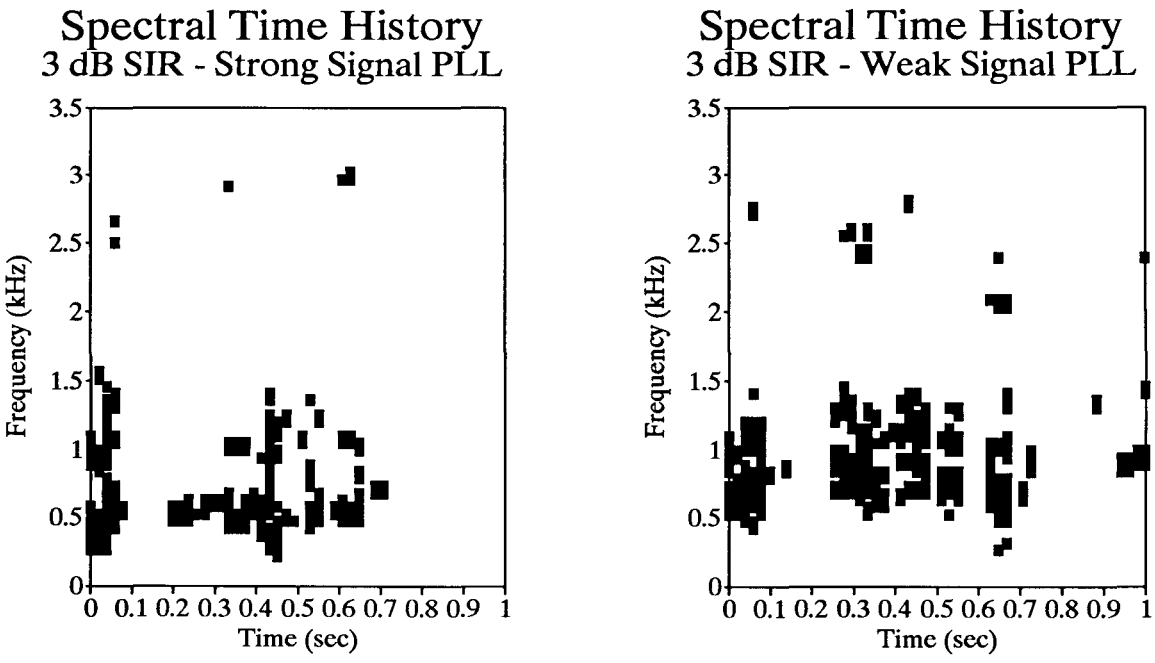

canceller's components include: four analog multipliers, four summers, and four first-order amplitude-estimate filters. All of these parts are commercially available as small-scale integrated circuits, and could be implemented as parts separate from the PLL's, if necessary. They add only a small amount of complexity relative to the two PLL's, and therefore should not cause a canceller design to exceed one chip.

Upgrades to the tower (base station) equipment are less of a problem. The base-station receivers are owned and operated by the service providers. This is important because it makes modifying the receivers a centrally controllable task, and eliminates the problem of providing the fixed receiver owners with extra incentives to upgrade, as required for the mobiles. Since the base stations don't have as strict size and weight restrictions as the mobiles do, more complicated, physically larger receivers could be used in the base stations if they provide any advantage.

Even if the canceller is produced on one chip and upgrade of the towers is easily done, distribution to mobile subscribers may be difficult. A service taking advantage of the interference cancellers would have to provide for continuing service of receivers without the cancellers, and therefore would face some of the same potential compatibility problems as proposed new digital cellular systems do. One solution to providing continuing service is, as in the digital cellular proposals, to reallocate some of the bandwidth exclusively to the interference-cancelling receivers. One advantage that this approach enjoys over proposed digital cellular systems is that there is, as we have seen, a simple upgrade path to the new technology. Upgrade can be accomplished without having to replace the subscriber equipment completely. Replacement of the FM demodulator is the only required change, and this is likely to be a single-chip substitution.

In the past, some computer manufacturers have handled similar upgrades by charging the customer a small upgrade fee. In the computer industry, the customer is the main benefactor from the upgrade, while in the cellular case the service providers (and future subscribers who can now be accommodated) are obtaining most of the benefit. Provider costs and benefits ultimately get passed on to the subscriber, of course, but by not having to apply for an increased spectral allocation to carry more revenue-producing traffic, the provider avoids the large financial investment needed to handle

more subscribers. Therefore, it is logical that the service providers pay some portion, possibly all, of the subscriber upgrade costs.

Chapter V

Summary and Conclusions

In this thesis, a case has been made for using interference cancellation on multiaccess communications systems. Beginning with theoretical motivations for using the discoverable structure of interference that is due to other users of the system, we went on to show the feasibility of interference cancellation for a practical modulation scheme (FM). Analog FM interference cancellers were examined, including both prior and new work. On the basis of a new understanding of FM interference-canceller operation, improved and simpler interference cancellers were proposed, analyzed, and verified by simulation. We then examined cellular telephony, an important example of a multiaccess communications system, as a candidate for application of FM interference cancellers. Spectrum-efficiency gains provided by active interference cancellation were considered relative to the conventional passive approach of allowing propagation attenuation alone to mitigate interference. The FM interference cancellers were tested on the cellular telephone channel by computer simulation, demonstrating the practicality of the interference-canceller approach and its large potential for spectrum-efficiency gain.

It has been said that the radio spectrum is like real estate; they aren't making any more of it. It is, however, that the important quantity to conserve is not necessarily the bandwidth itself, but its ability to carry information. In geographically distributed systems, wasting the recoverable information present in strong interferers is, quite literally, wasting the channel's capacity to carry information. Even in high-capacity systems where coding techniques allow users to communicate on the same frequency, it is potentially feasible to improve interference resistance by decoding (demodulating), re-encoding, and then cancelling the interference. In Chapter II we saw that information theory motivates such use of interference cancellation. We saw that with sufficiently strong interference and a version of an interference-cancelling receiver, it was possible sometimes to perform multiaccess communication on the additive white Gaussian channel without any loss of capacity because of interference.

The price for this immunity to interference is more complicated receiver systems. However, in an age where even complex spread-spectrum systems are being seriously considered for public mobile communications [7], increasing the complexity of receivers is not necessarily prohibitive. This is

especially true for conventional analog-modulation schemes. Such modulation schemes have simple receivers, designed originally for a single-transmitter channel. As an example of a conventional modulation scheme, we then specialized to FM transmission to demonstrate that conventional single-transmitter-based receiver designs sometimes discard side information, such as the signal amplitude, which can be important in separating interfering signals. We also saw that a correct use of even a simple Frequency Division Multiple Access (FDMA) channel allocation scheme could potentially utilize the entire allocated channel capacity. Therefore, we need not necessarily look toward more complex multiple-access schemes, but we could pursue more powerful reception techniques with conventional modulation.

Chapter III introduced Cross-Coupled Phase-Locked Loops (CCPLL)-based FM interference-cancelling receivers as a candidate interference canceller for use in multiaccess communications. These receivers have been the subject of little prior publication, and until now have been applied primarily to military reception problems. The operation of the CCPLL interference canceller was examined. Based on an understanding of the operational principles behind the CCPLL interference canceller and on optimal estimation theory, new interference-cancelling systems were proposed, analyzed and simulated on an amplitude-preserving channel. Some of the new systems were made simpler than the original CCPLL by providing only one amplitude-tracking loop rather than the original two. Others had improved steady-state operation, obtained by forming the estimate of a signal's amplitude from an interference-cancelled reference. For application to a given channel, the parameters of these receivers, i.e., the loop bandwidth, the loop filter transfer function, and the amplitude-estimation filters, would be optimized, but for the purposes of this general feasibility demonstration, previously recommended values [18] were used, with no further attempt at optimization. Even without optimization, simulation of the interference cancellers of Chapter III demonstrated that reception of both of two co-channel FM interferers was possible with these cancellers, as suggested by information theory.

Chapter IV examined the potential for applications of these interference cancellers to the cellular telephone channel. At least one of the interference-cancelling receivers of Chapter IV performed well on this Rayleigh fading channel, possibly allowing for the reuse of a frequency even within the same

cell. Again, this application was made without optimization, and without the benefit of other techniques known to mitigate the effects of FM interference on the demodulated output, i.e., companding and pre-emphasis. More on this particular application can be found in Appendix A, Summary for the Cellular Industry.

The modern world is awash with multiuser communications channels. The demand for the existing spectrum is, as such, relentless. From mobile communications, to cordless phones, to commercial broadcast stations, systems must make allowances for interference. (The commercial broadcast station can be considered a multiuser communications system over a large geographical area that includes multiple stations assigned to the same frequency.) Most of these systems face much less severe reception environments than the cellular telephone channel. In more general mobile communications applications, the required level of voice quality can be far below cellular telephone standards, e.g., on a police, aircraft, or taxicab radio. Application of interference cancellers to these channels would not only allow several users to speak at once, something not possible on current systems, but would also allow the allocated bandwidth to support more user licenses. Application to these mobile channels would be similar to the cellular telephone channel since the cellular telephone channel is also a mobile channel.

For cordless phones the rapid fading nature of the cellular environment, primarily because of doppler-shifted paths, will not be present. Users of cordless phones in areas of high user density would benefit from the application of interference cancellers, since these communications systems operate on a small number of frequencies and are commonly observed to interfere frequently with one another. For commercial broadcast stations, the high signal-to-noise ratios can be taken advantage of, combined with more complicated encoding or modulation at the transmitter. Commercial stations could be placed closer together geographically, and listeners could then choose which station they wanted to hear by selecting from the interference-canceller outputs. All these applications would allow more efficient use of the spectrum over geographically distributed areas.

As a final note it is important to point out that the information-theoretic motivations for interference cancellation do not have anything to do with modulation type. While the cancellers demonstrated were for analog FM systems, similar cancellers could potentially be designed for coded digital-

modulation schemes. The redundancy and regularity of such schemes would probably make the interference cancellation even easier to implement, and more effective as well. Since the FM cancellers follow Carleial's proposed interference-cancelling topology, digital systems based on the same designs as these FM cancellers are quite likely. For systems that currently mitigate interference through coding techniques, i.e., CDMA systems, the addition of interference cancellation at the receiver input, fed by the decoded output, would conceivably allow the resulting system to tolerate still more interference in the channel. The gains presented here are simply manifestations of the fact that treating structured interference as completely random noise without trying to exploit the discoverable structure is wasteful of the information represented by that discoverable structure.

Appendix A

Summary for the Cellular Industry

The results here imply that it is possible that with the current modulation specification, a frequency may even be reused within its own cell. In this way, FM interference cancellation could easily provide at least a doubling of the call-carrying capacity of the allocated spectrum under the current modulation specification. More research into these systems, including field tests, is required; however, the current results indicate that the prospects for great rewards in terms of increased spectral efficiency are good.

In this thesis we examined cellular telephony as a candidate for application of FM interference cancellers. New FM interference cancellers were developed, and they were evaluated by computer simulation against the Rayleigh fading characteristic of the cellular telephone channel. These simulations demonstrated that at least one of the new receivers recovered high-quality voice transmission from both of two interfering FM signals at SIR's near 0 dB. High quality was achieved in one of the voice channels at 0 dB, while the other channel, while still good, had a small amount of interference-related corruption noticeable in its spectral output. The final measure of call quality, evaluation by subjective listeners, will require further experimentation.

During these simulations, no attempt was made to optimize the receiver parameters beyond the recommendations of earlier work [18], which were based primarily on conventional PLL receiver theory. This was done so as not to contaminate the tests by "special-casing" the receivers to the test input. Since these interference-cancelling receivers are coupled systems, it is reasonable to believe that they will have different optimal parameters from those of conventional PLL's. As a result, the performance of the interference-cancelling systems will probably improve with further development.

As the cellular communications industry grows, the need to utilize the available spectrum efficiently becomes increasingly vital. The need to accommodate an ever larger subscriber base has pushed the development of co-frequency channel interference-resistant multiple-access schemes [7]. These schemes must provide greater call capacity for geographic regions, allowing for future expansion. However, they are significantly more complicated than the conventional frequency division multiple

access (FDMA) FM techniques. One is forced to ask the question, "What could be gained by using more complicated receivers in the current FDMA systems?" Indeed, the basic receiver design in current systems is at least a decade old, and comparing its performance to that of a CDMA system is something like comparing today's desktop personal computers to programmable calculators of ten years ago. In December 1989, the FCC issued General Docket No. 88-411, "In the Matter of Advanced Technologies for the Public Safety Radio Services" [39], in which they posed the question of what further advances in analog technology could improve spectral efficiency. One answer to this question is the development of interference-cancelling receivers.

As a final note it is important to point out that the motivations for interference cancellation do not necessarily have anything to do with the modulation and coding specifications. While the cancellers demonstrated were for analog FM systems, similar cancellers could potentially be designed for coded digital-modulation schemes. The redundancy and regularity of such schemes would probably make the interference cancellation both easier to implement and more effective. Since the FM cancellers follow the information-theoretically proposed interference-cancelling topology [20], digital systems based on the same designs as these FM cancellers are quite possible. For systems that currently mitigate interference through coding techniques, i.e., CDMA systems, the addition of interference cancellation at the receiver input, fed by the decoded output, would conceivably allow the resulting system to tolerate even more interference in the channel. The gains presented here are simply manifestations of the fact that treating structured interference as completely random noise without trying to exploit the discoverable structure is wasteful of the information represented by that discoverable structure.

References

1. R.E. Ziemer, W.H. Tranter; *Principles of Communications Systems, Modulation, and Noise* , Houghton Mifflin, Boston, 1985.

2. G.R. Cooper, R.W. Nettleton; "A Spread-Spectrum Technique for High-Capacity Mobile Communications," *IEEE Transactions on Vehicular Technology* , vol. VT-27, pp. 264-275, 1978.

3. D. J. Goodman, P.S. Henry and V.K. Prabhu; "Frequency-hopped Multilevel FSK for Mobile Radio," *Bell System Technical Journal* , vol. 59, pp. 1257-1275, 1980.

4. W. W. Chapman; "Spread Spectrum Applications to Mobile Radio: Past, Present, Future," *IEEE Vehicular Technology Newsletter* , February 1985.

5. E. A. Gerianotis and M. B. Pursley; "Performance of Coherent Direct-Sequence Spread-Spectrum Communications over Specular Multipath Fading Channel," *IEEE Transactions on Communications* , vol. COM-33, pp. 502-508, 1985.

6. E. A. Gerianotis and M. B. Pursley; "Performance of Non-Coherent Direct-Sequence Spread-Spectrum Communications over Specular Multipath Fading Channel," *IEEE Transactions on Communications* , vol. COM-34, pp. 219-226, 1986.

7. PacTel Cellular, Quallcomm Inc.; "CDMA Cellular - The Next Generation," *Presentation Notes* , November 1989.

8. E. Baghdady; "New Developments in FM Reception and Their Application to the Realization of a System of 'Power-Division' Multiplexing," *IRE Transactions on Communications Systems* , vol. 7, pp. 147-161, 1959.

9. T.S. Sundresh, F.A. Cassara, H. Schachter; "Maximum a posteriori Estimator for Suppression of Interchannel Interference in FM Receivers," *IEEE Transactions on Communications* , vol. COM-25, pp. 1480-1485, 1977.

10. F.A. Cassara, H. Schachter; "Suppression of Interchannel Interference in FM Receivers," Polytechnic Rep. POLY EE79-056, July 1979.

11. F.A. Cassara, H. Schachter, G. Simowitz; "Cross-Coupled Phase-Locked Loop FM Demodulator," 22nd Midwest Symposium on Circuits and Systems, Univ. of Pa., Philadelphia, pp. 475-481, June 17-19, 1979.

12. F.A. Cassara, H. Schachter, G. Simowitz; "Acquisition Behavior of the Cross-Coupled Phase-Locked Loop FM Demodulator," *IEEE Transactions on Communications* , vol. COM-28, pp. 897-904, 1980.

13. Y. Bar-ness, F.A. Cassara, H. Schachter; "Cross-Coupled PLL Interference Canceller with Closed Loop Amplitude Control," 1982 IEEE Global Telecommunications Conference (84CH2069-3/84/0000-0530) (GLOBECOM '82), vol. 2, pp. 691-695, November 29 - December 2, 1982.

14. Y. Bar-ness, F.A. Cassara, H. Schachter; "Cross-Coupled PLL Interference Canceller with Closed Loop Amplitude Control," *IEEE Transactions on Communications* , vol. COM-32, pp. 195-199, 1984.

15. F.A. Cassara, R. DiFazio, H. Schachter; "Cross-Coupled Phase-Locked Loop Interference Canceller for Suppression of Electromagnetic Interference Caused by Wind Turbine Generators," 24th Midwest Symposium on Circuits and Systems, Univ. of New Mexico, Albuquerque, pp. 720-725, June 20-30, 1981.

16. S. Say, F.A. Cassara; "Experimental Results on the Cross-Coupled Phase-Locked Loop Interference Canceller with Closed Loop Amplitude Control," 1986 IEEE Military Communications Conference (CH2323-4/86/0000-0176) (MILCOM '86), vol. 3, pp. 47.1.1 - 47.1.5, October 5-9, 1986.

17. T. Jedrey, E. Satorius; "Fixed Point Implementation of Cross-Coupled Phase-Lock Loops," 1986 IEEE Military Communications Conference (CH2323-4/86/0000-0177) (MILCOM '86), vol. 3, pp. 47.2.1 - 47.2.5, October 5-9, 1986.

18. S. Say; "Vector-Locked Loop Interference Canceller," Ph.D. Dissertation, Polytechnic Institute of New York, June 1985.

19. Cellular Telecommunications Industry Association (CTIA); "CTIA Reports Record Subscriber Surge Total Tops 3.5 Million," *CTIA Press Release* , Feb. 6, 1990.

20. A.B. Carleial; "A Case Where Interference Does Not Reduce Capacity," *IEEE Transactions on Information Theory* , vol. IT-21, pp. 569-570, 1975.

21. W. Jakes; *Microwave Mobile Communication* , John Wiley & Sons, New York, 1974.

22. D. Tufts, J. Francis; "Estimation and Tracking of Parameters of Narrow-Band Signals by Iterative Processing," *IEEE Transactions on Information Theory* , vol. IT-23, pp. 742-751, 1977.

23. I. Bar-David, S. Shamai (Shitz); "Information Transfer by Envelope Constrained Signals Over the Additive White Gaussian Channel," *IEEE Transactions on Information Theory* , vol. IT-34, pp. 371-379, 1988.

24. R. McEliece ; *The Theory of Information and Coding* , Cambridge University Press, Cambridge, England, 1984.

25. J. Pierce, E. Posner; *Introduction to Communication Science and Systems* , Plenum Press, New York, 1980.

26. D. Divsalar, M.K. Simon; "The Design of Trellis Coded MPSK for Fading Channels: Performance Criteria," *IEEE Transactions on Communications* , vol. COM-36, pp. 1004-1012, 1988.

27. B. Widrow, J. Glover, Jr., J.M. McCool, J. Kaunitz, C.S. Williams, R.H. Hearn, J.R. Zeidler, E. Dong, M.D., and R.C. Goodlin, M.D.; "Adaptive Noise Cancelling: Principles and Applications," *Proceedings of the IEEE* , vol. 63, no. 12, pp. 1692-1716, 1975.

28. B. Widrow, S. Stearns; *Adaptive Signal Processing* , Prentice-Hall, Englewood Cliffs, New Jersey, 1985.

29. J. Bruck, V.P. Roychowdhury; "On the Number of Spurious Memories in the Hopfield Model," *IEEE Transactions on Information Theory* , vol. IT-36, pp. 393-397, 1990.

30. E. Baghdady; *Lectures on Communication System Theory* , McGraw Hill Book Company, Inc., New York, 1961.

31. K. Leentvaar, J. Flint; "The Capture Effect in FM Receivers," *IEEE Transactions on Communications* , vol. COM-24, pp. 531-539, 1976.

32. J.H. Roberts; "A Survey of Receiver Designs for Interference Suppression," International Conference on Radio Receivers and Associated Systems, University College of North Wales, pp. 129-133, July 1-4, 1986.

33. R. Guerin; "Queueing and Traffic in Cellular Radio," Ph.D. Dissertation, California Institute of Technology, 1986.

34. *Federal Communications Commission (FCC);* Washington, D.C. 20554, Report No. 81-161 29244, Sec. 11.

35. G.A. Arredondo, J.C. Feggeler, and J.I. Smith; "Voice and Data Transmission," *Bell System Technical Journal* (special issue on Advanced Mobile Phone Service (AMPS)), pp. 97-108, January 1979.

36. W. Gosling; "A Simple Mathematical Model of Co-Channel and Adjacent Channel Interference in Land Mobile Radio," *IEEE Transactions on Vehicular Technology* , vol. VT-29, pp. 361-364, 1980.

37. R. McEliece, W. Stark; "Channels with Block Interference," *IEEE Transactions on Information Theory* , vol. IT-30, pp. 44-53, 1984.

38. R. French; "The Effect of Fading and Shadowing on Channel Reuse in Mobile Radio," *IEEE Transactions on Vehicular Technology* , vol. VT-28, pp. 171-181, 1979.

39. *Federal Communications Commission (FCC);* Washington, D.C. 20554, General Docket No. 88-441. Reprinted in *IEEE Vehicular Technology Newsletter* , vol. 37 #1, pp. 17-18, February 1990.